UNIVERSITY OF CALIFORNIA,
IRVINE

Continuum and Discrete Approaches to Quantum Gravity

DISSERTATION

submitted in partial satisfaction of the requirements for the degree of

DOCTOR OF PHILOSOPHY

in Physics

by

Shao H. Liu

Dissertation Committee:
Professor Herbert Hamber, Chair
Professor Riley Newman
Professor Jonas Schultz

1996

The dissertation of Shao H. Liu is approved
and is acceptable in quality and form
for publication on microfilm:

Committee Chair

University of California, Irvine
1996

DEDICATION

To

My parents.

Contents

List of Figures

List of Tables

Acknowledgements

I would like to express my deep appreciation to my thesis advisor Professor Herbert Hamber for his generous support and guidance during my four years of physics research at University of California, Irvine. The weekly discussions we held in the past four years were both stimulating in thinking and educational. I became to gain a much deeper understanding in all aspects of particle physics, quantum gravity, and quantum statistical field theory, and gradually learned to apply knowledge to doing physics research. This work wouldn't be possible without his continuous encouragement.

I am grateful to my thesis committee members Professor Myron Bander, Professor Jonas Schultz, and Professor Riley Newman for their kind advice and support. Special thanks go to Professor Myron Bander who I have learned a lot from working together in the W^- decay project. Not only I have gained a deeper understanding of phenomenological particle physics, but most importantly I learned a creative way of doing physics research. I am in debt to Professor Dennis Silverman for his most honest advice on academic matters, which will sure have a great influence on my later professional career.

I am grateful to all the professors in the physics department I have worked with as a teaching assistant, Steven Barwick, James Rutledge, Andrew Lankford, Jon Lawrence, Gordon Shaw, Douglas Mills, William Molzon, Steven Ruden, John Rosendahl, Herbert Hamber, and William Heidbrink. It has been a great learning experience and a pleasure to work with them. I am thankful to the department coordinators Mindy Johnson, Barbara Thevanez, and Margaret Suniga for their tender care of the graduate students. I also thank John Rosendahl, Jim Kelly, Margaret Suniga, Cindy Fern for putting in time and effort to ensure smooth

operations in all the T.A. classes I taught.

I thank in particular my friend and mentor Dr. Marco Vekic. The project on random Ising model we worked together had been a great fun and a learning experience. Special thanks go to my friends Nitin Pandya, Edward Carolipio, Isable Leonor, Weidong Zhang, Jia-Jen Sun, Weifeng Zhang, and Michael Bantel. Their friendship has made my graduate studies at UC Irvine the most memorable.

Curriculum Vitae for Shao H. Liu

Department of Physics and Astronomy

University of California

Irvine, CA 92717

Phone: (714) 824-3124, Fax: (714) 824-2174

E-mail: lius@uci.edu, lius@sun1.ps.uci.edu

Date of Birth: February 18, 1968. **Citizenship:** U.S.

Education

1987-91 B.S. in Physics, University of California, Santa Barbara.

1991-96 Ph.D. in Physics, University of California, Irvine.

Advisor

Professor Herbert Hamber

Ph.D Thesis

Title: "Continuum and Discrete Approaches to Quantum Gravity"

Academic Awards

1991-92 UC Regents Fellowship, University of California, Irvine.

1995-96 UC Regents Dissertation Fellowship, University of California, Irvine.

Current Research

- Quantum Gravity, Perturbative Weak Field Expansion,

  Non-perturbative Lattice Methods.

- Electroweak Phenomenology, Extended Standard Model, Unification and Model Building, Supersymmetric Theories.
- QCD and Lattice Gauge Theory, Numerical Simulations.
- Designing parallel processing algorithms to run on the IBM Scalable POWERparallel (SP2) Supercomputer for lattice simulations of Quantum Gravity.

Conference Attended

1995 “The Top Quark and the Electroweak Interaction", XXIII SLAC Summer Institute.

Teaching Experience

- 1990-91 **Math, Physics tutor**, University of California, Santa Barbara.
- 1991-95 **Teaching Assistant**, University of California, Irvine.
- Discussion sections I taught include college level physics, and undergraduate and graduate quantum mechanics.

Computer Experience

- Computer Programming languages: C, C++, FORTRAN, PASCAL, BASIC.
- Operating Systems : UNIX, MS-DOS, MS-WINDOWS, Macintosh.
- One research project on Ising spin system in two dimensions involved writing a simulation program in FORTRAN. Calculations of the one-loop quantum corrections to the Newtonian gravity potential involved extensive use of Mathematica and tensor related packages.
- Currently designing parallel processing computer algorithms to run on the IBM Scalable POWERparallel Supercomputer for lattice simulations.

Research Summary

One-loop quantum corrections to the Newtonian potential

It is generally assumed that a quantum theory of gravity cannot lead to testable predictions, due to a lack of perturbative renormalizability of the Einstein-Hilbert action. In a recent work, Prof. H. Hamber and I consider two massive scalar particles interacting through an exchange of gravitons in a fixed four dimensional flat background. The leading-quantum corrections to the Newtonian potential was obtained from the one-loop amplitude contributions of twelve relevant Feynman diagrams. In addition to being in exact agreement with the classical relativistic corrections in the potential, our result also shows that the leading quantum correction is finite and slowly increasing with distance. This work was published in Phys. Lett. B357 (1995) 51-56.

Feynman Rules in Simplicial Quantum Gravity

In this paper we develop the general formalism for performing perturbative diagrammatic expansions in the lattice theory of quantum gravity. We obtain the *lattice* Feynman rules for pure gravity and scalar matter field coupled to gravity to one loop order. The exact correspondence between the lattice Feynman rules and continuum Feynman rules is established. As an application, the two-dimensional conformal anomaly due to a D-component scalar field is explicitly computed in perturbation theory. This work was submitted to Nuclear Physics B for publication (March, 1996).

Random Ising spins in two dimensions

We studied the properties of random Ising spins coupled to two dimensional gravity. In one model Ising spins are placed at the vertices of a flat triangulated lattice. The background lattice is allowed to fluctuate by varying the local coordination numbers through a “link flip" operation. The resulting model exhibits a

tricritical behavior, with the first order and the second order phase meeting at a tricritical point. The critical exponents were found to agree with those by **KPZ** and in the matrix model solution, which suggests that the values of the critical exponents are directly related to the randomness of the spin system, and are not affected by gravity. These works were published in Phys. Lett. B329 (1994) 444-449, and in Phys. Rev. D51 (1995) 4287-4294.

Transverse lepton polarization in polarized W^- decays

In this work, Prof. M. Bander and I investigated the possibility of determining the mass of the Higgs particle by examining the transverse polarization of the outgoing lepton pair in the decay of a W^-. The decay amplitude of the incoming polarized W^- is calculated to one-loop order in the context of Standard Model and extended Standard Model with multiple Higgs doublets. Due to a small contribution to the decay rate from the Higgs loop, measurements of the transverse polarization of outgoing leptons in future accelerators may yield information for the Higgs mass. Our calculation also shows a possible restriction on the free parameter β, the ratio of the vacuum expectation values of multiple Higgs doublets. This work was published in Phys. Rev. D52 (1995) 543-546.

Other research interests

Besides continuing on our research program in (lattice) Quantum Gravity, my most recent research interests extend to looking for new phenomenology physics beyond the Standard Model. Currently I am working on building a possible unified model with a smaller gauge group embedded in higher dimensions, an approach similar to non-abelian Kaluza-Klein theories. A possible supersymmetric extension of the model will be examined in the future.

Publications

1. *Dynamically Triangulated Ising Spins in Flat Space,* (with M. Veki¢, and H. Hamber,) Phys. Lett. **B329** (1994) 444-449;

2. *Random Ising Spins in Two Dimensions - A Flat Space Realization of the KPZ Exponents,* (with M. Veki¢, and H. Hamber,) Phys. Rev. **D51** (1995) 4287-4294;

3. *Transverse Lepton Polarization in Polarized W Decays,* (with M. Bander,) Phys. Rev. **D52** (1995) 543-546;

4. *On the Quantum Corrections to the Newtonian Potential,* (with H. Hamber,) Phys. Lett. **B357** (1995) 51-56;

5. *Feynman Rules for Simplicial Gravity,* (with H. Hamber,) (accepted for publication in Nuclear Physics B, 1996.)

Reference letters from

Prof. Herbert Hamber
Department of Physics
University of California
Irvine, CA 92717
hhamber@uci.edu

Prof. Myron Bander
Department of Physics
University of California
Irvine, CA 92717
mbander@funth.ps.uci.edu

Prof. Dennis Silverman
Department of Physics
University of California
Irvine, CA 92717
djsilver@uci.edu

ABSTRACT OF DISSERTATION

Belief Rivision and Machine Discovery

by

Shao Liu

Doctor of Philosophy in Physics

University of California, Irvine, 1996

Professor Herbert Hamber, Chair

This thesis covers three important aspects of the study of quantum gravity: 1) the Feynman diagrammetic weak field expansion; 2) the analytical expansion of simplicial gravity in small momentum limit, and 3) the non-perturbative lattice simulations. We first calculate the leading long-distance quantum correction to the Newtonian potential for heavy spinless particles. The potential is extracted from the evaluation of all graviton exchange diagrams contributed to the scalar-graviton scattering amplitude. The calculation correctly reproduces the leading classical relativistic post-Newtonian correction. The sign of the perturbative quantum correction indicates that, in the absence of a cosmological constant, quantum effects lead to a slow increase of the gravitational coupling with distance.

We further develop the general formalism for performing perturbative diagrammatic expansions in the lattice theory of quantum gravity. The results help established a precise correspondence between continuum and lattice quantities in the low momentum limit, and should be a useful guide for non-perturbative studies of gravity. The Feynman rules for Regge's simplicial lattice formulation of gravity are derived in detail in two dimensions. As an application, the two-dimensional conformal anomaly due to a D-component scalar field is explicitly computed in perturbation theory.

In the computer simulation aspect of quantum gravity, a model describing Ising spins with short range interactions moving randomly in a two dimensional flat space is considered. The model is analogous to a dynamically triangulated Ising model coupled to gravity on a flat surface. A presence of a hard core repulsion among Ising spins is introduced to prevent the spins from overlapping. As a function of coupling strength and hard core repulsion, the model exhibits a multicritical behavior, with the first order and the second order transition lines terminating at a tricritical point. The thermal and magnetic exponents computed at the tricritical point are consistent with the KPZ (Knizhnik, Ployakov, Zamolodchikov) values associated with Ising spins, and with the exact two-matrix model solution of the random Ising model, introduced previously to describe the effects of fluctuating geometries. It suggests that this new set of exponents are due to the randomness of the lattice, and not to gravity introduced in the KPZ model.

Chapter 1

Introduction

Quantum gravity is a subject of great interest in its own right. Construction of a successful quantized theory can in principle help us to understand [1]

- the dynamics of gravity during the expansion of the universe at the immediate post big bang era, the Planck time, $10^{-42}s$. Typically it may be responsible for triggering the inflationary evolution that many feel it is a necessary stage for the very early expanding universe [2, 3, 4]. Some difficulties hinged in the standard hot big bang model, such as the homogeneity problem, the horizon problem, the flatness problem, the monopole problem may find natural solutions in the context of inflationary model.

- spacetime regions with intense gravity force. Examples of these spacetime regions are: the surroundings of black holes, cosmic strings, domain walls, etc. [5]. The singularity nature of these objects can be possibly avoided with a correct theory of quantum gravity. A theory of quantum gravity will also provide accurate descriptions of black hole radiation [6], thermodynamics inside black holes [7, 8, 9, 10], and formulation of quantum cosmology [11, 12].

- how gravity can possibly provide a fundamental cut-off at the Planck energy $10^{28}eV$ for quantum field theory. Quantum gravity in this context is regarded as a necessary ingredient of an unifying theory of all known forces.

Different approaches to quantize gravity based on our understandings and/or assumptions of gravity have been proposed since the advent of quantum mechanics discovered at the early century. Current popular theories are

- Lagrangian formation of quantum gravity. Gravity is quantized like other known forces: electromagnetic, weak (electroweak), and strong force. One starts with a Lagrangian describing the interactions of the field particles; the theory is then quantized by putting the constructed Lagrangian in the Feynman path integral. The lack of analytical methods in solving the path integral in general leaves the perturbation method as the predominent method used in analyzing the theory. In perturbative quantum gravity, the genuine metric is separated into two parts, a fixed background Minkowski spacetime metric $\eta_{\mu\nu}$, and a perturbation metric $h_{\mu\nu}$ representing the fluctuation of the spacetime geometry due to quantum gravity interaction. The action S is expanded in series in terms of the perturbation metric, $h_{\mu\nu}$. Corresponding Feynman rules to each order of the $h_{\mu\nu}$ are subsequently developed, such as the propagator of the field particles (gravitons), and the interaction vertices among gravitons and material particles. The biggest obstacle presented in this approach is the problem of the renormalizability of the theory. A simple power counting method shows that gravity in this approach is non-renormalizable to all loop orders. Explicit calculations to two loops have also verified that the theory is non-renormalizable in perturbation theory.

- Regge simplicial formulation. The spacetime is divided into many tiny blocks, simplexes. The interior of each block is flat, and the curvature of the continuum spacetime is concentrated on the vertices, hinges. The fluctuation of the metric is represented by the changing in the volume of the simplex, edge lengths, and the angles at the hinges. The continuum Lagrangian is rewritten in the simplicial form. There are essentially two ways to study the

simplicial gravity: the lattice perturbative method, and the computer simulation method. The lattice perturbative method is very similar to the continuum perturbative method. Starting with the lattice Lagrangian, one series expands the lattice Lagrangian in terms of the dynamical variables, edge lengths. Lattice Feynman rules are subsequently enumerated (see detailed discussions in chapter 3.) Once the Feynman rules are developed, analytical results can be obtained by performing loop calculations. The computer simulation method employs a quite different approach. In this method, one relies on fast computers to simulate the sum of all possible metrics and spacetime points through a Monte-Carlo algorithm. This method is essentially non-perturbative.

- Supergravity and superstrings. Quantum gravity in these theories are better behaved with improved renormalizability due to the added supersymmetry between bosonic and fermionic degrees of freedom. They are also hoped to provide the necessary mechanisms to unify all the known forces as quantum gravity is needed in these theories (superstring) to cancel the gauge anomaly. String objects as the fundamental building blocks of matter also remove the point, local notion of the spacetime, an "unpleasant" feature of point particle quantum field theory.

- new canonical quantization of gravity proposed by Abhay Ashtekar, 1986. A new set of canonical variables are found to tremendously simplify the structure of constraints in gravity. This work supports the idea of quantum gravity being non-perturbative [13, 14].

In this thesis, the first two methods will be used to study quantum gravity. It is a general assumption that a quantum theory of gravity cannot lead to testable predictions, due to a lack of perturbative renormalizability of the Einstein-Hilbert action. Chapter 2 starts with a brief review of the fundamentals of quantum gravity

in the Lagrangian path integral approach. The action is simply taken as the Hilbert-Einstein action (without the higher derivative curvature terms of the form R^2). A weak field expansion of the theory is developed by writing the metric composed of a static flat Minkowski metric plus a weak perturbation metric. Derivation of the Feynman rules to the first loop order for pure gravity and also gravity coupled to massive scalar field is presented. Using the Feynman rules developed, we calculate the interaction potential of two massive scalar particles generated by an exchange of gravitons in a fixed four dimensional flat background. By evaluating the twelve relevant one-loop Feynman diagrams, we show that our results for the classical relativistic corrections to the potential agrees exactly with those obtained earlier by Y. Iwasaki. More interestingly we obtain a finite leading quantum correction to the potential that increases slowly with distance.

One disadvantage of the weak field expansion of quantum gravity developed in chapter 2 is that all calculated results are necessarily perturbative. However, many may argue that quantum gravity is essentially non-perturbative in nature. The only non-perturbative way to deal with quantum gravity we know so far is the simplicial formulation. This leads to the next topic of my study, simplicial gravity. In chapter 3 we develop the general formalism for performing perturbative diagrammatic expansions in the *lattice* theory of quantum gravity. We obtain the *lattice* Feynman rules for pure gravity and scalar matter field coupled to gravity to one loop order. The exact correspondence between the lattice Feynman rules and continuum Feynman rules is established. As an application, the two-dimensional conformal anomaly due to a D-component scalar field is explicitly computed in perturbation theory. The result in the small momentum limit is found to agree with those obtained by the continuum weak field theory.

While analytical results of high loop orders of quantum gravity are usually difficult to obtain in both the weak field expansion method and the diagrammatic ex-

pansion method of the lattice theory, it is much “easier" to obtain non-perturbative results by performing Monte Carlo simulations of simplicial gravity. Chapter 4 presents our studies of the properties of random Ising spins coupled to two dimensional gravity. Ising spins are placed at the vertices of a flat triangulated lattice. The background lattice is allowed to fluctuate by varying the local coordination numbers through a “link flip" operation. The resulting model exhibits a tricritical behavior, with the first order and the second order phase lines meeting at a tricritical point. The critical exponents are found to agree with those obtained by **KPZ** and in the matrix model solution. This suggests that the values of the critical exponents are directly related to the randomness of the spin system, and are not affected by gravity.

Chapter 2

On the Quantum Corrections to the Newtonian Potential

2.1 Introduction

It is generally assumed that a quantum theory of gravity cannot lead to testable predictions, due to a lack of perturbative renormalizability of the Einstein-Hilbert action [16, 17, 18, 19, 20]. Recently an interesting possibility has been raised [21] that quantitative results can be obtained in the low energy limit of quantum gravity without concerning details of the short distance behavior (renormalizability) of gravity. In this chapter we will examine this possibility by explicitly calculating the leading long distance quantum corrections to the Newtonian potential for two massive spinless particles to the order of $O(G\hbar/c^3r^3)$.

The existence of a universal long distance quantum correction to the Newtonian potential should be applicable to a wide class of gravity theories. A more general class of gravity is to have higher derivative curvature terms in the form of $\alpha R^{\mu\nu}R_{\mu\nu} + \beta R^2$ added to the pure Einstein-Hilbert theory[22]. This modification of the Lagrangian has been shown to improve the renormalizability of the theory significantly at the short distance scale, e.g. Planck scale, $l_p = (G\hbar/c^3)^{1/2}$. However, these terms do not contribute to the gravity potential at the large distance scale, and will not be considered for the present purpose. Another modification of the

theory is to have a cosmological constant added to the pure Einstein-Hilbert action. The addition of a cosmological constant would in principle complicate the perturbative treatment significantly due to the need to expand the metric in a non-flat spacetime background. In the following treatment of the quantum corrections to the Newtonian potential, we will simply assume it is zero. This assumption may be partially justified by the fact that the physical cosmological constant is measured experimentally to be vanishingly small at a large distance scale (macroscopic), and thus bears no effect on our potential calculations. It is thus sufficient to consider the action as the pure Einstein-Hilbert theory only as long as we restrict ourselves to the low energy limit (long distance scale) of the theory.

In this chapter we will explicitly show how the leading classical and quantum corrections to the static potential is obtained by evaluating a complete set of diagrams contributing to the scattering amplitude for heavy spinless particles in the low momentum transfer limit. Our results for the static potential indicate a slow increase of gravitational interactions with distance due to the quantum corrections.

2.2 One Loop Amplitudes

Before describing the calculation, it will be useful to first clarify out conventions and notation. We shall expand around the flat Minkowski space-time metric, with signature given by $\eta_{\mu\nu} = \text{diag}(1,-1,-1,-1)$. The Einstein-Hilbert action is given by

$$S_{\text{E}} = +\frac{1}{16\pi G}\int dx\,\sqrt{-g(x)}\,R(x)\,, \tag{2.2.1}$$

with $g(x) = \det(g_{\mu\nu})$ and R the scalar curvature. The presence of a non-vanishing cosmological constant will in general introduce additional momentum independent vertices. For a simplified treatment of the potential calculation, we shall assume the cosmological term is zero since it may have little effect on the quantum corrections to the gravity potential at a very large scale, as argued in the previous

section.

The quantized theory of gravity is obtained by performing the path integral integrations of all possible spacetime metric and coordinates. The path integral is given by

$$Z[g] = \int D[g(x)] e^{iS[g(x)]}. \tag{2.2.2}$$

While no analytical method is found to solved the theory exactly, perturbation theory is the method we will use in the following calculations.

In perturbation theory the metric $g_{\mu\nu}(x)$ is expanded around the flat metric $\eta_{\mu\nu}$ [19],

$$g_{\mu\nu}(x) \;=\; \eta_{\mu\nu} + \kappa\, h_{\mu\nu}(x) \tag{2.2.3}$$

with the expansion parameter $\kappa^2 = 32\pi G$. The inverse of the $g_{\mu\nu}(x)$ is given by

$$g^{\mu\nu}(x) \;=\; \eta^{\mu\nu} - \kappa\, h^{\mu\nu}(x) + \kappa^2\, h^{\mu}_{\lambda}\, h^{\lambda\nu}(x) + O(h^3). \tag{2.2.4}$$

We shall only keep the expansion to the orders of κ^2 for the one loop calculations followed. Once the action is expanded out in the graviton field $h_{\mu\nu}(x)$, the spacetime indices are then raised and lowered using the flat metric (in the following I will not make the distinction between upper and lower indices in most cases even thought they are actually raised and lowered by the background Minkowski spacetime.)

The expansion of metric determinant $g_{\mu\nu}(x)$ in terms of $h_{\mu\nu}$ is given by

$$\begin{aligned}
\sqrt{-g_{\mu\nu}(x)} &= e^{\frac{1}{2}\, Tr\, \ln(\eta_{\mu\nu} + \kappa\, h_{\mu\nu})} \\
&= 1 + \frac{\kappa}{2}(Tr(h) - \frac{\kappa}{2} Tr(h^2)\,) + \frac{\kappa}{8}(Tr(h) - \frac{\kappa}{2} Tr(h^2)\,)^2 + O(\kappa^3) \\
&= 1 + \frac{\kappa}{2}\, h^{\alpha}_{\alpha} - \frac{\kappa^2}{4}\, h^{\alpha}_{\beta}\, h^{\beta}_{\alpha} + \frac{\kappa^2}{8}\, (h^{\alpha}_{\alpha})^2 + O(\kappa^3).
\end{aligned} \tag{2.2.5}$$

The expansion of the Ricci curvature $R_{\mu\nu}$ can be determined by first noting that

$$R_{\mu\nu} = \partial_\nu \Gamma^{\lambda}_{\mu\lambda} - \partial_\lambda \Gamma^{\lambda}_{\mu\nu} + \Gamma^{\sigma}_{\mu\lambda}\, \Gamma^{\lambda}_{\nu\sigma} - \Gamma^{\sigma}_{\mu\nu}\, \Gamma^{\lambda}_{\lambda\sigma}, \tag{2.2.6}$$

where the Levi-Civita connection written in terms of the full metric $g_{\mu\nu}$ is given by

$$\begin{aligned}\Gamma^{\lambda}_{\mu\nu} &= \frac{1}{2}\, g^{\lambda\sigma}(\partial_\mu g_{\nu\sigma} + \partial_\nu g_{\mu\sigma} - \partial_\sigma g_{\mu\nu}) \\ &= \frac{1}{2}(\eta^{\lambda\sigma} - \kappa\, h^{\lambda\sigma} + \kappa^2\, h^{\lambda}_{\alpha} h^{\alpha\sigma}) \cdot \kappa\, (\partial_\mu h_{\nu\sigma} + \partial_\nu h_{\mu\sigma} - \partial_\sigma h_{\mu\nu}\,) \\ &= \frac{\kappa}{2}(\partial_\mu h^{\lambda}_{\nu} + \partial_\nu h_{\mu\lambda} - \partial^{\lambda} h_{\mu\nu}) \\ &\quad - \frac{\kappa^2}{2}\, h^{\lambda\nu}\, (\partial_\mu h_{\nu\sigma} + \partial_\nu h_{\mu\sigma} - \partial_\sigma h_{\mu\nu}) + O(h^3). \end{aligned} \tag{2.2.7}$$

Collecting the Lagrangian in powers of $h_{\mu\nu}$, we have

$$L(h^2) = \frac{1}{2}\, (h_{\rho\lambda,\sigma} h_{\rho\lambda,\sigma} - 2\, h_{\sigma\lambda,\rho} h_{\sigma\rho,\lambda} + 2\, h_{\lambda\lambda,\rho} h_{\sigma\rho,\sigma} - h_{\lambda\lambda,\rho} h_{\sigma\sigma,\rho}), \tag{2.2.8}$$

$$\begin{aligned} L(h^3) &= -\frac{\kappa}{2}\, [\, h_{\tau\tau}\{h_{\sigma\lambda,\rho} h_{\sigma\rho,\lambda} - \frac{1}{2}\, h_{\rho\lambda,\sigma} h_{\rho\lambda,\sigma} - h_{\lambda\lambda,\rho} h_{\sigma\rho,\sigma} + \frac{1}{2} h_{\lambda\lambda,\rho} h_{\sigma\sigma,\rho}\} \\ &\quad +\ h_{\mu\nu}\{h_{\rho\lambda,\mu} h_{\rho\lambda,\nu} - 2\, h_{\mu\lambda,\rho} h_{\nu\rho,\lambda} + 2\, h_{\mu\lambda,\rho} h_{\nu\lambda,\rho} + 2\, h_{\lambda\lambda,\rho} h_{\mu\rho,\nu} - 2\, h_{\lambda\lambda,\rho} h_{\mu\nu,\rho} \\ &\quad + 2\, h_{\lambda\mu,\lambda} h_{\rho\rho,\nu} - 2\, h_{\lambda\lambda,\mu} h_{\rho\rho,\nu} + 2\, h_{\lambda\rho,\lambda} h_{\mu\nu,\rho} - 4\, h_{\lambda\mu,\rho} h_{\lambda\rho,\nu}\}\,]. \end{aligned} \tag{2.2.9}$$

The theory of pure gravity describes the interactions among the graviton gauge particles. We are also interested in gravity coupled to material particles through the exchange of gravitons. The Lagrangian for scalar fields coupled to gravity is given by

$$L_{scalar} = \frac{1}{2}\sqrt{-g}\, (g^{\mu\nu}\ \partial_\mu \phi\ \partial_\nu \phi - m^2 \phi^2) \tag{2.2.10}$$

In terms of perturbed metric $h_{\mu\nu}$, L_{scalar} can be written as:

$$L(\phi^2) = \frac{1}{2}(\partial_\mu \phi \partial_\mu \phi - m^2 \phi^2), \tag{2.2.11}$$

$$L(h\phi^2) = \frac{\kappa}{2}[\, - h_{\mu\nu} \partial_\mu \phi \partial_\nu \phi + \frac{1}{2} h_{\rho\rho} (\partial_\lambda \phi \partial_\lambda \phi - m^2 \phi^2)], \tag{2.2.12}$$

$$\begin{aligned} L(h^2\phi^2) &= \frac{\kappa^2}{2}[\, h_{\mu\rho} h_{\nu\rho} \partial_\mu \phi \partial_\nu \phi - \frac{1}{2} h_{\rho\rho} h_{\mu\nu} \partial_\mu \phi \partial_\nu \phi \\ &\quad + (\frac{1}{8} h_{\rho\rho} h_{\lambda\lambda} - \frac{1}{4} h_{\rho\lambda} h_{\rho\lambda})(\partial_\rho \phi \partial_\rho \phi - m^2 \phi^2)]. \end{aligned} \tag{2.2.13}$$

The Feynman rules can be determined quite straightforwardly. The graviton propagator is given by

$$D_{\mu\nu,\alpha\beta}(p) \;=\; \frac{i}{2}\,\frac{\eta_{\mu\alpha}\eta_{\nu\beta}+\eta_{\mu\beta}\eta_{\nu\alpha}-\frac{2}{d-2}\,\eta_{\mu\nu}\eta_{\alpha\beta}}{p^2+i\varepsilon}. \tag{2.2.14}$$

It is clear from the above expression that the graviton propagator diverges in two dimensions. It simply reflects the fact that gravity does not exist in exactly two dimensions. The propagator for the scalar particle is

$$D(k) = \frac{i}{k^2-m^2}. \tag{2.2.15}$$

The interaction among scalar particles and gravitons is described by the Feynman vertices. For the scalar-scalar-graviton, we have

$$V_{\mu\nu}(k_1,k_2,q) \;=\; \frac{i\kappa}{2}\,[\eta_{\mu\nu}(k_1\cdot k_2-m^2)-k_{1\mu}k_{2\nu}-k_{1\nu}k_{2\mu}]; \tag{2.2.16}$$

for scalar-scalar-graviton-graviton vertex, we have

$$\begin{aligned} V_{\alpha\beta,\mu\nu}(k_1,k_2,q_1,q_2) \;=\; & \frac{i\kappa^2}{2}\{(\eta_{\alpha\beta}\eta_{\mu\nu}-\eta_{\alpha\mu}\eta_{\beta\nu}-\eta_{\alpha\nu}\eta_{\beta\mu})(k_1\cdot k_2-m^2) \\ & +\;\eta_{\alpha\beta}(k_{1\beta}k_{2\nu}+k_{1\nu}k_{2\beta})+\eta_{\alpha\nu}(k_{1\beta}k_{2\mu}+k_{1\mu}k_{2\beta}) \\ & +\;\eta_{\beta\mu}(k_{1\alpha}k_{2\mu}+k_{1\nu}k_{2\alpha})+\eta_{\beta\nu}(k_{1\alpha}k_{2\mu}+k_{1\mu}k_{2\alpha}) \\ & -\;\eta_{\alpha\beta}(k_{1\mu}k_{2\nu}+k_{1\nu}k_{2\mu})-\eta_{\mu\nu}(k_{1\alpha}k_{2\beta}+k_{1\beta}k_{2\alpha})\;\}. \end{aligned} \tag{2.2.17}$$

The Feynman rules developed above are well suited for many kinds of gravity perturbation calculation. (These Feynman rules will be used to compare with the lattice Feynman rules developed in chapter 3 in the lowest momentum limit.) However, in the following we shall adopt a different metric expansion method [27]. This expansion method of the metric has the advantage of having simpler Feynman rules for the tripled graviton vertex and for the two-scalar and two-graviton vertex. Let's define the small fluctuation graviton field $h_{\mu\nu}(x)$ via the expansion

$$g^{\mu\nu}(x)\sqrt{-g(x)} \;=\; \eta^{\mu\nu}+\kappa\,h^{\mu\nu}(x). \tag{2.2.18}$$

The expansion of the determinant in d-dimension is

$$\begin{aligned}\sqrt{-g(x)} &= e^{\frac{1}{d-2}Tr\,\ln(\eta_{\alpha\beta}+\kappa\, h_{\alpha\beta})} \\ &= 1+\frac{\kappa}{d-2}\,h^{\alpha}_{\alpha}-\frac{\kappa^2}{2(d-2)}h^{\alpha}_{\beta}\,h^{\beta}_{\alpha}+\frac{\kappa^2}{2(d-2)^2}\,(h^{\alpha}_{\alpha})^2+O(h^3). \qquad (2.2.19)\end{aligned}$$

The expansion of the scalar curvature can be performed similary. Collecting the Lagrangian in powers of $h_{\mu\nu}$, we have

$$L(h^2)=\frac{1}{2}\partial_\mu h_{\nu\lambda}\;\partial_\mu h_{\nu\lambda}-\frac{1}{2(d-2)}\;\partial_\mu h_{\nu\nu}\;\partial_\mu h_{\rho\rho}-\partial_\mu h_{\mu\nu}\;\partial_\rho h_{\rho\nu}, \qquad (2.2.20)$$

$$\begin{aligned}L(h^3) &= \frac{\kappa}{2}h_{\sigma\rho}(\partial_\rho h_{\mu\kappa}\partial_\sigma h_{\mu\kappa}-\frac{1}{d-2}\partial_\rho h_{\mu\mu}\;\partial_\sigma h_{\nu\nu}) \\ &+\;\kappa\, h_{\mu\tau}(\partial_\tau h_{\mu\sigma}\partial_\sigma h_{\lambda\tau}-\partial_\rho h_{\mu\kappa}\;\partial_\rho h_{\tau\kappa}+\frac{1}{d-2}\partial_\rho h_{\mu\tau}\partial_\rho h_{\nu\nu}). \qquad (2.2.21)\end{aligned}$$

The Lagrangian describing the coupling of gravity to scalar particles with mass m is the same as before, eq. (2. 2. 10). Its series expansion in terms of the perturbed metric $h_{\mu\nu}$ via. the new expansion method is

$$L(\phi^2 h)=\frac{\kappa}{2}(\;h^{\mu\nu}\;\partial_\mu\phi\;\partial_\nu\phi-\frac{1}{d-2}m^2\;h^{\mu}_{\mu}\;\phi^2), \qquad (2.2.22)$$

$$L(\phi^2h^2)=-\frac{\kappa^2}{2}m^2\phi^2\;(-\frac{1}{2(d-2)}h^{\alpha}_{\beta}\;h^{\beta}_{\alpha}+\frac{1}{2(d-2)^2}(h^{\mu}_{\mu})^2). \qquad (2.2.23)$$

One can again extract the Feynman rules in a similar fashion. It is convenient to keep the Feynman rule expressions in d dimensions. This becomes necessary when dimensional regularization is used in $4-\varepsilon$ dimensions. The graviton propagator is simply given by

$$D_{\alpha\beta,\mu\nu}(p) \;=\; \frac{i}{2}\;\frac{\eta_{\alpha\mu}\eta_{\beta\nu}+\eta_{\alpha\nu}\eta_{\beta\mu}-\eta_{\alpha\beta}\eta_{\mu\nu}}{p^2}. \qquad (2.2.24)$$

Note that the graviton propagator is well defined in any dimensions in this expansion method. However, the interaction vertices of gravitons will involve with coefficients of $1/\,(d-2)$, which become divergent in two dimensions.

The scalar particle propagator is the same as before

$$D_(p) = \frac{i}{p^2 - m^2}. \tag{2.2.25}$$

The two scalar-one graviton vertex is given by

$$V_{\mu\nu}(p_1, p_2) = \frac{i\kappa}{2}\left(p_{1\mu}p_{2\nu} + p_{1\nu}p_{2\mu} - \frac{2}{d-2}\, m^2\, \eta_{\mu\nu}\right). \tag{2.2.26}$$

The two scalar-two graviton vertex is given by

$$V_{\mu\nu,\rho\sigma} = \frac{i\kappa^2 m^2}{2(d-2)}\left(\eta_{\mu\lambda}\eta_{\nu\sigma} + \eta_{\mu\sigma}\eta_{\nu\lambda} - \frac{2}{d-2}\, \eta_{\mu\nu}\eta_{\lambda\sigma}\right), \tag{2.2.27}$$

where one pair of indices (μ, ν) is associated with one graviton line, and the other pair (λ, σ) is associated with the second graviton line. The three-graviton vertex $V_{\alpha_1\beta_1,\alpha_2\beta_2,\alpha_3\beta_3}(q^1, q^2, q^3)$ is given by

$$\begin{aligned}
V(q^1, q^2, q^3) \;=\; & -\frac{i\kappa}{2}[q^2_{(\alpha_1} q^3_{\beta_1)}\,(2\,\eta_{\alpha_2(\alpha_3}\eta_{\beta_3)\beta_2} - \frac{2}{d-2}\,\eta_{\alpha_2(\beta_2}\,\eta_{\alpha_3)\beta_3}) \\
& +\; q^1_{(\alpha_2} q^3_{\beta_2)}\,(2\,\eta_{\alpha_1(\alpha_3}\eta_{\beta_3)\beta_1} - \frac{2}{d-2}\,\eta_{\alpha_1(\beta_1}\,\eta_{\alpha_3)\beta_3}) \\
& + q^1_{(\alpha_3} q^2_{\beta_3)}\,(2\,\eta_{\alpha_1(\alpha_2}\eta_{\beta_2)\beta_1} - \frac{2}{d-2}\,\eta_{\alpha_1(\beta_1}\,\eta_{\alpha_2)\beta_2}) \\
& +\; 2\, q^3_{(\alpha_2}\eta_{\beta_2)(\alpha_1}\eta_{\beta_1)(\alpha_3} q^2_{\beta_3)} + 2\, q^1_{(\alpha_3}\eta_{\beta_3)(\alpha_2}\eta_{\beta_2)(\alpha_1} q^3_{\beta_1)} \\
& +\; 2\, q^2_{(\alpha_1}\eta_{\beta_1)(\alpha_3}\eta_{\beta_3)(\alpha_2} q^1_{\beta_2)}) + q^2\cdot q^3\,(\frac{2}{d-2}\,\eta_{\alpha_1(\alpha_2}\eta_{\beta_2)\beta_1}\eta_{\alpha_3\beta_3} \\
& +\; \frac{2}{d-2}\,\eta_{\alpha_1(\alpha_3}\eta_{\beta_3)\beta_1}\eta_{\alpha_2\beta_2} - 2\,\eta_{\alpha_1(\alpha_2}\eta_{\beta_2)(\alpha_3}\eta_{\beta_3)\beta_1}) \\
& +\; q^1\cdot q^3\,(\frac{2}{d-2}\,\eta_{\alpha_2(\alpha_1}\eta_{\beta_1)\beta_2}\eta_{\alpha_3\beta_3} + \frac{2}{d-2}\,\eta_{\alpha_2(\alpha_3}\eta_{\beta_3)\beta_2}\eta_{\alpha_1\beta_1} \\
& -\; 2\,\eta_{\alpha_2(\alpha_1}\eta_{\beta_1)(\alpha_3}\eta_{\beta_3)\beta_2}) + q^1\cdot q^2\,(\frac{2}{d-2}\,\eta_{\alpha_3(\alpha_1}\eta_{\beta_1)\beta_3}\eta_{\alpha_2\beta_2} \\
& +\; \frac{2}{d-2}\,\eta_{\alpha_3(\alpha_2}\eta_{\beta_2)\beta_3}\eta_{\alpha_1\beta_1} - 2\,\eta_{\alpha_3(\alpha_1}\eta_{\beta_1)(\alpha_2}\eta_{\beta_2)\beta_3})\,].
\end{aligned} \tag{2.2.28}$$

A gauge fixing term [28, 29] has to be introduced to give raise to the Feddev-Popov ghost fields, and it has the form

$$\frac{1}{\kappa^2}\left(\partial_\mu\sqrt{-g(x)}g^{\mu\nu}\right)^2. \tag{2.2.29}$$

The ghost Lagrangian is

$$L_{ghost} = \xi_\nu[\eta_{\nu\lambda}\,\partial_\alpha\partial^\alpha - \kappa(h_{\mu\nu,\lambda\mu} - h_{\mu\rho}\eta_{\nu\lambda}\,\partial_\mu\partial_\rho - h_{\mu\rho,\mu}\,\eta_{\nu\lambda}\,\partial_\rho + h_{\mu\nu,\mu}\,\partial_\lambda)\ ]\ \xi_\lambda\,. \tag{2.2.30}$$

The propagator for the ghost is

$$D_{\mu\nu}(p) = \frac{i\eta_{\mu\nu}}{p^2}. \tag{2.2.31}$$

The ghost-ghost-graviton vertex is

$$V_{\lambda,\mu,\alpha\beta} = i\kappa[\,-\eta_{\lambda(\alpha}k_{1\beta)}k_{2\mu} + \eta_{\lambda(\mu}k_{2\alpha)}k_{3\beta}]. \tag{2.2.32}$$

To lowest order in G, the contribution to the potential from the single graviton exchange diagram can be computed easily. In momentum space the static potential is obtained as

$$-G\ m_1\ m_2\ \frac{4\pi}{\tilde{q}^2} \tag{2.2.33}$$

where $\tilde{q}$ is the momentum transfer (see also [30]). It is simply the familiar Newtonian gravity potential, as expected.

Higher order corrections in G are computed by evaluating contributions to the interaction coming from the complete set of one-loop diagrams, Figs. 2.1, 2.2. One notices that the relevant length scale appearing with the Einstein-Hilbert action for pure gravity is the Planck length $l_p = (G\hbar/\,c^3)^{1/2}$. On the other hand the action for the scalar particle involves only the combination $mc/\,\hbar$, the inverse Compton wavelength associated with the heavy sources. This is also clearly seen from the path integral phase contribution for a single particle, which is given by

$$\frac{imc^2}{\hbar}\int_{\tau(a)}^{\tau(b)} d\tau\sqrt{g_{\mu\nu}(x(\tau))\frac{dx^\mu}{d\tau}\frac{dx^\nu}{d\tau}}\ \ , \tag{2.2.34}$$

When one considers the lowest order contribution to the gravitational interaction due to single graviton exchange one obtains a contribution to the static gravitational potential proportional to $(\hbar/\,c)(mc^2/\,\hbar)^2(G\hbar/\,c^3) = m^2G$. At order G^2 one finds

contributions both of order $(\hbar / c)(mc^2 / \hbar)^2(G\hbar / c^3)^2 = m^2\hbar G^2 / c^3$ and of order $(\hbar / c)(mc^2 / \hbar)^3(G\hbar / c^3)^2 = m^3G^2 / c$. The first one represents a genuine quantum correction proportional to $\hbar$, while in the second type of contribution the $\hbar$'s have canceled, and the resulting correction represents a classical relativistic correction. The latter involves the Schwarzschild radius of the massive particle, $2Gm / c^2$.

These considerations lead us to believe that Feynman diagram perturbation theory should be able to reproduce the classical relativistic corrections, which are independent of $\hbar$. And indeed it is shown by the authors of Ref. [31, 32] that classical relativistic corrections can be obtained by considering the tree graphs connected to an arbitrarily high number of external classical sources. Calculation of these classical relativistic corrections is performed in Ref. [33] using the diagrammatic method. In the paper, by explicitly evaluating the scattering amplitude of two massive scalar particles, Iwasaki is able to show that the corrections of order G^2 correctly and completely reproduce the leading classical relativistic corrections appearing in the Einstein-Hoffmann-Infeld effective post-Newtonian Hamiltonian.

The remaining of this chapter will be focused on the computation of the one loop scattering amplitude. By including a complete set of one loop diagrams, we will be able to calculate all first-order corrections in G, which will include both the classical relativistic $O(G^2m^2/c^2)$ and the quantum mechanical $O(\hbar G^2/c^3)$ corrections to the classical Newtonian potential energy. The classical relativistic in potential will be identical to those obtained by Iwasaki. The relevant topologically distinct Feynman diagrams are shown in Figs. 2.1 and 2.2.

In the following we will first compute the relevant amplitudes in momentum space as a function of the total momentum transfer squared $\tilde{q}^2$. They are then evaluated using dimensional regularization in $4-\varepsilon$ dimensions, using the Feynman parametric representation for combining propagator denominators. For small $\tilde{q}^2$ the contributions arising from each diagram can be separated into two types of

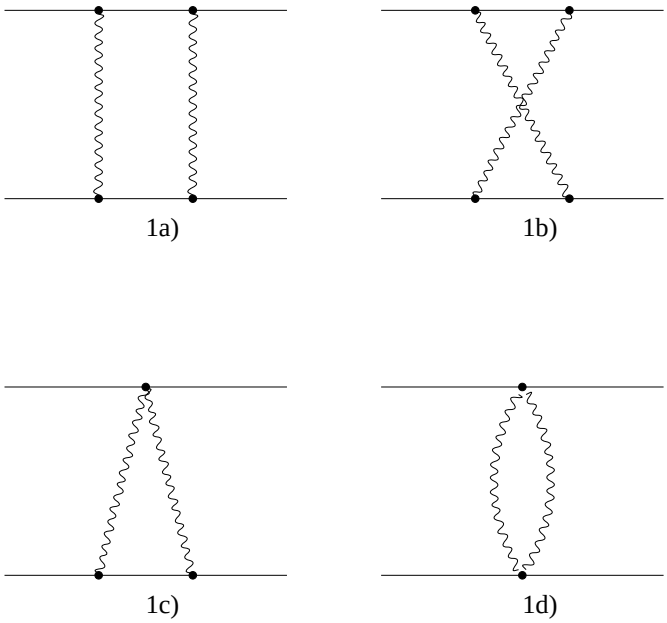

Figure 2.1: Some one loop graviton exchange diagrams.

terms, one describing the classical relativistic correction proportional to $1/\sqrt{\tilde{q}^2}$, and the other describing the leading quantum correction proportional to $\log \tilde{q}^2$. The final answer to the Newtonian potential is then obtained by performing the necessary momentum and parametric integrations. In our calculations, due to the vast amount of algebraic manipulations involved in doing the index contractions, computer algebra was employed throughout the calculation in order to ensure the correctness of the results.

Transformation from the momentum space to the usual coordinate space can be done with the help of the following equations

$$\int \frac{d^3\tilde{q}}{(2\pi)^3} e^{-i\tilde{q}\cdot\tilde{x}} \frac{1}{\tilde{q}^2} \to \frac{1}{4\pi r}\,. \tag{2.2.35}$$

$$\int \frac{d^3\tilde{q}}{(2\pi)^3} e^{-i\tilde{q}\cdot\tilde{x}} \frac{1}{\sqrt{\tilde{q}^2}} \to \frac{1}{2\pi r^2}\,. \tag{2.2.36}$$

$$\int \frac{d^3\tilde{q}}{(2\pi)^3} e^{-i\tilde{q}\cdot\tilde{x}} \log \tilde{q}^2 \to -\frac{1}{2\pi r^3}\,. \tag{2.2.37}$$

A nontrivial check of the calculation is provided by the expected equality, for each diagram involving massless particles only, of the coefficient of the $2/\,\varepsilon$ ultraviolet divergence and of the coefficient of the $-\log\tilde{q}^2$ contribution, which would appear as one single logarithmic term $\log\,(\Lambda^2/\,\tilde{q}^2)$ in the presence of an explicit ultraviolet cutoff Λ.

2.3 Results and Discussion

After converting the expressions for the individual diagrams to coordinate space, one obtains the following results. One has the Newtonian potential correction from Figs. 2.1, diagram 1a

$$+\frac{3}{4}\,G^2\,\frac{m_1m_2(m_1+m_2)}{r^2}+2\,G^2\,\frac{m_1m_2}{\pi r^3}, \tag{2.3.38}$$

from diagram 1b

$$+\frac{3}{4}\,G^2\,\frac{m_1m_2(m_1+m_2)}{r^2}+2\,G^2\,\frac{m_1m_2}{\pi r^3}, \tag{2.3.39}$$

from diagram 1c

$$-\,G^2\,\frac{m_1m_2(m_1+m_2)}{r^2}+8\,G^2\,\frac{m_1m_2}{\pi r^3}, \tag{2.3.40}$$

from diagram 1d

$$-10\,G^2\,\frac{m_1m_2}{\pi r^3}, \tag{2.3.41}$$

from Figs. 2.2, diagram 2b

$$+\frac{16}{3}\,G^2\,\frac{m_1m_2}{\pi r^3}, \tag{2.3.42}$$

and from diagram 2d

$$+\frac{23}{3}\,G^2\,\frac{m_1m_2}{\pi r^3}. \tag{2.3.43}$$

From diagrams 2e and 2g one obtains the graviton and ghost vacuum polarization contribution

$$-\frac{206}{30}\,G^2\,\frac{m_1m_2}{\pi r^3}. \tag{2.3.44}$$

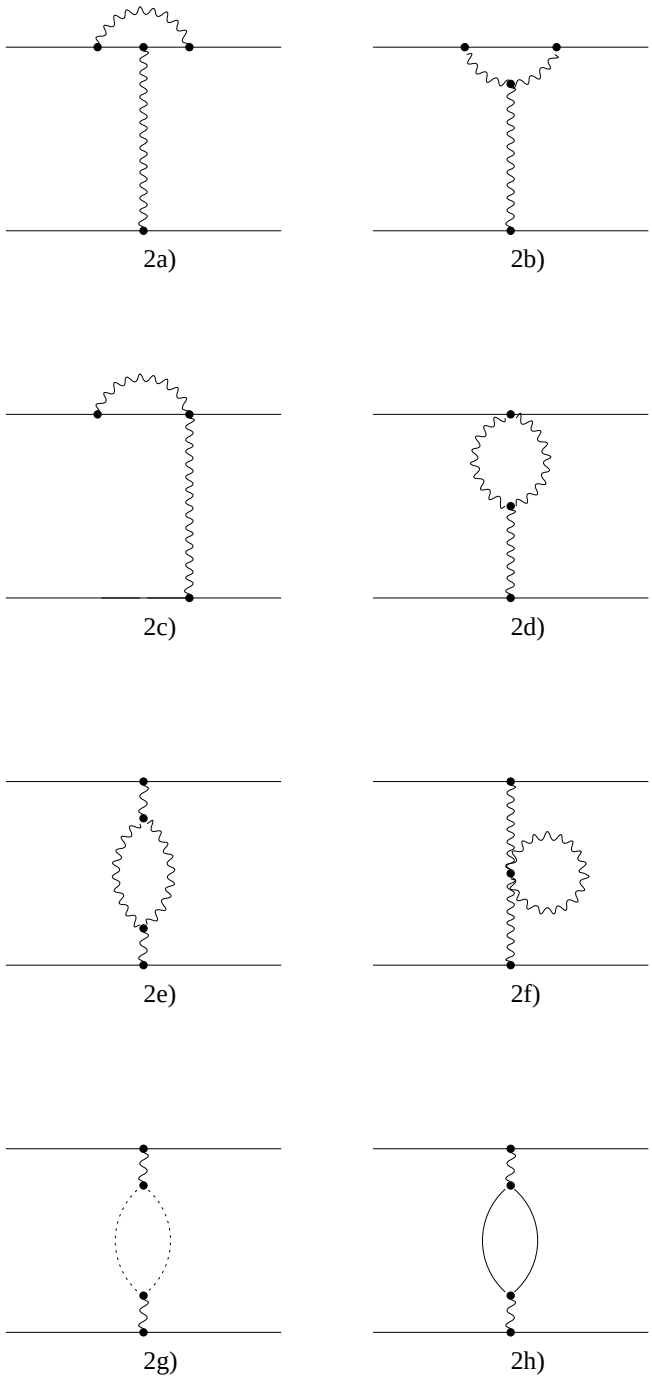

Figure 2.2: Additional one loop graviton exchange diagrams.

This last contribution was also computed in Ref. [27]. We have verified that the Slavnov-Taylor identity for the vacuum polarization $\Pi_{\alpha\beta\gamma\delta}(q)$,

$$q_\mu q_\nu \, D_{\mu\lambda\alpha\beta}(q) \, \Pi_{\alpha\beta\gamma\delta}(q) \, D_{\gamma\delta\nu\sigma}(q) \; = 0 \tag{2.3.45}$$

is indeed satisfied to this order. In Ref. [19] the vacuum polarization was computed using a somewhat different expansion for the metric field, and a coordinate invariant expression for the one-loop counterterms was given in terms of operators quadratic in the curvature.

Diagram 2h represents the contribution to the vacuum polarization due to one *massless* scalar particle,

$$-\frac{1}{20} \, G^2 \, \frac{m_1 m_2}{\pi r^3}. \tag{2.3.46}$$

Its contribution to the vacuum polarization satisfies separately the Slavnov-Taylor identity, as one would expect from the covariant conservation law for the energy-momentum tensor associated with matter. Explicit calculations of diagrams 2a and 2c show that they do not give any correction terms in the form of $1/\sqrt{\tilde{q}^2}$ and $\log \tilde{q}^2$, and thus give no rise to any classical relativistic or quantum correction. Diagram 2f vanishes identically in dimensional regularization. Diagrams 2b, 2d, 2e, 2g and 2h give only quantum mechanical corrections, involving closed graviton loops in all cases, except 2b.

The sum of all contributions from diagrams 1a to 2g is therefore

$$+\frac{1}{2} \, G^2 \, \frac{m_1 m_2 (m_1 + m_2)}{r^2} + \frac{122}{15} \, G^2 \, \frac{m_1 m_2}{\pi r^3}. \tag{2.3.47}$$

The contribution of n species of massless scalar particles to the vacuum polarization (arising from diagram 2h) changes the quantum correction to the potential to

$$+\frac{1}{60}(488 - 3n) \, G^2 \, \frac{m_1 m_2}{\pi r^3}, \tag{2.3.48}$$

which represents a relatively small modification to the result for pure gravity if n is small. Massless particles of higher spin will contribute additional terms to the vacuum polarization.

Putting back in the appropriate powers of c and $\hbar$, one obtains the following final answer for the corrected potential in pure gravity, valid to order G^2

$$V(r) = -G\frac{m_1 m_2}{r}\left[1 - \frac{G(m_1+m_2)}{2c^2 r} - \frac{122G\hbar}{15\pi c^3 r^2}\right]. \tag{2.3.49}$$

Two very different length scales enter in the correction to the static Newtonian potential, namely the Schwarzschild radii of the heavy sources, $2Gm_i/c^2$, and the Planck length $(G\hbar/c^3)^{1/2}$. As a consequence there are two independent dimensionless parameters that appear in the correction term, involving the ratio of these two scales with respect to the distance r. Presumably the above calculation is meaningful only if these two length scales are much smaller than the distance r.

Similar calculations have been performed in the work of Ref. [21]. There the starting point is to calculate the scattering amplitude in the limit of small momentum transfer. The potential is defined as the non-relativistic limit of the one particle reducible graphs in the crossed channel, which represents therefore a subset of the graphs considered here. We should point out that the results we obtain are in complete agreement with the expected classical relativistic correction, as derived for example from the expansion of the Schwarzschild metric [35]. The sign of the quantum correction of our result is found to be the same as in Ref. [21], and the magnitude of the correction is comparable. The sign of the quantum correction we obtain indicate that gravitational interactions increase (slowly) with distance, which shows similarities with the evolution of the coupling constant in pure Yang-Mills theories, but differs in sign from the QED radiative corrections to the static Coulomb potential. This result is also in agreement with the intuitive expectation that gravity couples universally to all forms of energy, and cannot be easily screened by quantum fluctuations.

Recently the authors of Ref. [25] have computed the corrections to the static Newtonian potential following the method of Ref. [49], thus extending to the next order in G the calculation of Ref. [50]. In their work the radiative corrections to the

potential are obtained by considering correlations between the action contributions from two heavy particle world lines, separated by a fixed geodesic distance. The results they obtain appear to correctly reproduce the classical relativistic correction, but arise from only a subset of two diagrams among the four which lead to the classical correction in Ref. [33]. In this last reference the ladder and crossed ladder diagrams give, using the same metric expansion, additional contributions which appear to be necessary in order to obtain the correct classical relativistic correction. These diagrams involve recoil of the massive particles, and have been neglected in the calculation of Ref. [25]. In our calculation we find that ladder and crossed ladder diagrams (1a and 1b), when carefully treated, contribute to the quantum correction. This probably explains why our results and the results of Ref. [25] differ in both sign and magnitude for the quantum correction.

It is unclear at present if higher loop order corrections in G can still lead to finite corrections in the long distance limit. Whether higher derivative terms or string theory is needed to control the ultraviolet divergences appearing at higher loops remains an open question [38]. There is also an issue of the non-perturbative definition of the Euclidean path integral for quantum gravity, which suffers from the problem of the unbounded fluctuations in the conformal mode, and for which an integration over complex conformal factors has been suggested, followed by an integration over conformal equivalence classes of metrics. In the framework of perturbation theory we did not have to deal with these difficult problems.

Chapter 3

Feynman Rules in Simplicial Quantum Gravity

3.1 Introduction

In the quantization of gravitational interactions one expects non-perturbative effects to play an important role. One formulation available for studying such effects is Regge's simplicial lattice theory of gravity [39]. It is the only lattice model with a local gauge invariance [40], and the only model known to contain gravitons in four dimensions [41]. A number of fundamental issues in quantum gravity, such as the existence of non-trivial ultraviolet fixed points of the renormalization group in four dimensions and the recovery of general relativity at large distances, can in principle be addressed in such a model. The presence of a local gauge invariance, which is analogous to the diffeomorphism group in the continuum, makes the model attractive as a regulated theory of gravity [42], while the existence of a phase transition in three and four dimensions [43, 44, 45, 46] (but not in two [47, 48]) suggests the existence of a (somewhat unusual) lattice continuum limit. A detailed discussion of the properties of the two phases characterizing four-dimensional gravity, and of the associated critical exponents, can be found in [45]. Recently calculations have progressed to the point that a first calculation of the

Newtonian potential from the correlation of heavy particle world lines, following the proposal of [49], has become feasible [50]. These results indicate that in the lattice quantum theory the potential is indeed attractive, and has the correct heavy mass dependence. In the same work a general scaling theory for gravitational correlations, valid in the vicinity of the fixed point, was put forward.

In view of this recent progress it would appear desirable to further elucidate the correspondence between continuum and lattice theories. The weak field expansion is available to systematically develop this correspondence, and it is well known that such an expansion can be carried out in both formulations. Not unexpectedly, it is technically somewhat more complex in the lattice theory due to the presence of additional vertices, as happens in ordinary lattice gauge theories. In the past most perturbative studies of lattice gravity have focused on the lowest order terms, and in particular the lattice graviton propagators [41, 47, 51]. As such, these did not probe directly important, genuinely quantum-mechanical, aspects of the theory. A systematic weak field expansion is generally useful, since it allows one in principle to determine subleading lattice corrections to the continuum results, which can be relevant in the analysis of the numerical non-perturbative results in the full theory.

More importantly, the weak field expansion can be used to compare with known results in the continuum, and some are known in two dimensions [94, 53]. A related motivation comes from trying to understand the recently discovered discrepancy between the critical exponents for matter coupled to gravity in two dimensions as computed in the lattice regularized model for gravity [83, 55], and the corresponding conformal field theory predictions [82, 57]. Particularly significant in this respect appears to be the recent realization that the conformal field theory exponents describe two-dimensional random systems in *flat* space, and do not correspond to "gravitational" dressing of correlators [59, 60].

The plan of this chapter is as follows. We shall first introduce our notation and

describe the gravitational action, including matter fields. We will limit our discussion mostly to the two-dimensional case, although it can be easily generalized to higher dimensions. The subsequent sections will then be devoted to the systematic development of the lattice weak field expansion. The results presented here will help elucidate the correspondence between the lattice and continuum theories, and bring out the role of local gauge invariance in the lattice theory. We will develop the Feynman rules for gravity coupled to a scalar field, and as an application compute the conformal anomaly in two dimensions.

3.2 The Discretized Theory

In this section we shall briefly review the construction of the action describing the gravitational field on the lattice, and use the occasion to define the notation used later in the chapter. In concrete examples we will often refer, because of its simplicity, to the two-dimensional case, where a number of results can be derived easily and transparently. In a number of instances though important aspects of the discussion will be quite general, and not restricted to specific aspects of the two-dimensional case.

It is well known that in two dimensions quantum gravity can be defined on a two-dimensional surface consisting of a network of flat triangles. The underlying lattice may be constructed in a number of ways. Points may be distributed randomly on the surface and then joined to form triangles according to some algorithm. An alternative procedure is to start with a regular lattice, like a tessellation of the two sphere or a lattice of squares divided into triangles by drawing in parallel sets of diagonals, and then allow the edge lengths to vary, which will introduce curvature localized on the vertices. For arbitrary assignments of edge lengths, consistent with the imposition of the triangle inequalities constraints, such a lattice is

in general far from regular, and resembles more a random lattice. In the following though we will narrow down the discussion, and think of the "regular" lattice as consisting of a network of triangles with a fixed coordination number of six, although many of the results in this work are expected to be quite general and should not depend significantly on the specific choice of local coordination numbers.

The elementary degrees of freedom on the lattice are the edge lengths, with the correspondence between continuum and lattice degrees of freedom given locally by

$$\{g_{\mu\nu}(x)\}_{x\varepsilon\mathcal{M}} \to \left\{l_i^2\right\}_{i=1\ldots N_1} \quad , \tag{3.2.1}$$

where the index i ranges over all N_1 edges in the lattice. From the well known relationship between the induced metric in a simplex and its squared edge lengths,

$$g_{ij}(l^2) = \tfrac{1}{2}\left[l_{0i}^2 + l_{0j}^2 - l_{ij}^2\right] \quad . \tag{3.2.2}$$

one then has the essentially unique functional measure contribution

$$\int \prod_x dg_{\mu\nu}(x) \quad \to \quad \int_0^\infty \prod_i dl_i^2 \quad , \tag{3.2.3}$$

supplemented by the additional constraint that the triangle inequalities be satisfied for all quantum fluctuations of the edge lengths [40]. Both the continuum metric and the lattice edge lengths imply some redundancy due to local gauge invariance of the action, which therefore requires gauge-fixing when performing perturbation theory due to the presence of the exact gauge zero modes [41] (the triangle inequalities, which violate gauge invariance by imposing a cutoff on the gauge orbits, are in fact not seen to *any* order in the weak field expansion). [1] A gauge fixing term is not required in non-perturbative studies, since the contributions from the gauge zero modes are expected to cancel exactly between numerator and denominator in the functional integral for observables, as discussed for example in [42].

[1] A small breaking of gauge invariance causes well known problems in perturbation theory. There are rather convincing arguments that this is not necessarily the case non-perturbatively, if the breaking can be considered small [62, 63], as in the present case

For a given action, the dynamics of the lattice will give rise to some average lattice spacing $a_0 = [\langle l^2 \rangle]^{\frac{1}{2}}$, which in turn will supply the ultraviolet cutoff needed to define the quantum theory. It should be stressed that in the following we shall restrict our attention to the *lattice* theory, which is defined in terms of its lattice degrees of freedom *only*. Since it is our purpose to describe an ultraviolet regulated theory of quantum gravity, we shall follow the usual procedure adopted when discussing lattice field theories, and describe, in the spirit of Regge's original idea, the model exclusively in terms of its primary, lattice degrees of freedom: the squared edge lengths. As such, the theory does not require any additional *ad-hoc* regulators for defining conical singularities, for example.

3.2.1 Curvature and Discretized Action

In simplicial gravity the curvature is concentrated on the hinges, which are subspaces of dimensions $d-2$, and is entirely determined from the assignment of the edge lengths. In two dimensions the hinges correspond to the vertices, and δ_h, the deficit angle at a hinge, is defined by

$$\delta_h = 2\pi - \sum_{\substack{\text{triangles } t \\ \text{meeting at h}}} \theta_t \quad , \tag{3.2.4}$$

where θ_t is the dihedral angle associated with the triangle t at the vertex h (see Figs. 3.1). In d dimensions several d-simplexes meet on a $(d-2)$-dimensional hinge, with the deficit angle defined by

$$\delta_h(l^2) = 2\pi - \sum_{\substack{\text{d-simplexes} \\ \text{meeting on h}}} \theta_d(l^2) \quad . \tag{3.2.5}$$

Useful formulas for the cosine of the dihedral angles can be found in [43]. In two dimensions the dihedral angle is obtained from

$$\cos\theta_d = \frac{l_{01}^2 + l_{02}^2 - l_{12}^2}{2 l_{01} l_{02}} \quad . \tag{3.2.6}$$

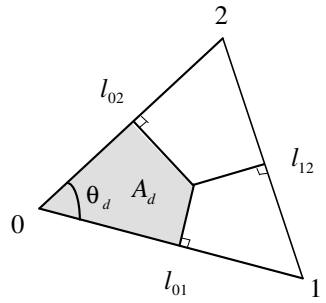

Figure 3.1: Dual area A_d associated with vertex 0, and the corresponding dihedral angle θ_d.

(for the labeling see Figs. 3.1).

It is useful to introduce a dual lattice following, for example, the *Dirichlet-Voronoi* cell construction (see [64, 65] and references therein), which consists in introducing perpendicular bisectors in each triangle and joining the resulting vertices. It provides for a natural subdivision of the original lattice in a set of non-overlapping exhaustive cells (see Figs. 3.2), and furthermore has a natural generalization to higher dimensions.

The vertices of the original lattice then reside on circumscribed circles, centered on the vertices of the dual lattice. For the vertex 0 the dihedral dual volume contribution is given by

$$A_d(l^2) = \frac{1}{16A}\left[l_{12}^2(l_{01}^2 + l_{02}^2) - (l_{01}^2 - l_{02}^2)^2\right] \quad . \tag{3.2.7}$$

It should be pointed out that the above subdivision is not unique. Alternatively, one can introduce a *baricenter* for each triangle, defined as the point equidistant from all three vertices, and again join the resulting vertices. The baricentric dihedral volume is given simply by

$$A_d(l^2) = A/3 \quad . \tag{3.2.8}$$

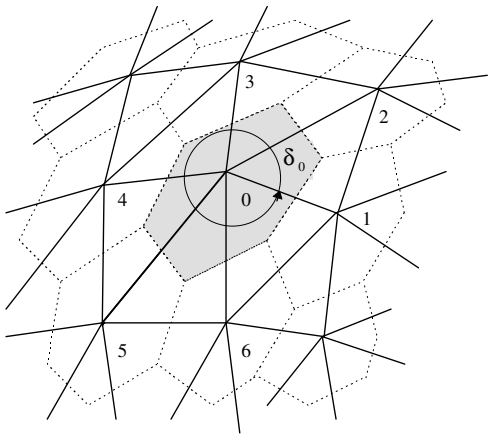

Figure 3.2: Original simplicial lattice (continuous lines) and dual lattice (dotted lines) in two dimensions. The shaded region corresponds to the dual area associated with vertex 0.

For the baricentric subdivision one then has simply

$$A_h = \tfrac{1}{3} \sum_{\substack{\text{triangles t} \\ \text{meeting at h}}} A_t \quad . \tag{3.2.9}$$

A_h can also be taken to be the area of the cell surrounding h in the dual lattice, with

$$A_h = \sum_{\substack{\text{triangles t} \\ \text{meeting at h}}} A_d \quad , \tag{3.2.10}$$

with the dual area contribution for each triangle A_d given in Eq. (3.2.7). In general, if the original lattice has local coordination number q_i at the site i, then the dual cell centered on i will have q_i faces. A fairly complete set of formulae for dual volumes relevant for lattice gravity and their derivation can be found in [43]. In the following we shall refer to the Voronoi cell construction as the "*dual subdivision*", while we will call the baricentric cell construction the "*baricentric subdivision*".

It is well known that two-dimensional Einstein gravity is trivial because the Einstein action is constant and the Ricci tensor vanishes identically. When a cos-

mological constant term and a curvature-squared term are included in the action,

$$I = \int d^2x \sqrt{g} \left[\lambda - kR + aR^2 \right] \ , \tag{3.2.11}$$

the classical solutions have constant curvature with $R = \pm\sqrt{\lambda / a}$ (there being no real solutions for $\lambda < 0$). The theory with the Einstein action and a cosmological constant is metrically trivial, having neither dynamical degrees of freedom nor field equations, although non-trivial interactions can arise from the functional measure. The lattice action corresponding to pure gravity is

$$I(l^2) = \sum_h A_h \left[\lambda - 2k R_h + a R_h^2 \right] \ , \tag{3.2.12}$$

with local volume element A_h and the local curvature given by $R_h = 2\delta_h / A_h$. In the limit of small fluctuations around a smooth background, $I(l^2)$ corresponds to the above continuum action [47]. For a manifold of fixed topology the term proportional to k can be dropped, since $\sum_h \delta_h = 2\pi\chi$, where χ is the Euler characteristic. The curvature-squared leads to non-trivial interactions in two dimensions, although the resulting theory is not unitary.

A number of results have been obtained from the above pure gravitational action. Arguments based on perturbation theory about two dimensions (where the gravitational coupling is dimensionless and the Einstein theory becomes renormalizable) suggest that there should be no non-trivial ultraviolet fixed point of the renormalization group in two dimensions. Explicit calculations in the lattice theory have shown conclusively that this is indeed the case in the absence of matter [47, 83, 48], as well as in the presence of scalar matter for a sufficiently small number of components [66].

3.2.2 Scalar Field

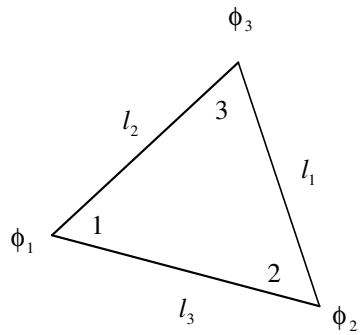

Figure 3.3: Labeling of edges and scalar fields used in the construction of the scalar field action.

A scalar field can be introduced, as the simplest type of dynamical matter that can be coupled to the gravitational degrees of freedom. The continuum action is

$$I[g,\phi] = \tfrac{1}{2}\int d^2x\,\sqrt{g}\,[\,g^{\mu\nu}\,\partial_\mu\phi\,\partial_\nu\phi + (m^2+\xi R)\phi^2]\ , \tag{3.2.13}$$

The dimensionless coupling ξ is arbitrary. Two special cases are the minimal ($\xi = 0$) and the conformal ($\xi = \frac{1}{6}$) coupling case; in the following we will mostly consider the case $\xi = 0$.

On the lattice consider a scalar ϕ_i and define this field at the vertices of the simplexes. The corresponding lattice action can be obtained through the usual procedure which replaces the original continuum metric with the induced metric on the lattice, written in terms of the edge lengths [41, 51]. Here we shall consider only the two-dimensional case; the generalization to higher dimensions is straightforward. It is convenient to use the notation of Figs. 3.3, which will bring out more readily the symmetries of the resulting lattice action. Here coordinates will be picked in each triangle along the (1,2) and (1,3) directions.

To construct the scalar lattice action, one performs in two dimensions the re-

placement

$$g_{\mu\nu}(x) \longrightarrow g_{ij}(\Delta) = \begin{pmatrix} l_3^2 & \frac{1}{2}(-l_1^2+l_2^2+l_3^2) \\ \frac{1}{2}(-l_1^2+l_2^2+l_3^2) & l_2^2 \end{pmatrix} \quad , \tag{3.2.14}$$

which then gives

$$\det g_{\mu\nu}(x) \longrightarrow \det g_{ij}(\Delta) = \tfrac{1}{4}\left\{2(l_1^2l_2^2+l_2^2l_3^2+l_3^2l_1^2) - l_1^4 - l_2^4 - l_3^4\right\} \equiv 4A_\Delta^2 \quad , \tag{3.2.15}$$

and also

$$g^{\mu\nu}(x) \longrightarrow g^{ij}(\Delta) = \frac{1}{\det g(\Delta)} \begin{pmatrix} l_2^2 & \frac{1}{2}(l_1^2-l_2^2-l_3^2) \\ \frac{1}{2}(l_1^2-l_2^2-l_3^2) & l_3^2 \end{pmatrix} \quad . \tag{3.2.16}$$

For the scalar field derivatives one writes [67, 68]

$$\partial_\mu\phi\,\partial_\nu\phi \longrightarrow \Delta_i\phi\Delta_j\phi = \begin{pmatrix} (\phi_2-\phi_1)^2 & (\phi_2-\phi_1)(\phi_3-\phi_1) \\ (\phi_2-\phi_1)(\phi_3-\phi_1) & (\phi_3-\phi_1)^2 \end{pmatrix} \quad , \tag{3.2.17}$$

which corresponds to introducing finite lattice differences defined in the usual way by

$$\partial_\mu\phi \longrightarrow (\Delta_\mu\phi)_i = \phi_{i+\mu} - \phi_i \quad . \tag{3.2.18}$$

Here the index μ labels the possible directions in which one can move from a point in a given triangle. The discrete scalar field action then takes the form

$$I(l^2,\phi) = \tfrac{1}{16}\sum_\Delta \frac{1}{A_\Delta}\left[l_1^2(\phi_2-\phi_1)(\phi_3-\phi_1) + l_2^2(\phi_3-\phi_2)(\phi_1-\phi_2) + l_3^2(\phi_1-\phi_3)(\phi_2-\phi_3)\right] \quad . \tag{3.2.19}$$

Using the identity

$$(\phi_i-\phi_j)(\phi_i-\phi_k) = \tfrac{1}{2}\left[(\phi_i-\phi_j)^2 + (\phi_i-\phi_k)^2 - (\phi_j-\phi_k)^2\right] \quad , \tag{3.2.20}$$

one obtains after some re-arrangements the simpler expression [67]

$$I(l^2,\phi) = \tfrac{1}{2}\sum_{<ij>} A_{ij}\left(\frac{\phi_i-\phi_j}{l_{ij}}\right)^2 \quad , \tag{3.2.21}$$

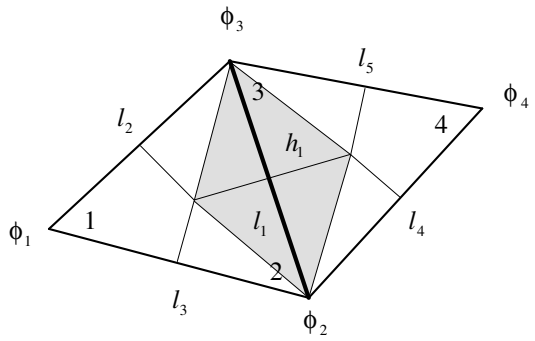

Figure 3.4: Dual area associated with the edge l_1 (shaded area), and the corresponding dual link h_1.

where A_{ij} is the dual (Voronoi) area associated with the edge ij. In terms of the edge length l_{ij} and the dual edge length h_{ij}, connecting neighboring vertices in the dual lattice, one has $A_{ij} = \frac{1}{2} h_{ij} l_{ij}$ (see Figs. 3.4). Other choices for the lattice subdivision will lead to a similar formula for the lattice action, but with the Voronoi dual volumes replaced by their appropriate counterparts in the new lattice.

For the edge of length 1 the dihedral dual volume contribution is given by

$$A_{l_1} = \frac{l_1^2(l_2^2 + l_3^2 - l_1^2)}{16 A_{123}} + \frac{l_1^2(l_4^2 + l_5^2 - l_1^2)}{16 A_{134}} = \tfrac{1}{2}\, l_1 h_1 \ , \tag{3.2.22}$$

with h_1 is the length of the edge dual to l_1. The baricentric dihedral volume for the same edge would be simply

$$A_{l_1} = (A_{123} + A_{134}) / \, 3 \ . \tag{3.2.23}$$

It is well known that one of the disadvantages of the Voronoi construction is the lack of positivity of the dual volumes, as already pointed out in [43]. Thus some of the weights appearing in Eq. (3.2.21) can be negative for such an action. On the other hand, for the baricentric subdivision this problem does not arise, as the areas A_{ij} are always positive due to the enforcement of the triangle inequalities. It

is immediate to generalize the action of Eq. (3.2.21) to higher dimensions, with the two-dimensional Voronoi volumes replaced by their higher dimensional analogs.

Mass and curvature terms can be added to the action, so that the total scalar action contribution becomes

$$I(l^2, \phi) = \tfrac{1}{2} \sum_{<ij>} A_{ij} \left(\frac{\phi_i - \phi_j}{l_{ij}} \right)^2 + \tfrac{1}{2} \sum_i A_i \left(m^2 + \xi R_i \right) \phi_i^2 \quad . \tag{3.2.24}$$

The term containing the discrete analog of the scalar curvature involves the quantity

$$A_i R_i \equiv \sum_{h \supset i} \delta_h \sim \sqrt{g}\, R \quad . \tag{3.2.25}$$

In the above expression for the scalar action, A_{ij} is the area associated with the edge l_{ij}, while A_i is associated with the site i. Again there is more than one way to define the volume element A_i, [43], but under reasonable assumptions, such as positivity, one expects to get equivalent results in the lattice continuum limit. In the following we shall only consider the simplest form for the scalar action, with $m^2 = \xi = 0$.

3.3 Lattice Weak field Expansion

One of the simplest problems which can be studied analytically in the continuum as well as on the lattice is the analysis of small fluctuations about some classical background solution. In the continuum, the weak field expansion is often performed by expanding the metric and the action about flat Euclidean space

$$g_{\mu\nu} = \delta_{\mu\nu} + \kappa h_{\mu\nu} \quad . \tag{3.3.26}$$

In four dimensions $\kappa = \sqrt{32\pi G}$, which shows that the weak field expansion there corresponds to an expansion in powers of G. In two dimensions this is no longer the case and the relation between κ and G is lost; instead one should regard κ as a dimensionless expansion parameter which is eventually set to one, $\kappa = 1$,

at the end of the calculation. The procedure will be sensible as long as wildly fluctuating geometries are not important in two dimensions (on the lattice or in the continuum). The influence of the latter configurations can only be studied by numerical simulations of the full path integral [47, 83].

In the lattice case the weak field calculations can be carried out in three [51] and four [41] dimensional flat background space with the Regge-Einstein action. One finds that the Regge gravity propagator indeed agrees exactly with the continuum result [69] in the weak-field limit. As a result, the existence of gravitational waves and gravitons in the discrete lattice theory has been established (indeed it is the only lattice theory of gravity for which such a result has been obtained).

In the following we shall consider in detail only the two-dimensional case, although similar calculations can in principle be performed in higher dimensions, with considerable more algebraic effort. In pure gravity case the Einstein-Regge action is a topological invariant in two dimensions, and one has to consider the next non-trivial invariant contribution to the action. We shall therefore consider a two-dimensional lattice with the higher derivative action of Eq. (3.2.12) and $\lambda = 0$,

$$I(l^2) = 4a \sum_{\text{hinges h}} \frac{\delta_h^2}{A_h} \quad . \tag{3.3.27}$$

The weak field expansion for such a term has largely been done in [47], and we will first recall here the main results. Since flat space is a classical solution for such an R^2–type action, one can take as a background space a network of unit squares divided into triangles by drawing in parallel sets of diagonals (see Figs. 3.5). This is one of an infinite number of possible choices for the background lattice, and a rather convenient one. Physical results should in the end be insensitive to the choice of the background lattice used as a starting point for the weak field expansion.

It is also convenient to use the binary notation for vertices described in references [41]. As discussed in the previous section, the edge lengths on the lattice correspond

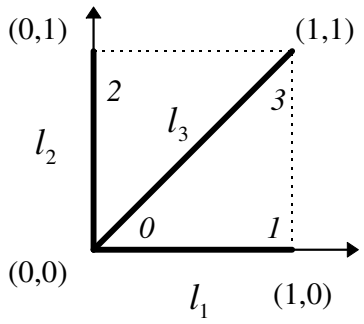

Figure 3.5: Notation for the weak-field expansion about the rigid square lattice.

to the metric degrees of freedom in the continuum. The edge lengths are thus allowed to fluctuate around their flat space values,

$$l_i = l_i^0(1 + \varepsilon_i) \ , \tag{3.3.28}$$

with $l_1^0 = l_2^0 = 1$ and $l_3^0 = \sqrt{2}$ for our choice of lattice. The second variation of the action is then expressed as a quadratic form in the ε's,

$$\delta^2 I = 4a \sum_{ij} \varepsilon_i M_{ij} \varepsilon_j \ . \tag{3.3.29}$$

The properties of M_{ij} are best studied by going to momentum space. One assumes that the fluctuation ε_i at the point i, j steps in one coordinate direction and k steps in the other coordinate direction from the origin, is related to the corresponding ε_i at the origin by

$$\varepsilon_i^{(j+k)} = \omega_1^j \, \omega_2^k \, \varepsilon_i^{(0)} \ , \tag{3.3.30}$$

where $\omega_i = e^{-ik_i}$ and k_i is the momentum in the direction i. The matrix M then reduces to a 3×3 matrix M_ω with components given by [47]

$$\begin{aligned}
(M_\omega)_{11} &= 2 + \omega_1 - 2\omega_2 - 2\omega_1\omega_2 + \omega_1\omega_2^2 + c.c. \\
(M_\omega)_{12} &= 2 - \omega_1 - \bar{\omega}_2 - \omega_1\omega_2 - \bar{\omega}_1\bar{\omega}_2 - \omega_1^2 - \bar{\omega}_2^2 + \omega_1^2\omega_2 + \bar{\omega}_1\bar{\omega}_2^2 + 2\omega_1\bar{\omega}_2
\end{aligned}$$

$$
\begin{aligned}
(M_\omega)_{13} &= 2(-1+2\omega_1-\bar\omega_1+\omega_2-\bar\omega_2-\omega_1\omega_2+2\bar\omega_1\bar\omega_2+\bar\omega_2^2-\bar\omega_1\bar\omega_2^2-\omega_1\bar\omega_2) \\
(M_\omega)_{33} &= 4(2-2\omega_1-2\omega_2+\omega_1\omega_2+\bar\omega_1\omega_2+c.c.)
\end{aligned}
\tag{3.3.31}
$$

with the other components easily obtained by symmetry. The change of variables

$$
\varepsilon_1' = \varepsilon_1 \quad \varepsilon_2' = \varepsilon_2 \quad \varepsilon_3' = \tfrac{1}{2}(\varepsilon_1+\varepsilon_2)+\varepsilon_3 \quad . \tag{3.3.32}
$$

leads for small momenta to the matrix M'_ω given by

$$
M'_\omega = l^4 \begin{pmatrix} k_2^4 & k_1^2k_2^2 & -2k_1k_2^3 \\ k_1^2k_2^2 & k_1^4 & -2k_1^3k_2 \\ -2k_1k_2^3 & -2k_1^3k_2 & 4k_1^2k_2^2 \end{pmatrix} + O(k^5) \quad . \tag{3.3.33}
$$

This expression is identical to what one obtains from the corresponding weak-field limit in the continuum theory. To see this, one defines as usual the small fluctuation field $h_{\mu\nu}$ about flat space, which then gives

$$
\sqrt{g}\,R^2 = (h_{11,22}+h_{22,11}-2h_{12,12})^2 + O(h^3) \quad . \tag{3.3.34}
$$

In momentum space, each derivative ∂_ν produces a factor of k_ν, and one has

$$
\sqrt{g}\,R^2 = h_{\mu\nu}\,V_{\mu\nu,\rho\sigma}\,h_{\rho\sigma} \quad , \tag{3.3.35}
$$

where $V_{\mu\nu,\rho\sigma}$ coincides with M' above (when the metric components are re-labeled according to $11\to 1,\ 22\to 2,\ 12\to 3$).

It is easy to see the reason for the change of variables in Eq. (3.3.32). Given the three edges in Figure 5, one can write for the metric at the origin

$$
g_{ij} = \begin{pmatrix} l_1^2 & \frac{1}{2}(l_3^2-l_1^2-l_2^2) \\ \frac{1}{2}(l_3^2-l_1^2-l_2^2) & l_2^2 \end{pmatrix} \quad . \tag{3.3.36}
$$

Inserting $l_i = l_i^0(1+\varepsilon_i)$, with $l_i^0 = 1$ for the body principals ($i = 1,2$) and $l_i^0 = \sqrt{2}$ for the diagonal ($i = 3$), one then obtains

$$
l_1^2 = (1+\varepsilon_1)^2 \quad = \quad 1+h_{11}
$$

$$\begin{aligned} l_2^2 = (1+\varepsilon_2)^2 &= 1 + h_{22} \\ \tfrac{1}{2} l_3^2 = (1+\varepsilon_3)^2 &= 1 + \tfrac{1}{2}(h_{11}+h_{22}) + h_{12} \quad , \end{aligned} \tag{3.3.37}$$

which can be inverted to give

$$\begin{aligned} \varepsilon_1 &= \tfrac{1}{2} h_{11} - \tfrac{1}{8} h_{11}^2 + O(h_{11}^3) \\ \varepsilon_2 &= \tfrac{1}{2} h_{22} - \tfrac{1}{8} h_{22}^2 + O(h_{22}^3) \\ \varepsilon_3 &= \tfrac{1}{4}(h_{11}+h_{22}+2h_{12}) - \tfrac{1}{32}(h_{11}+h_{22}+2h_{12})^2 + O(h^3) \end{aligned} \tag{3.3.38}$$

which was used in Eq. (3.3.32). Thus the matrix M_ω was brought in the continuum form after performing a suitable local rotation from the local edge lengths to the local metric components.

A similar weak field expansion can be performed for the cosmological constant term, although strictly speaking flat space is no longer a classical solution in the presence of such a term [47]. One then obtains a contribution to the second variation of the action of the form

$$L_\omega = \frac{\lambda}{2} \begin{pmatrix} -1 & 0 & 1+\bar{\omega}_2 \\ 0 & -1 & 1+\bar{\omega}_1 \\ 1+\omega_2 & 1+\omega_1 & -4 \end{pmatrix} \quad . \tag{3.3.39}$$

In the weak field limit, and with the same change of variables as described for the matrix M_ω, this leads to

$$L'_\omega = -\frac{\lambda}{2} \begin{pmatrix} 1 & -1 & 0 \\ -1 & 1 & 0 \\ 0 & 0 & 4 \end{pmatrix} + O(k) \quad . \tag{3.3.40}$$

The local gauge invariance of the R^2-action is reflected in the presence of two exact zero modes in M_ω of Eq. (3.3.31). As discussed in Ref. [70], the eigenvalues

of the matrix M_ω are given by

$$\begin{aligned}
\lambda_1 &= 0 \\
\lambda_2 &= 0 \\
\lambda_3 &= 24 - 9(\omega_1 + \bar{\omega}_1 + \omega_2 + \bar{\omega}_2) + 4(\omega_1\bar{\omega}_2 + \bar{\omega}_1\omega_2) \\
&\quad + \omega_1\omega_2^2 + \omega_1^2\omega_2 + \bar{\omega}_1\bar{\omega}_2^2 + \bar{\omega}_1^2\bar{\omega}_2 \quad .
\end{aligned} \tag{3.3.41}$$

It should be noted that the exact zero modes appear for arbitrary ω_i, and not just for small momenta.

It is clear that if one were interested in doing lattice perturbation theory with such an R^2 action, one would have to add a lattice gauge fixing term to remove the zero modes, such as the lattice analog of

$$\frac{1}{\kappa^2}\left(\partial_\mu\sqrt{g(x)}g^{\mu\nu}\right)^2 \quad , \tag{3.3.42}$$

and then add the necessary Fadeev-Popov nonlocal ghost determinant. A similar term would have to be included as well if one were to pick the lattice analog of the conformal gauge [94]. If one is *not* doing perturbation theory, then of course the contribution of the zero modes will cancel out between the numerator and denominator in the Feynman path integral representation for operator averages, and such a term is not needed, as in ordinary lattice formulations of gauge theories.

The above zero modes correspond to the lattice analogs of diffeomorphisms. It is easy to see that the eigenvectors corresponding to the two zero modes can be written as

$$\begin{pmatrix} \varepsilon_1(\omega) \\ \varepsilon_2(\omega) \\ \varepsilon_3(\omega) \end{pmatrix} = \begin{pmatrix} 1-\omega_1 & 0 \\ 0 & 1-\omega_2 \\ \frac{1}{2}(1-\omega_1\omega_2) & \frac{1}{2}(1-\omega_1\omega_2) \end{pmatrix} \begin{pmatrix} \chi_1(\omega) \\ \chi_2(\omega) \end{pmatrix} \quad , \tag{3.3.43}$$

where $\chi_1(\omega)$ and $\chi_2(\omega)$ are arbitrary functions (the above result is not restricted to two dimensions; completely analogous zero modes are found for the Regge action

in three [51] and four [41] dimensions, leading to expressions rather similar to Eq. (3.3.43), with d gauge zero modes in d dimensions; their explicit form can be found in the quoted references). In position space one then has

$$\begin{aligned}
\varepsilon_1(n) &= \chi_1(n) - \chi_1(n+\hat{\mu}_1) \\
\varepsilon_2(n) &= \chi_2(n) - \chi_2(n+\hat{\mu}_2) \\
\varepsilon_3(n) &= \tfrac{1}{2}\chi_1(n) + \tfrac{1}{2}\chi_2(n) - \tfrac{1}{2}\chi_1(n+\hat{\mu}_1+\hat{\mu}_2) - \tfrac{1}{2}\chi_2(n+\hat{\mu}_1+\hat{\mu}_2)
\end{aligned} \tag{3.3.44}$$

Using the correct relation between induced metric perturbations and edge length variations,

$$\delta g_{ij} = \begin{pmatrix} \delta l_1^2 & \frac{1}{2}(\delta l_3^2 - \delta l_1^2 - \delta l_2^2) \\ \frac{1}{2}(\delta l_3^2 - \delta l_1^2 - \delta l_2^2) & \delta l_2^2 \end{pmatrix} \quad , \tag{3.3.45}$$

one can easily show that the above corresponds to the discrete analog of the familiar expression

$$\delta g_{\mu\nu} = -\partial_\mu \chi_\nu - \partial_\nu \chi_\mu \quad , \tag{3.3.46}$$

which indeed describes the correct gauge variation in the weak field limit. In the discrete case it reflects the invariance of the lattice action under local deformations of the simplicial manifold which leave the local curvatures unchanged [40]. The above relationships express in the continuum the well-known fact that metrics related by a coordinate transformation describe the same physical manifold. Since the continuum metric degrees of freedom correspond on the lattice to the values of edge lengths squared, one expects to find analogous deformations of the edge lengths that leave the lattice geometry invariant, the latter being specified by the local *lattice* areas and curvatures, in accordance with the principle of discussing the geometric properties of the lattice theory in terms of lattice quantities only. This invariance is spoiled by the presence of the triangle inequalities, which places a constraint on how far the individual edge lengths can be deformed. In the per-

turbative, weak field expansion about a fixed background the triangle inequalities are not seen to any order in perturbation theory, they represent non-perturbative constraints.

The above invariance of the lattice action is a less trivial realization of the exact local gauge invariance found already in one dimension

$$\delta l_n = \chi_{n+1} - \chi_n \quad , \tag{3.3.47}$$

where the χ_n's represent continuous gauge transformations defined on the lattice vertices [71]. The invariance of the quantum theory is again broken by the triangle inequalities, which in one dimension reduces to the requirement that the edge lengths be positive. Such a breaking is unavoidable in any lattice regularization as it cannot preserve the invariance under scale transformations, which are just special cases of diffeomorphisms.

The weak field expansion for the purely gravitational part can be carried out to higher order, and the Feynman rules for the vertices of order h^3, h^4, … in the R^2-action of Eq. (3.2.12) can be derived. Since their expressions are rather complicated, they will not be recorded here.

3.3.1 Feynman Rules

Let us consider next the scalar action of Eq. (3.2.21),

$$\tfrac{1}{2}\int d^2x\,\sqrt{g}\,g^{\mu\nu}\,\partial_\mu\phi\,\partial_\nu\phi \;\sim\; \tfrac{1}{2}\sum_{<ij>} A_{ij}\left(\frac{\phi_i-\phi_j}{l_{ij}}\right)^2 \quad . \tag{3.3.48}$$

In the continuum, the Feynman rules are obtained by first expanding out the action in the weak fields $h_{\mu\nu}(x)$,

$$\begin{aligned}\tfrac{1}{2}\int d^2x\,\sqrt{g}g^{\mu\nu}\,\partial_\mu\phi\,\partial_\nu\phi \;=\; & \tfrac{1}{2}\int d^2x\,(\partial\phi)^2 + \tfrac{1}{2}\int d^2x\,h_{\mu\nu}\left\{\tfrac{1}{2}\delta_{\mu\nu}(\partial\phi)^2 - \partial_\mu\phi\,\partial_\nu\phi\right\} \\ & + \frac{1}{2}\int d^2x\,\{h_{\mu\rho}h_{\nu\rho}\partial_\mu\phi\partial_\nu\phi - \frac{1}{2}\,h_{\rho\rho}h_{\mu\nu}\partial_\mu\phi\partial_\nu\phi \\ & + (\,\frac{1}{8}\,h_{\rho\rho}h_{\lambda\lambda} - \frac{1}{4}h_{\rho\lambda}h_{\rho\lambda}\,)\,\partial_\alpha\phi\partial_\alpha\phi\,\} + O(h^3\phi^2)\ . \end{aligned} \tag{3.3.49}$$

and then by transforming the resulting expressions to momentum space.

On the lattice the action is again expanded in the small fluctuation fields ε_i, which depend on the specific choice of parameterization for the flat background lattice. We will first discuss the lattice of Figure 2.6(a), with the choice of labeling according to Figure 2.5. Figures 2.6(a) and 2.6(b) correspond to two different gauge choices for the background metric which are physically equivalent; there are many others. The fluctuations in the edge lengths ε_i (see Eq. (3.3.28)) and the scalar fields ϕ at the point i, j steps in one coordinate direction and k steps in the other coordinate direction from the origin, are related to the corresponding ε_i and ϕ at the origin by

$$\varepsilon_i^{(j+k)} \;=\; \omega_1^j \, \omega_2^k \, \varepsilon_i^{(0)} \quad , \tag{3.3.50}$$

where $\omega_i = e^{-ik_i}$ and k_i is the momentum in the direction i.

$$\phi^{(j+k)} \;=\; \omega'^j_{\ 1} \, \omega'^k_{\ 2} \, \phi_i^{(0)} \quad , \tag{3.3.51}$$

where $\omega'_i = e^{-ip_i}$. In practice it is actually more convenient to redefine the edge variables at the midpoints of the links, since this choice neatly removes later a set of complex phase factors from the Feynman rules. For the edge lengths we therefore define the lattice Fourier transforms as

$$\begin{aligned}
\varepsilon_1(n) &= \int_{-\pi}^{\pi}\int_{-\pi}^{\pi} \frac{d^2k}{(2\pi)^2}\, e^{-ik\cdot n - ik_1/2}\, \varepsilon_1(k) \\
\varepsilon_2(n) &= \int_{-\pi}^{\pi}\int_{-\pi}^{\pi} \frac{d^2k}{(2\pi)^2}\, e^{-ik\cdot n - ik_2/2}\, \varepsilon_2(k) \\
\varepsilon_3(n) &= \int_{-\pi}^{\pi}\int_{-\pi}^{\pi} \frac{d^2k}{(2\pi)^2}\, e^{-ik\cdot n - ik_1/2 - ik_2/2}\, \varepsilon_3(k) \quad ,
\end{aligned} \tag{3.3.52}$$

while we still define the scalar field on the vertices, and therefore the Fourier transform in the usual way,

$$\phi(n) = \int_{-\pi}^{\pi}\int_{-\pi}^{\pi} \frac{d^2p}{(2\pi)^2}\, e^{-ip\cdot n}\, \phi(p) \quad . \tag{3.3.53}$$

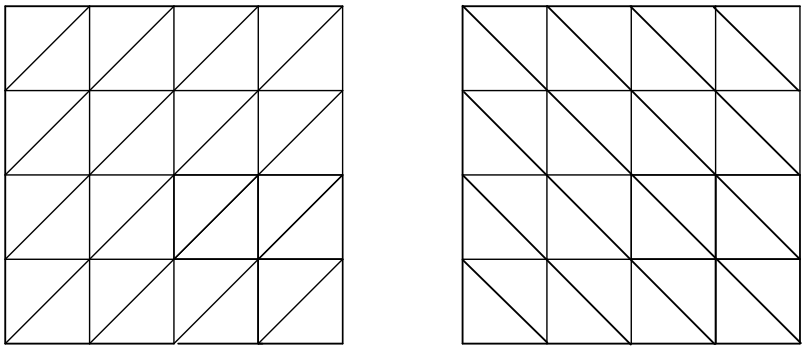

(a) (b)

Figure 3.6: Two equivalent triangulation of flat space, based on different subdivisions of the square lattice.

These formulae are easy to generalize to higher dimensions when a simplicial subdivision of a hypercubic lattice is employed, as first suggested in [41].

The kinetic energy term for the scalar field can naturally be decomposed as a sum of three terms

$$\begin{aligned} I &= \frac{1}{2}\sum_{<ij>} A_{ij}(\frac{\phi_i-\phi_j}{l_{ij}})^2 \\ &= \frac{1}{2}\sum_{horizontal} A_{ij}^{(h)}(\frac{\phi_i-\phi_j}{1+\varepsilon_1})^2 + \frac{1}{2}\sum_{vertical} A_{ij}^{(v)}(\frac{\phi_i-\phi_j}{1+\varepsilon_2})^2 \\ &\quad + \frac{1}{2}\sum_{diagonal} A_{ij}^{(d)}(\frac{\phi_i-\phi_j}{1+\varepsilon_3})^2 \ , \end{aligned} \tag{3.3.54}$$

where $< ij >$ labels an edge connecting sites i and j. We have separated the sum over all edges into sums over horizontal, vertical, and diagonal edges. The series expansion of each term in the sums with respect to an edge length fluctuation in a particular direction is given by the following expressions

$$\begin{aligned} \frac{A_{ij}^{(h)}}{(1+\varepsilon_1)^2} &= \frac{1}{4} - \frac{1}{2}\varepsilon_1 + \frac{1}{2}\varepsilon_3 \\ &\quad + \frac{1}{2}\varepsilon_1^2 + \frac{1}{4}\varepsilon_2^2 + \frac{3}{4}\varepsilon_3^2 \end{aligned}$$

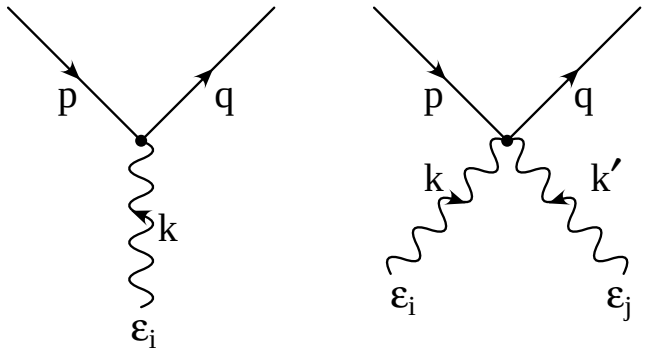

Figure 3.7: Labeling of momenta for the scalar-graviton vertices.

$$+\frac{1}{2}\,\varepsilon_1\varepsilon_2-\varepsilon_1\varepsilon_3-\varepsilon_2\varepsilon_3+O(\varepsilon_i^3)\ \ ; \tag{3.3.55}$$

$$\begin{aligned}\frac{A_{ij}^{(v)}}{(1+\varepsilon_2)^2} &= \frac{1}{4}-\frac{1}{2}\,\varepsilon_2+\frac{1}{2}\,\varepsilon_3\\ &\quad+\frac{1}{4}\,\varepsilon_1^2+\frac{1}{2}\,\varepsilon_2^2+\frac{3}{4}\,\varepsilon_3^2\\ &\quad+\frac{1}{2}\,\varepsilon_1\varepsilon_2-\varepsilon_1\varepsilon_3-\varepsilon_2\varepsilon_3+O(\varepsilon_i^3)\ \ ;\end{aligned} \tag{3.3.56}$$

$$\begin{aligned}\frac{A_{ij}^{(d)}}{(1+\varepsilon_3)^2} &= \frac{1}{4}\,\varepsilon_1+\frac{1}{4}\,\varepsilon_2-\frac{1}{2}\,\varepsilon_3\\ &\quad-\frac{1}{8}\,\varepsilon_1^2-\frac{1}{8}\,\varepsilon_2^2-\frac{1}{4}\,\varepsilon_3^2\\ &\quad-\frac{1}{2}\,\varepsilon_1\varepsilon_2+\frac{1}{2}\,\varepsilon_1\varepsilon_3+\frac{1}{2}\,\varepsilon_2\varepsilon_3+O(\varepsilon_i^3)\ \ .\end{aligned} \tag{3.3.57}$$

The 0-th order term in ε gives the scalar field propagator

$$\frac{1}{4\,\sum_\mu \sin^2(\frac{p_\mu}{2})}, \tag{3.3.58}$$

which is the usual scalar propagator for the square lattice, and coincides with the continuum one for small momenta.

The higher order terms give, after transforming to momentum space, the Feynman rules for the vertices. For the trilinear vertex associated with $\varepsilon_1(k)\phi(p)\phi(q)$ one

finds

$$-2\sin(\frac{p_1}{2})\sin(\frac{q_1}{2})+\cos(\frac{k_2}{2})\sin(\frac{p_1+p_2}{2})\sin(\frac{q_1+q_2}{2}) \quad ; \tag{3.3.59}$$

for the vertex $\varepsilon_2(k)\phi(p)\phi(q)$ one obtains

$$-2\sin(\frac{p_2}{2})\sin(\frac{q_2}{2})+\cos(\frac{k_1}{2})\sin(\frac{p_1+p_2}{2})\sin(\frac{q_1+q_2}{2}) \quad ; \tag{3.3.60}$$

and for the vertex $\varepsilon_3(k)\phi(p)\phi(q)$ one has

$$\begin{aligned} &2\cos(\tfrac{k_2}{2})\sin(\tfrac{p_1}{2})\sin(\tfrac{q_1}{2})+2\cos(\tfrac{k_1}{2})\sin(\tfrac{p_2}{2})\sin(\tfrac{q_2}{2}) \\ &\quad -2\sin(\tfrac{p_1+p_2}{2})\sin(\tfrac{q_1+q_2}{2}) \quad . \end{aligned} \tag{3.3.61}$$

In order to compare the lattice Feynman rules with the usual continuum ones, one needs to perform a transformation from the ε_i variables to the metric fluctuation $h_{\mu\nu}$. The correspondence between the two is given in Eqs. (3.2.13), (3.3.37) and (3.3.38). However, one must be careful in doing the transformation since ε_3 contains contributions to all h_{11}, h_{22}, and h_{12}. The exact correspondence is given by the following relation. After writing

$$\begin{aligned} &a\varepsilon_1+b\varepsilon_2+c\varepsilon_3+A\varepsilon_1^2+B\varepsilon_2^2+C\varepsilon_3^2 \\ &\quad +D\varepsilon_1\varepsilon_2+E\varepsilon_1\varepsilon_3+F\varepsilon_2\varepsilon_3, \end{aligned} \tag{3.3.62}$$

one can use the relationships between ε_i and $h_{\mu\nu}$ of Eq. (3.3.37) to obtain

$$\begin{aligned} &(\tfrac{a}{2}+\tfrac{c}{4})\,h_{11}+(\tfrac{b}{2}+\tfrac{c}{4})\,h_{22}+\tfrac{c}{4}\,h_{12}+\tfrac{c}{4}\,h_{21} \\ &+(-\tfrac{a}{8}-\tfrac{c}{32}+\tfrac{A}{4}+\tfrac{C}{16}+\tfrac{E}{8})\,h_{11}^2+(-\tfrac{b}{8}-\tfrac{c}{32}+\tfrac{B}{4}+\tfrac{C}{16}+\tfrac{F}{8})\,h_{22}^2 \\ &+(-\tfrac{c}{16}+\tfrac{C}{8}+\tfrac{D}{4}+\tfrac{E}{8}+\tfrac{F}{8})\,h_{11}\,h_{22}+(-\tfrac{c}{16}+\tfrac{C}{8}+\tfrac{E}{8})\,h_{11}\,h_{12} \\ &+(-\tfrac{c}{16}+\tfrac{C}{8}+\tfrac{F}{8})\,h_{11}\,h_{21}+(-\tfrac{c}{16}+\tfrac{C}{8}+\tfrac{F}{8})\,h_{22}\,h_{12} \\ &+(-\tfrac{c}{16}+\tfrac{C}{8}+\tfrac{F}{8})\,h_{22}\,h_{21}+(-\tfrac{c}{32}+\tfrac{C}{16})\,h_{12}^2+(-\tfrac{c}{16}+\tfrac{C}{8})\,h_{12}\,h_{21} \quad . \end{aligned} \tag{3.3.63}$$

With the aid of the above equation, one can then easily rewrite the Feynman rules in terms of $h_{\mu\nu}\phi^2$. For the vertex $h_{11}(k)\phi(p)\phi(q)$ one has

$$-4\,(1-\tfrac{1}{2}\cos\tfrac{k_2}{2})\sin(\tfrac{p_1}{2})\sin(\tfrac{q_1}{2})+2\cos(\tfrac{k_1}{2})\sin(\tfrac{p_2}{2})\sin(\tfrac{q_2}{2})$$

$$-2\,(1-\cos\tfrac{k_2}{2})\sin(\tfrac{p_1+p_2}{2})\sin(\tfrac{q_1+q_2}{2})\ \ . \tag{3.3.64}$$

When expanded out for small momenta it gives

$$\frac{1}{2}\,(-p_1\,q_1+p_2\,q_2)=\frac{1}{2}\,(p\cdot q-2\,p_1\,q_1)\ \ . \tag{3.3.65}$$

For the vertex $h_{22}(k)\phi(p)\phi(q)$ one obtains

$$\begin{aligned}&2\cos(\tfrac{k_2}{2})\sin(\tfrac{p_1}{2})\sin(\tfrac{q_1}{2})-4\,(1-\tfrac{1}{2}\cos\tfrac{k_1}{2})\sin(\tfrac{p_2}{2})\sin(\tfrac{q_2}{2})\\&-2\,(1-\cos\tfrac{k_1}{2})\sin(\tfrac{p_1+p_2}{2})\sin(\tfrac{q_1+q_2}{2})\ \ ,\end{aligned} \tag{3.3.66}$$

and its leading continuum approximation is given by

$$\frac{1}{2}\,(-p_2\,q_2+p_1\,q_1)=\frac{1}{2}\,(p\cdot q-2\,p_2\,q_2)\ \ . \tag{3.3.67}$$

For the vertex $h_{12}(k)\phi(p)\phi(q)$ ($=h_{21}(k)\phi(p)\phi(q)$) one has

$$\begin{aligned}&2\cos(\tfrac{k_2}{2})\sin(\tfrac{p_1}{2})\sin(\tfrac{q_1}{2})+2\cos(\tfrac{k_1}{2})\sin(\tfrac{p_2}{2})\sin(\tfrac{q_2}{2})\\&-2\sin(\tfrac{p_1+p_2}{2})\sin(\tfrac{q_1+q_2}{2})\ \ ,\end{aligned} \tag{3.3.68}$$

and its leading continuum approximation is given by

$$-\frac{1}{2}\,(p_1\,q_2+p_2\,q_1)\ \ . \tag{3.3.69}$$

Written in Lorentz covariant form, the leading continuum approximations for the vertices $h_{\mu\nu}(k)\phi(p)\phi(q)$ can be grouped together as

$$\frac{1}{2}\,(\delta_{\mu\nu}p\cdot q-p_\mu\,q_\nu-p_\nu\,q_\mu) \tag{3.3.70}$$

which is now identical to the usual continuum Feynman rule, derived from the original continuum action (see eq.(2.2.16), chapter 2.)

One can proceed in a similar way for the higher order vertices. The Feynman rules for the 2-scalar 2-graviton vertex written in the component forms are:
for the vertex $\varepsilon_1(k)\varepsilon_1(k')\phi(p)\phi(q)$,

$$\begin{aligned}&2\sin(\tfrac{p_1}{2})\sin(\tfrac{q_1}{2})+\cos(\tfrac{k_1+k_2+k_1'+k_2'}{2})\sin(\tfrac{p_2}{2})\sin(\tfrac{q_2}{2})\\&-\tfrac{1}{2}\cos(\tfrac{k_2+k_2'}{2})\sin(\tfrac{p_1+p_2}{2})\sin(\tfrac{q_1+q_2}{2})\ \ ;\end{aligned} \tag{3.3.71}$$

for the vertex $\varepsilon_2(k)\varepsilon_2(k')\phi(p)\phi(q)$,

$$\cos(\tfrac{k_1+k_2+k_1'+k_2'}{2})\sin(\tfrac{p_1}{2})\sin(\tfrac{q_1}{2}) + 2\sin(\tfrac{p_2}{2})\sin(\tfrac{q_2}{2}) - \tfrac{1}{2}\cos(\tfrac{k_1+k_1'}{2})\sin(\tfrac{p_1+p_2}{2})\sin(\tfrac{q_1+q_2}{2}) \quad ; \tag{3.3.72}$$

for the vertex $\varepsilon_3(k)\varepsilon_3(k')\phi(p)\phi(q)$,

$$3\cos(\tfrac{k_2+k_2'}{2})\sin(\tfrac{p_1}{2})\sin(\tfrac{q_1}{2}) + 3\cos(\tfrac{k_1+k_1'}{2})\sin(\tfrac{p_2}{2})\sin(\tfrac{q_2}{2}) - \sin(\tfrac{p_1+p_2}{2})\sin(\tfrac{q_1+q_2}{2}) \quad ; \tag{3.3.73}$$

for the vertex $\varepsilon_1(k)\varepsilon_2(k')\phi(p)\phi(q)$,

$$2\cos(\tfrac{k_1'+k_2'}{2})\sin(\tfrac{p_1}{2})\sin(\tfrac{q_1}{2}) + 2\cos(\tfrac{k_1+k_2}{2})\sin(\tfrac{p_2}{2})\sin(\tfrac{q_2}{2}) - 2\cos(\tfrac{k_2-k_1'}{2})\sin(\tfrac{p_1+p_2}{2})\sin(\tfrac{q_1+q_2}{2}) \quad ; \tag{3.3.74}$$

for the vertex $\varepsilon_1(k)\varepsilon_3(k')\phi(p)\phi(q)$,

$$-4\cos(\tfrac{k_2'}{2})\sin(\tfrac{p_1}{2})\sin(\tfrac{q_1}{2}) - 4\cos(\tfrac{k_1+k_2+k_1'}{2})\sin(\tfrac{p_2}{2})\sin(\tfrac{q_2}{2}) + 2\cos(\tfrac{k_2}{2})\sin(\tfrac{p_1+p_2}{2})\sin(\tfrac{q_1+q_2}{2}) \quad ; \tag{3.3.75}$$

for the vertex $\varepsilon_2(k)\varepsilon_3(k')\phi(p)\phi(q)$,

$$-4\cos(\tfrac{k_1+k_2+k_2'}{2})\sin(\tfrac{p_1}{2})\sin(\tfrac{q_1}{2}) - 4\cos(\tfrac{k_1'}{2})\sin(\tfrac{p_2}{2})\sin(\tfrac{q_2}{2}) + 2\cos(\tfrac{k_1}{2})\sin(\tfrac{p_1+p_2}{2})\sin(\tfrac{q_1+q_2}{2}). \tag{3.3.76}$$

After writing again the ε_i fields in terms of the $h_{\mu\nu}$ fields (see Eq. (3.3.37)), one obtains the Feynman rules for the vertex $h_{11}(k)h_{11}(k')\phi(p)\phi(q)$,

$$\begin{aligned}&(6 - \tfrac{1}{2}\cos\tfrac{k_2}{2} + \tfrac{3}{2}\cos\tfrac{k_2+k_2'}{2} - 4\cos\tfrac{k_2'}{2})\sin(\tfrac{p_1}{2})\sin(\tfrac{q_1}{2})\\ &+ (\tfrac{3}{2}\cos\tfrac{k_1+k_1'}{2} - 4\cos\tfrac{k_1'+k_1+k_2}{2} + 2\cos\tfrac{k_1+k_2+k_1'+k_2'}{2} - \tfrac{1}{2}\cos\tfrac{k_1}{2})\sin(\tfrac{p_2}{2})\sin(\tfrac{q_2}{2})\\ &+ (\cos\tfrac{k_2}{2} - \cos\tfrac{k_2+k_2'}{2})\sin(\tfrac{p_1+p_2}{2})\sin(\tfrac{q_1+q_2}{2}) \quad .\end{aligned} \tag{3.3.77}$$

The above expression should be symmetrized in k and k' to reflect the fact that an edge is shared between two neighboring triangles. For small momenta its leading

continuum approximation is given by

$$\frac{1}{4}\,(\,-p\cdot q+4\,p_1q_1)\quad . \tag{3.3.78}$$

For the vertex $h_{22}(k)h_{22}(k')\phi(p)\phi(q)$,

$$\begin{aligned}(\tfrac{3}{2}\cos\tfrac{k_2+k_2'}{2}-4\cos\tfrac{k_1+k_2+k_2'}{2}+2\cos\tfrac{k_1+k_2+k_1'+k_2'}{2}-\tfrac{1}{2}\cos\tfrac{k_2}{2})\sin(\tfrac{p_1}{2})\sin(\tfrac{q_1}{2})\\ +(6-4\cos\tfrac{k_1'}{2}+\tfrac{3}{2}\cos\tfrac{k_1+k_1'}{2}-\tfrac{1}{2}\cos\tfrac{k_1}{2})\sin(\tfrac{p_2}{2})\sin(\tfrac{q_2}{2})\\ +(\cos\tfrac{k_1}{2}-\cos\tfrac{k_1+k_1'}{2})\sin(\tfrac{p_1+p_2}{2})\sin(\tfrac{q_1+q_2}{2})\quad ,\end{aligned} \tag{3.3.79}$$

and its leading continuum approximation for small momenta is given by

$$\frac{1}{4}\,(\,-p\cdot q+4\,p_2q_2)\quad . \tag{3.3.80}$$

For the vertex $h_{11}(k)h_{22}(k')\phi(p)\phi(q)$,

$$\begin{aligned}2(\,-\cos\tfrac{k_2'}{2}+\cos\tfrac{k_1'+k_2'}{2}+\tfrac{3}{4}\cos\tfrac{k_2+k_2'}{2}-\cos\tfrac{k_1+k_2+k_2'}{2}-\tfrac{1}{4}\cos\tfrac{k_2}{2})\sin(\tfrac{p_1}{2})\sin(\tfrac{q_1}{2})\\ +2(\,-\cos\tfrac{k_1'}{2}+\tfrac{3}{4}\cos\tfrac{k_1+k_1'}{2}+\cos\tfrac{k_1+k_2}{2}-\cos\tfrac{k_1+k_2+k_1'}{2}-\tfrac{1}{4}\cos\tfrac{k_1}{2})\sin(\tfrac{p_2}{2})\sin(\tfrac{q_2}{2})\\ +(\cos\tfrac{k_1}{2}-2\cos\tfrac{k_1'-k_2}{2}+\cos\tfrac{k_2}{2})\sin(\tfrac{p_1+p_2}{2})\sin(\tfrac{q_1+q_2}{2})\quad ,\end{aligned} \tag{3.3.81}$$

and its leading continuum approximation for small momenta is

$$-\frac{1}{4}\,p\cdot q\quad . \tag{3.3.82}$$

For the vertex $h_{11}(k)h_{12}(k')\phi(p)\phi(q)$ ($=h_{11}(k)h_{21}(k')\phi(p)\phi(q)$),

$$\begin{aligned}\tfrac{1}{2}\,(\,-\cos\tfrac{k_2}{2}-4\cos\tfrac{k_2'}{2}+3\cos\tfrac{k_2+k_2'}{2})\sin(\tfrac{p_1}{2})\sin(\tfrac{q_1}{2})\\ +\tfrac{1}{2}\,(\,-\cos\tfrac{k_1}{2}+3\cos\tfrac{k_1+k_1'}{2}-4\cos\tfrac{k_1+k_2+k_1'}{2})\sin(\tfrac{p_2}{2})\sin(\tfrac{q_2}{2})\\ +\cos(\tfrac{k_2}{2})\sin(\tfrac{p_1+p_2}{2})\sin(\tfrac{q_1+q_2}{2})\quad ,\end{aligned} \tag{3.3.83}$$

and its leading continuum approximation for small momenta is

$$\frac{1}{4}\,(p_1q_2+p_2q_1)\quad . \tag{3.3.84}$$

For the vertex $h_{22}(k)h_{12}(k')\phi(p)\phi(q)$ ($= h_{22}(k)h_{21}(k')\phi(p)\phi(q)$),

$$\begin{aligned}
&\tfrac{1}{2}\,(-\cos\tfrac{k_2}{2}+3\cos\tfrac{k_2+k_2'}{2}-4\cos\tfrac{k_1+k_2+k_2'}{2})\sin(\tfrac{p_1}{2})\sin(\tfrac{q_1}{2})\\
&+\tfrac{1}{2}\,(-\cos\tfrac{k_1}{2}-4\cos\tfrac{k_1'}{2}+3\cos\tfrac{k_1+k_1'}{2})\sin(\tfrac{p_2}{2})\sin(\tfrac{q_2}{2})\\
&+\cos(\tfrac{k_1}{2})\sin(\tfrac{p_1+p_2}{2})\sin(\tfrac{q_1+q_2}{2})\ ,
\end{aligned}\tag{3.3.85}$$

and its leading continuum approximation for small momenta is

$$\frac{1}{4}\,(p_1q_2+p_2q_1)\ .\tag{3.3.86}$$

For the vertex $h_{12}(k)h_{12}(k')\phi(p)\phi(q)$ ($= h_{21}(k)h_{21}(k')\phi(p)\phi(q) = \frac{1}{2}\,[h_{12}(k)h_{21}(k')$ $\phi(p)\phi(q) + h_{21}(k)h_{12}(k')\phi(p)\phi(q)]$),

$$\begin{aligned}
&\tfrac{1}{2}(-\cos\tfrac{k_2}{2}+3\cos\tfrac{k_2+k_2'}{2})\sin(\tfrac{p_1}{2})\sin(\tfrac{q_1}{2})\\
&+\tfrac{1}{2}(-\cos\tfrac{k_1}{2}+3\cos\tfrac{k_1+k_1'}{2})\sin(\tfrac{p_2}{2})\sin(\tfrac{q_2}{2})\ ,
\end{aligned}\tag{3.3.87}$$

and its leading continuum approximation for small momenta is

$$\frac{1}{4}\,p\cdot q\ .\tag{3.3.88}$$

The above lattice Feynman rules for the 2-graviton 2-scalar vertex in terms of $h_{\mu\nu}$ can be compared to the continuum Feynman rules, which are given by the following expression

$$\begin{aligned}
V_{\mu\nu,\alpha\beta} \;=\; &(1/4)\,[\,\delta_{\mu\alpha}\,(p_\nu q_\beta+p_\beta q_\nu)+\delta_{\mu\beta}\,(p_\nu q_\alpha+p_\alpha q_\nu)\\
&+\delta_{\nu\alpha}\,(p_\mu q_\beta+p_\beta q_\mu)+\delta_{\nu\beta}\,(p_\mu q_\alpha+p_\alpha q_\mu)-\delta_{\mu\nu}\,(p_\alpha q_\beta+p_\beta q_\alpha)\\
&-\delta_{\alpha\beta}\,(p_\mu q_\nu+p_\nu q_\mu)+(\delta_{\mu\nu}\delta_{\alpha\beta}-\delta_{\mu\alpha}\delta_{\nu\beta}-\delta_{\mu\beta}\delta_{\nu\alpha}\,)\,p\cdot q\,]\ .
\end{aligned}\tag{3.3.89}$$

Again one sees that the 2-graviton 2-scalar vertex in the leading continuum approximation reduces completely to the continuum Feynman rules (see eq.(2.2.17), chapter 2.)

In order to see how much the lattice Feynman rules depend on a particular lattice triangulation, one can derive the Feynman rules for the lattice obtained by

a reflection with respect to the vertical axis (see Figure 6b). It turns out that these Feynman rules can simply be obtained by performing the following substitutions in all the above formulae for the vertices,

$$p_1 \to -p_1, q_1 \to -q_1, k_1 \to -k_1, k_1' \to -k_1' \quad , \tag{3.3.90}$$

which indeed corresponds to a reflection about the vertical axis. In this case the leading continuum approximation of the lattice Feynman rules are again identical to the continuum Feynman rules. One therefore concludes that the two inequivalent lattice triangulations give the same physical results, at least to the first leading continuum order (for momenta which are small compared to the ultraviolet cut-off). This should not come as a surprise, since the two lattices correspond to two equivalent parameterizations of flat space, with an action that is parameterization invariant, at least for small deformations.

3.3.2 Conformal Anomaly

As an application, we will compute the graviton self-energy using the lattice Feynman rules developed above. There are two diagrams contributing to the lattice graviton self-energy, namely the vacuum polarization loop and the tadpole diagram shown in Figs. 3.8.

The evaluation of the above diagrams corresponds to a functional integration over the scalar field, performed to lowest order in the weak field expansion, and with a scalar field measure deriving from the functional measure

$$\int_0^\infty \prod_{\text{edges ij}} dl_{ij}^2 \, F_\varepsilon[l] \times \int_{-\infty}^{\infty} \prod_{\text{sites i}} \prod_a d\phi_i^a \quad ; \tag{3.3.91}$$

the specific form of the gravitational measure will not matter in the following calculation since only the scalar field is integrated over. The relevant expressions

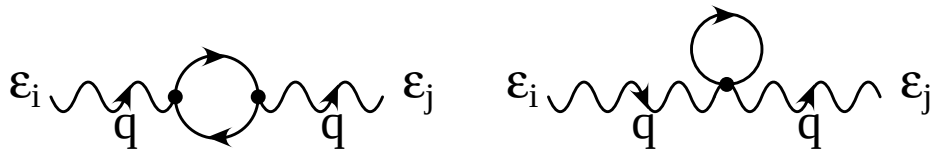

Figure 3.8: Lowest order diagrams contributing to the conformal anomaly.

for the vacuum polarization loop diagram, written in component form, are then

$$\begin{aligned} V_{\varepsilon_1,\varepsilon_1}(q) &= \frac{1}{2}\int_{-\pi}^{\pi}\int_{-\pi}^{\pi}\frac{d^2p}{(2\pi)^2}\left\{-2\sin\frac{p_1}{2}\sin\frac{p_1+q_1}{2}\right. \\ &\quad \left.+\cos\frac{q_2}{2}\sin\frac{p_1+p_2}{2}\sin\frac{p_1+q_1+p_2+q_2}{2}\right\}^2 \\ &\quad \times\frac{1}{16[\ \sum_\mu \sin^2(\frac{p_\mu}{2})\ ][\ \sum_\mu \sin^2(\frac{p_\mu+q_\mu}{2})\ ]}, \end{aligned} \tag{3.3.92}$$

$$\begin{aligned} V_{\varepsilon_2,\varepsilon_2}(q) &= \frac{1}{2}\int_{-\pi}^{\pi}\int_{-\pi}^{\pi}\frac{d^2p}{(2\pi)^2}\left\{-2\sin\frac{p_2}{2}\sin\frac{p_2+q_2}{2}\right. \\ &\quad \left.+\cos\frac{q_1}{2}\sin\frac{p_1+p_2}{2}\sin\frac{p_1+q_1+p_2+q_2}{2}\right\}^2 \\ &\quad \times\frac{1}{16[\ \sum_\mu \sin^2(\frac{p_\mu}{2})\ ][\ \sum_\mu \sin^2(\frac{p_\mu+q_\mu}{2})\ ]}, \end{aligned} \tag{3.3.93}$$

$$\begin{aligned} V_{\varepsilon_3,\varepsilon_3}(q) &= \frac{1}{2}\int_{-\pi}^{\pi}\int_{-\pi}^{\pi}\frac{d^2p}{(2\pi)^2}\left\{2\cos\frac{q_2}{2}\sin\frac{p_1}{2}\sin\frac{p_1+q_1}{2}\right. \\ &\quad \left.+2\cos\frac{q_1}{2}\sin\frac{p_2}{2}\sin\frac{p_2+q_2}{2}-2\sin\frac{p_1+p_2}{2}\sin\frac{p_1+q_1+p_2+q_2}{2}\right\}^2 \\ &\quad \times\frac{1}{16[\ \sum_\mu \sin^2(\frac{p_\mu}{2})\ ][\ \sum_\mu \sin^2(\frac{p_\mu+q_\mu}{2})\ ]}, \end{aligned} \tag{3.3.94}$$

$$\begin{aligned} V_{\varepsilon_1,\varepsilon_2}(q) &= \frac{1}{2}\int_{-\pi}^{\pi}\int_{-\pi}^{\pi}\frac{d^2p}{(2\pi)^2}\left\{(-2\sin\frac{p_1}{2}\sin\frac{p_1+q_1}{2}+\cos\frac{q_2}{2}\sin\frac{p_1+p_2}{2}\right. \\ &\quad \times\sin\frac{p_1+q_1+p_2+q_2}{2})\times(-2\sin\frac{p_2}{2}\sin\frac{p_2+q_2}{2}+ \\ &\quad \left.\cos\frac{q_1}{2}\sin\frac{p_1+p_2}{2}\sin\frac{p_1+q_1+p_2+q_2}{2})\right\} \\ &\quad \times\frac{1}{16[\ \sum_\mu \sin^2(\frac{p_\mu}{2})\ ][\ \sum_\mu \sin^2(\frac{p_\mu+q_\mu}{2})\ ]}. \end{aligned} \tag{3.3.95}$$

$$
\begin{aligned}
V_{\varepsilon_1,\varepsilon_3}(q) &= \frac{1}{2}\int_{-\pi}^{\pi}\int_{-\pi}^{\pi}\frac{d^2p}{(2\pi)^2}\Big\{(-2\sin\frac{p_1}{2}\sin\frac{p_1+q_1}{2}+\cos\frac{q_2}{2}\sin\frac{p_1+p_2}{2} \\
&\times\sin\frac{p_1+q_1+p_2+q_2}{2})\times(2\cos\frac{q_2}{2}\sin\frac{p_1}{2}\sin\frac{p_1+q_1}{2}+ \\
&2\cos\frac{q_1}{2}\sin\frac{p_2}{2}\sin\frac{p_2+q_2}{2}-2\sin\frac{p_1+p_2}{2}\sin\frac{p_1+q_1+p_2+q_2}{2})\Big\} \\
&\times\frac{1}{16[\ \sum_\mu \sin^2(\frac{p_\mu}{2})\ ][\ \sum_\mu \sin^2(\frac{p_\mu+q_\mu}{2})\ ]}. \qquad (3.3.96)
\end{aligned}
$$

$$
\begin{aligned}
V_{\varepsilon_2,\varepsilon_3}(q) &= \frac{1}{2}\int_{-\pi}^{\pi}\int_{-\pi}^{\pi}\frac{d^2p}{(2\pi)^2}\Big\{(-2\sin\frac{p_2}{2}\sin\frac{p_2+q_2}{2}+\cos\frac{q_1}{2}\sin\frac{p_1+p_2}{2} \\
&\times\sin\frac{p_1+q_1+p_2+q_2}{2})\times(2\cos\frac{q_2}{2}\sin\frac{p_1}{2}\sin\frac{p_1+q_1}{2}+ \\
&2\cos\frac{q_1}{2}\sin\frac{p_2}{2}\sin\frac{p_2+q_2}{2}-2\sin\frac{p_1+p_2}{2}\sin\frac{p_1+q_1+p_2+q_2}{2})\Big\} \\
&\times\frac{1}{16[\ \sum_\mu \sin^2(\frac{p_\mu}{2})\ ][\ \sum_\mu \sin^2(\frac{p_\mu+q_\mu}{2})\ ]}. \qquad (3.3.97)
\end{aligned}
$$

For zero external momentum q all the quantities $V_{\varepsilon_i,\varepsilon_j}$'s are infrared finite, and one finds

$$
\begin{aligned}
V_{\varepsilon_1,\varepsilon_1}(q=0) &= \frac{1}{16}\left(1-\frac{2}{\pi}\right) \\
V_{\varepsilon_2,\varepsilon_2}(q=0) &= \frac{1}{16}\left(1-\frac{2}{\pi}\right) \\
V_{\varepsilon_3,\varepsilon_3}(q=0) &= \frac{1}{8}\left(1-\frac{2}{\pi}\right) \\
V_{\varepsilon_1,\varepsilon_2}(q=0) &= 0 \\
V_{\varepsilon_1,\varepsilon_3}(q=0) &= -\frac{1}{16}\left(-1+\frac{1}{\pi}\right) \\
V_{\varepsilon_2,\varepsilon_3}(q=0) &= -\frac{1}{16}\left(-1+\frac{1}{\pi}\right)
\end{aligned} \qquad (3.3.98)
$$

The q^2-dependent terms are the ones that are of physical importance. Expanding the lattice integrals for small external momentum one obtains for example

$$
V_{\varepsilon_1,\varepsilon_1}(q1=q2=q)=\frac{1}{16}\left(1-\frac{2}{\pi}\right)+\frac{1}{96\pi}q^2+O(q^4)\ , \qquad (3.3.99)
$$

which can be compared with the continuum result for the metric vacuum polarization

$$\Pi_{11,11} = \frac{1}{96\pi} q^2 + O(q^4) \quad . \tag{3.3.100}$$

The expressions relevant for the tadpole diagram, written in component form, are

$$\begin{aligned} T_{\varepsilon_1,\varepsilon_1}(q) &= \int_{-\pi}^{\pi}\int_{-\pi}^{\pi} \frac{d^2p}{(2\pi)^2} \left\{ 2\sin^2(\frac{p_1}{2}) + \sin^2(\frac{p_2}{2}) - \frac{1}{2}\sin^2(\frac{p_1+p_2}{2}) \right\} \\ &\quad \times \frac{1}{4\,[\,\sum_\mu \sin^2(\frac{p_\mu}{2})]}. \end{aligned} \tag{3.3.101}$$

$$\begin{aligned} T_{\varepsilon_2,\varepsilon_2}(q) &= \int_{-\pi}^{\pi}\int_{-\pi}^{\pi} \frac{d^2p}{(2\pi)^2} \left\{ \sin^2(\frac{p_1}{2}) + 2\sin^2(\frac{p_2}{2}) - \frac{1}{2}\sin^2(\frac{p_1+p_2}{2}) \right\} \\ &\quad \times \frac{1}{4\,[\,\sum_\mu \sin^2(\frac{p_\mu}{2})]}. \end{aligned} \tag{3.3.102}$$

$$\begin{aligned} T_{\varepsilon_3,\varepsilon_3}(q) &= \int_{-\pi}^{\pi}\int_{-\pi}^{\pi} \frac{d^2p}{(2\pi)^2} \left\{ 3\sin^2(\frac{p_1}{2}) + 3\sin^2(\frac{p_2}{2}) - \sin^2(\frac{p_1+p_2}{2}) \right\} \\ &\quad \times \frac{1}{4\,[\,\sum_\mu \sin^2(\frac{p_\mu}{2})]}. \end{aligned} \tag{3.3.103}$$

$$\begin{aligned} T_{\varepsilon_1,\varepsilon_2}(q) &= \int_{-\pi}^{\pi}\int_{-\pi}^{\pi} \frac{d^2p}{(2\pi)^2} \cos\frac{q_1+q_2}{2} \left\{ 2\sin^2(\frac{p_1}{2}) + 2\sin^2(\frac{p_2}{2}) \right. \\ &\quad \left. -2\sin^2(\frac{p_1+p_2}{2}) \right\} \times \frac{1}{4\,[\,\sum_\mu \sin^2(\frac{p_\mu}{2})]}. \end{aligned} \tag{3.3.104}$$

$$\begin{aligned} T_{\varepsilon_1,\varepsilon_3}(q) &= \int_{-\pi}^{\pi}\int_{-\pi}^{\pi} \frac{d^2p}{(2\pi)^2} \cos\frac{q_2}{2} \left\{ -4\sin^2(\frac{p_1}{2}) - 4\sin^2(\frac{p_2}{2}) + 2\sin^2(\frac{p_1+p_2}{2}) \right\} \\ &\quad \times \frac{1}{4\,[\,\sum_\mu \sin^2(\frac{p_\mu}{2})]}. \end{aligned} \tag{3.3.105}$$

$$\begin{aligned} T_{\varepsilon_2,\varepsilon_3}(q) &= \int_{-\pi}^{\pi}\int_{-\pi}^{\pi} \frac{d^2p}{(2\pi)^2} \cos\frac{q_1}{2} \left\{ -4\sin^2(\frac{p_1}{2}) - 4\sin^2(\frac{p_2}{2}) + 2\sin^2(\frac{p_1+p_2}{2}) \right\} \\ &\quad \times \frac{1}{4\,[\,\sum_\mu \sin^2(\frac{p_\mu}{2})]}. \end{aligned} \tag{3.3.106}$$

The first three integrals are q-independent, while in the last three the q-dependence factorizes. One finds

$$\begin{aligned} T_{\varepsilon_1,\varepsilon_1}(q) &= \frac{3}{8} - \frac{1}{4\pi} \\ T_{\varepsilon_2,\varepsilon_2}(q) &= \frac{3}{8} - \frac{1}{4\pi} \\ T_{\varepsilon_3,\varepsilon_3}(q) &= \frac{3}{4} - \frac{1}{2\pi} \\ T_{\varepsilon_1,\varepsilon_2}(q) &= \cos(\frac{q_1+q_2}{2}) \left(\frac{1}{2} - \frac{1}{\pi}\right) \\ T_{\varepsilon_1,\varepsilon_3}(q) &= \cos(\frac{q_2}{2}) \left(-1 + \frac{1}{\pi}\right) \\ T_{\varepsilon_2,\varepsilon_3}(q) &= \cos(\frac{q_1}{2}) \left(-1 + \frac{1}{\pi}\right) \end{aligned} \tag{3.3.107}$$

The terms in $T_{\varepsilon_i,\varepsilon_j}(q)$ are required to cancel some of the unwanted, including non-covariant, terms in $V_{\varepsilon_i,\varepsilon_j}(q)$. Also, a number of contributions to the lattice vacuum polarization can be shown to contribute to a renormalization of the cosmological constant. It should be noted here that the lattice form of the cosmological constant term (which just corresponds to the total area of the triangulated manifold) contains, in contrast to the continuum, momentum dependent terms [47]. The reason for this is that the lattice area terms couple neighboring edges, and lead therefore to some residual local interactions between the edges variables, as shown in Eq. (3.3.39).

Eventually one needs to rotate the final answer for the vacuum polarization from the ε_i to the $h_{\mu\nu}$ variables, which is achieved to linear order (and for small q) by the matrix

$$V = \begin{pmatrix} \frac{1}{2} & 0 & 0 \\ 0 & \frac{1}{2} & 0 \\ \frac{1}{4} & \frac{1}{4} & \frac{1}{2} \end{pmatrix} \quad . \tag{3.3.108}$$

with $\varepsilon(q) = V \cdot h(q)$ (see Eq. (3.3.38)). Since the integration over the scalar gives

$$I_{eff} = -\tfrac{1}{2} \int \frac{d^2q}{(2\pi)^2}\, h(q) \cdot \Pi(h) \cdot h(q) = -\tfrac{1}{2} \int \frac{d^2q}{(2\pi)^2}\, \varepsilon(q) \cdot \Pi(\varepsilon) \cdot \varepsilon(q) \ , \qquad (3.3.109)$$

one obtains the correspondence between the two polarization quantities,

$$\Pi(h) = V^{-1} \cdot \Pi(\varepsilon) \cdot V \ , \qquad (3.3.110)$$

correct to lowest order in the weak field expansion.

Analytical evaluations of the remaining integrals in terms of Bessel functions will be presented elsewhere [72]. In the following we will calculate the graviton self-energy using the lattice Feynman rules in the leading continuum order, by doing a continuum approximation to the integrands valid for small momenta. The procedure is justified for integrands that are sharply peaked in the low momentum region, and neglects the effects due to presence of a high momentum cutoff.

The calculation is most easily done by using the Feynman rules in terms of $h_{\mu\nu}$ in the Lorentz covariant form, which were given before. The vacuum polarization loop contributing to the graviton self-energy then reduces to

$$\begin{aligned} V_{\mu\nu,\alpha\beta}(q) &= \frac{1}{2} \int \frac{d^2p}{(2\,\pi)^2} \frac{t_{\mu\nu}(p,q)\, t_{\alpha\beta}(p,q)}{p^2\,(p+q)^2} \\ t_{\mu\nu}(p,q) &= \frac{1}{2}\,[\,\delta_{\mu\nu} p\cdot(p+q) - p_\mu\,(p_\nu + q_\nu) - p_\nu\,(p_\mu + q_\mu)\,] \ . \end{aligned} \qquad (3.3.111)$$

The calculation of the integral is easily done using dimensional regularization. One obtains

$$V_{\mu\nu,\alpha\beta}(q) = \frac{1}{48\,\pi}\,(q^2\delta_{\mu\nu} - q_\mu q_\nu)\,\frac{1}{q^2}\,(q^2\delta_{\alpha\beta} - q_\alpha q_\beta) \ . \qquad (3.3.112)$$

As expected, the tadpole contribution $T_{\mu\nu,\alpha\beta}(q)$ to the graviton self-energy is 0. The remaining graviton self-energy contribution is given by

$$\begin{aligned} \Pi_{\mu\nu,\alpha\beta}(q) &= V_{\mu\nu,\alpha\beta}(q) + T_{\mu\nu,\alpha\beta}(q) \\ &= \frac{1}{48\,\pi}\,(q^2\delta_{\mu\nu} - q_\mu q_\nu)\,\frac{1}{q^2}\,(q^2\delta_{\alpha\beta} - q_\alpha q_\beta) \ . \end{aligned} \qquad (3.3.113)$$

The above result is valid for one real massless scalar field. For a D-component scalar field, the above result would get multiplied by a factor of D. Then the effective action, obtained from integrating out the scalar degrees of freedom, and to lowest order in the weak field expansion, is given by

$$I_{eff} = -\tfrac{1}{2} \int \frac{d^2q}{(2\pi)^2}\, h_{\mu\nu}(q)\, \Pi_{\mu\nu\rho\sigma}(q)\, h_{\rho\sigma}(-q) \quad , \tag{3.3.114}$$

with the scalar vacuum polarization given by

$$\Pi_{\mu\nu\rho\sigma}(q) = \frac{D}{48\pi} (q_\mu q_\nu - \delta_{\mu\nu} q^2) \frac{1}{q^2} (q_\rho q_\sigma - \delta_{\rho\sigma} q^2) \quad . \tag{3.3.115}$$

In the lattice analog of the continuum conformal gauge,

$$g_{\mu\nu}(x) = \delta_{\mu\nu}\, e^{\varphi(x)} \quad , \tag{3.3.116}$$

one can write for the scalar curvature

$$(q_\mu q_\nu - \delta_{\mu\nu} q^2) h_{\mu\nu}(q) = R(q) = q^2 \varphi(q) \quad , \tag{3.3.117}$$

and therefore re-write the effective action in the form

$$I_{eff}(\varphi) = -\frac{D}{96\pi} \int \frac{d^2q}{(2\pi)^2}\, \varphi(q)\, q^2 \varphi(-q) \quad , \tag{3.3.118}$$

which in real space becomes the well-known Liouville action

$$I_{eff}(\varphi) = -\frac{D}{96\pi} \int d^2x \left[(\partial_\mu \varphi)^2 + (\lambda - \lambda_c)\, e^{\varphi} \right] \quad . \tag{3.3.119}$$

One therefore completely recovers the result derived perturbatively from the continuum Feynman rules, as given for example in [53]).

In the continuum, the effective action term of Eq. (3.3.119) arising from the conformal anomaly can be written in covariant form as

$$\tfrac{1}{2} \int d^2x\, d^2y\, R\sqrt{g}(x)\, \langle x | \frac{1}{-\partial^2 + m^2} | y \rangle\, R\sqrt{g}(y) \quad , \tag{3.3.120}$$

where ∂^2 is the continuum covariant Laplacian, $\partial^2 \equiv \partial_\mu(\sqrt{g} g^{\mu\nu} \partial_\nu)$, and $m^2 \to 0$. In two dimensions and for flat space, $\langle x | \frac{1}{\partial^2} | y \rangle \sim \frac{1}{2\pi} \log |x-y|$. Using the correspondence

between lattice and continuum curvature operators derived in [43], its lattice form gives rise to an effective long-range interaction between deficit angles of the type

$$\tfrac{1}{2} \sum_{\text{hinges}\, h,h'} \delta_h \left[\frac{1}{-\Delta + m^2}\right]_{h,h'} \delta_{h'} \quad , \tag{3.3.121}$$

where Δ is the nearest-neighbor covariant lattice Laplacian, as obtained from the discrete scalar action, and $m^2 \to 0$ an infrared mass regulator. This result was given in [47]; see also the recent discussion in [73].

In general one cannot expect the lattice expression for the vacuum polarization to match completely the continuum expression already at the lowest order of perturbation theory. Since there is *no* small parameter controlling the weak field expansion in two dimensions, it is difficult to see why the first few orders on the lattice should suffice. Indeed in the weak field expansion the background lattice is usually taken to be regular, which leads to a set of somewhat preferred lattice directions for high momenta, which are close to the momentum cutoff at $\pm\pi$. It would seem though that this is an artifact of the choice of background lattice (which is necessarily rigid), and whose effects are eventually washed out when the fluctuations is the edge lengths are properly accounted for in higher order in the weak field expansion. The fact that the conformal mode in fact remains massless in two dimensions in the full numerical, non-perturbative treatment of the lattice theory was shown in [83, 66], without the necessity of any sort of fine-tuning of bare parameters.

The gravitational contribution to the effective action in the lattice conformal gauge can, at least in principle, be computed in a similar way. Let us sketch here how the analogous lattice calculation would proceed; a more detailed discussion of the relevant calculations will be presented elsewhere. In the continuum the metric perturbations are naturally decomposed into conformal and diffeomorphism parts,

$$\delta g_{\mu\nu}(x) = g_{\mu\nu}(x)\ \delta\varphi(x) + \nabla_\mu \chi_\nu(x) + \nabla_\nu \chi_\mu(x) \quad . \tag{3.3.122}$$

where ∇_ν denotes the covariant derivative. A similar decomposition can be done for the lattice degrees of freedom, by separating out the lattice gauge transformations [40] (which act on the vertices and change the edge lengths without changing the local curvatures) from the conformal transformations (which change the local volumes and curvatures) in Eq. (3.3.45). The explicit form for the lattice diffeomorphisms, to lowest order in the lattice weak field expansion, is given in Eq. (3.3.43), which makes it obvious that such a decomposition can indeed be performed on the lattice. After rewriting the gravitational functional measure in terms of conformal and diffeomorphism degrees of freedom,

$$[dg] \;=\; [d\varphi][d\chi]\,[\det\,(L^{+}L)]^{\frac{1}{2}} \quad , \tag{3.3.123}$$

which involves the Jacobian of the operator L, which in the continuum is determined from

$$(L^{+}L\;\chi)_\mu = \nabla^\nu(\nabla_\mu\chi_\nu + \nabla_\nu\chi_\mu - g_{\mu\nu}\nabla^\rho\chi_\rho) \quad , \tag{3.3.124}$$

one has for the effective action contribution in the conformal gauge, and to lowest order in the weak field expansion,

$$[\det\,(L^{+}L)]^{-\frac{1}{2}} \;\sim\; \exp\left\{-I_{\mathit{eff}}(\varphi)\right\} \quad . \tag{3.3.125}$$

The lattice form of L depends on the specific form of the lattice gauge fixing term. On the lattice the functional integration is performed over the edge lengths, see Eq. (3.2.3). The lattice conformal gauge choice corresponds to an assignment of edge lengths such that

$$g_{ij}(n) = \begin{pmatrix} l_3^2 & \frac{1}{2}(-l_1^2+l_2^2+l_3^2) \\ \frac{1}{2}(-l_1^2+l_2^2+l_3^2) & l_2^2 \end{pmatrix} \;\approx\; \delta_{ij}\,e^{\varphi(n)} \quad . \tag{3.3.126}$$

The lattice fields $\varphi(n)$ are defined on the lattice vertices. So are the gauge degrees of freedom $\chi_\mu(n)$, as can be seen from Eq. (3.3.44). It should therefore be clear that the choice of lattice conformal gauge corresponds to a re-assignment of edge

lengths about each vertex which leaves the local curvature unchanged but brings the induced metric into diagonal form; it corresponds to a choice of approximately right-angle triangles at each vertex [70].

A diagrammatic calculation, similar to the one for the scalar field contribution, gives in the continuum the celebrated result [53]

$$\Pi_{\mu\nu\rho\sigma}(q) = \frac{13}{48\pi}\,(q_\mu q_\nu - \delta_{\mu\nu}q^2)\,\frac{1}{q^2}\,(q_\rho q_\sigma - \delta_{\rho\sigma}q^2) \quad . \tag{3.3.127}$$

As a consequence the total Liouville action for the field $\varphi = \frac{1}{\partial^2}R$ becomes

$$I_{\mathit{eff}}(\varphi) \;=\; \frac{26-D}{96\pi}\int d^2x\,\left[(\partial_\mu\varphi)^2 + (\lambda-\lambda_c)\,e^{\varphi}\right] \quad , \tag{3.3.128}$$

Thus to lowest order in the weak field expansion the critical value of D for which the action vanishes is $D_c = 26$, but this number is expected to get modified by higher order quantum corrections. In any case, for sufficiently large D one expects an instability to develop. Numerical nonperturbative studies of two-dimensional gravity suggest that in the lattice theory the correction is large, and one finds that the threshold of instability moves to $D_c \approx 13$ [66]. It is unclear if this critical value can be regarded as truly universal, and independent for example on the detailed choice of gravitational measure.

3.4 Conclusions

In the previous section we have presented results relevant for the weak field expansion of lattice gravity. We have shown the precise correspondence between continuum and lattice degrees of freedom within the context of such an expansion. To avoid unnecessary technical complications, most of our discussion has focused on the two-dimensional case, but the methods presented here can be applied to any dimension. In the purely gravitational case, we have shown that the presence of

zero modes is tied to the existence of a local invariance of the gravitational action. This invariance corresponds precisely to the diffeomorphisms in the continuum, with appropriate deformations in the edge lengths playing the role of local gauge variations of the metric in the continuum.

We have then derived the Feynman rules for gravity coupled to a massless scalar field, to lowest order in the weak field expansion. Although the lattice Feynman rules for the edge length vertices appear to be rather unwieldy, they actually reduce to the familiar continuum form when re-expressed in terms of the weak field metric field, and we have presented this important result in detailed form. As an application, the two-dimensional conformal anomaly due to a massless scalar field was computed by diagrammatic methods. We have given explicitly the relevant lattice integrals, which involve among other things a new diagram, the tadpole term, which vanishes in the continuum but is necessary on the lattice for canceling unwanted terms. Finally we have shown that in the leading continuum approximation the expected continuum form for the anomaly is obtained, with the correct coefficient.

The procedure followed here in deriving the Feynman rules for lattice gravity works in any dimension, including therefore the physical case of four dimensions. The lack of perturbative renormalizability in four dimensions is not ameliorated though by the presence of an explicit lattice cutoff, and non-perturbative searches for an ultraviolet fixed point and a lattice continuum limit are still required.

Chapter 4

Random Ising Spins in Two Dimensions - A Flat Space Realization of the KPZ Exponents

4.1 Introduction

In this chapter we will discuss the computer simulation aspect of quantum gravity. More specifically we will consider the dynamics of random Ising spins coupled to gravity in two dimensions. The continuum space is divided into a random lattice. Ising spins with spin either up or down are placed at the vertices of the lattice, and are allowed to move randomly on a discretized version of a fluid surface. The lattice geometry is allowed to fluctuate by varying the local coordination number through a "link flip" operation which varies the local connectivity [77]. The transformation from the continuum spacetime to lattice (after a Wick rotation) essentially turns the field theory into a statistical mechanics theory. Our study of this "statistical" system consists of several steps. The first step is to determine if this system has a phase transition. Whether a phase transition has taken placed is manifested by the singular (or vanishing) nature of some thermodynamic functions at the phase transition point. The phase diagram can be mapped out by a carefully study of these thermodynamic functions. After the phase transition has taken place, the initial symmetry of the system may no longer be preserved by the new ground

state. In this case, the system is said to have undergone a spontaneous symmetry breaking. This breaking of the symmetry has a great relevance in quantum field theory as the masses of gauge field particles are generated in this manner, known as the Higgs mechanism. In the regular (Onsagar) Ising model, magnetization can be spontaneously generated even in the absence of an external magnetic field. Another interesting thing happened at the critical point is that the correlation length of the system becomes infinite. The details of the underlying lattice is no longer revalent, and the continuous spacetime symmetries of the field theory are restored. In this chapter, we will be interested in measuring thermodynamical quantities, such as spontaneous magnetization per spin, zero field susceptibility, latent heat, average energy per spin, and specific heat, in our dynamically triangulated random Ising model. The phase transition diagram will be constructed by examining the behavior of these quantities.

After the phase diagram of the theory has been established, we are next to determine the order of the phase transition, as well as the critical exponents characterizing the universality class of the system. One of the most interesting aspect of critical phenomena is that many systems with different lattice structures have the exact critical exponents which allow us to classify them by their universality property.

Before we actually go into the Ising model on random surface, it is useful to give a brief review of the exactly solvable Onsager Ising model on two dimensions [78, 79, 80]. Consider a two dimensional flat surface divided into square lattice. Each site of the lattice is labeled by a vector of a pair integers,

$$n = (n_x, n_y). \tag{4.1.1}$$

A spin variable $s(n)$ with spin value +1 (up) or −1 (down) is placed at the site n.

The action describing the model is

$$S = -J \sum_{n,\mu} s(n)s(n+\mu), \tag{4.1.2}$$

where μ is an unit vector connecting the two neighboring spins. The Ising spin interaction is local; it only interacts with its four nearest neighbors. We further choose the coupling parameter J positive such that the system results in a lower energy state when the neighboring two spins have both +1 or both −1 spins. The system is called ferromagnetic (as contrast to anti-ferromagnetic when $J < 0$.) The system posses a global symmetry. When all spins flip their values, the action S remains unchanged. This global symmetry can be explicitly broken by introducing an external magnetic field B to the action

$$S = -J \sum_{n,\nu} s(n)s(n+\nu) - B \sum_{n} s(n). \tag{4.1.3}$$

The partition function of the statistical system is given by

$$Z = \sum_{configs} e^{-\beta S}, \tag{4.1.4}$$

where the sum runs over all possible spin configurations. On a lattice of N sites, there are 2^N possible configurations. $\beta = 1/kT$ is the inversed Ising temperature.

Some interesting thermodynamic quantities are: free energy

$$F = -\beta\ T\ \ln Z\ ; \tag{4.1.5}$$

magnetization per site

$$M = \frac{1}{N}\frac{\partial F}{\partial B}\ ; \tag{4.1.6}$$

magnetic susceptibility per site

$$\begin{aligned} \chi &= \frac{\partial M}{\partial B}\ |_{B=0} \\ &= \frac{1}{NkT}[\ <(s_{tot} - < s_{tot} >)^2 >\ ]\ ; \end{aligned} \tag{4.1.7}$$

and the specific heat

$$C = -T\frac{\partial^2 F}{\partial T^2}. \tag{4.1.8}$$

The system can undergo a spontaneous magnetization even in the absence of external magnetic field B when the temperature T is below the critical value T_c. Above T_c the system is completely random, and exhibits no magnetization. The magnetization M is thus served as a local order parameter characterizing the phase transition of the Ising system. At the phase transition region, many thermodynamic quantities obey some scaling laws: for the magnetization,

$$M \sim (T_c - T)^{\beta}, \tag{4.1.9}$$

where β is called the magnetization critical exponent; for the spin-spin correlation function,

$$\begin{aligned} \Gamma(n) &= < s(n)s(0) > \\ &\sim |n|^{-(d-2+\eta)}, \ T = T_c ; \end{aligned} \tag{4.1.10}$$

for the correlation length,

$$\xi(T) \sim (T - T_c)^{-\nu} ; \tag{4.1.11}$$

for the susceptibility,

$$\chi \sim (T - T_c)^{-\gamma} ; \tag{4.1.12}$$

for the specific heat,

$$C \sim (T - T_c)^{-\alpha} ; \tag{4.1.13}$$

and for the magnetization when a small external magnetic field B is applied,

$$m \sim B^{1/\delta}, \ T = T_c . \tag{4.1.14}$$

The critical exponents are solved exactly in the two dimensional Ising model (Onsaga). They are $\beta = 1/8$, $\eta = 1/4$, $\nu = 1$, $\gamma = 7/4$, $\alpha = 0$, and $\delta = 15$. Furthermore,

these critical indices are related as follows

$$\begin{aligned}
\beta &= \frac{1}{2}\nu(d-2+\eta), \\
\gamma &= \nu(2-\eta), \\
\alpha &= 2-\nu d, \\
\delta &= (d+2-\eta)/(d-2+\eta).
\end{aligned} \tag{4.1.15}$$

There are thus essentially only two independent critical exponents in the regular Ising model in two dimensions. A very important property of these critical exponents is that these values are shared by many physical systems with different lattice structures. Anisotropic lattices of the Ising model having the same critical indices are said to belong to the same universality class.

Exact solution of the Ising model on a random surface is solved in matrix model methods [74]. In this model, in addition to all 2^N spin configurations summed over, all planar graphs with the topology of sphere and N vertices are summed over in the action. The phase transition of this model is found to be third order instead of second order in regular Ising model. This work has been extented to study the properties of random Ising spins coupled to two-dimensional gravity. More recently, work based on both series expansions [75, 76] and numerical simulations [77, 81] has verified and extended the original results. Remarkably, the same critical exponents have been found using consistency conditions derived from conformal field theory for central charge $c = \frac{1}{2}$ [82], which should again apply to Ising spins. It is generally believed that the new values for the Ising critical exponents are due to the random fluctuations of the surface in which the spins are embedded, and therefore intimately tied to the intrinsic fractal properties of fluctuating geometries. It comes therefore as a surprise that in our study of non-random Ising spins, placed on a randomly fluctuating geometry but with fixed spin coordination number, exhibits the same critical behavior as in flat space, without

any observed "gravitational" shift of the exponents [83].

The natural question to ask is to what extent the values of the critical Ising exponents found by KPZ for $c = \frac{1}{2}$ and in the matrix model solution ($\alpha = -1$, $\beta = 1/2$, $\gamma = 2$, $\eta = 2/3$, $\nu = 3/2$ [74, 82]) are due to the *annealed* randomness of the lattice, and to what extent they are due to the physical presence of a fluctuating background metric. The most straightforward way to answer this question is to investigate the critical properties of annealed random Ising spins, with interactions designed to mimic as closely as possible the dynamical triangulation model, but placed in flat two-dimensional space. It is well known that for a *quenched* random lattice the critical exponents are the same as on a regular lattice [84], as expected on the basis of universality, even though in two dimensions the Harris criterion (which applies to quenched impurities only) does not give a clear prediction, since the specific heat exponent vanishes, $\alpha = 0$, for Onsager's solution.

4.2 Formulation of the Model

In a square d-dimensional box of sides L with periodic boundary conditions we introduce a set of $N = L^d$ Ising spins $S_i = \pm 1$ with coordinates x_i^a, $i = 1 \ldots N$, $a = 1 \ldots d$, and average density $\rho = N/L^d = 1$. Both the spins and the coordinates will be considered as dynamical variables in this model. Interactions between the spins are determined by

$$I[x, S] \;=\; -\sum_{i<j} J_{ij}(x_i, x_j)\; W_{ij}\; S_i S_j - h \sum_i W_i\; S_i \quad , \tag{4.2.16}$$

with ferromagnetic coupling

$$J_{ij}(x_i, x_j) = \begin{cases} 0 & \text{if } |x_i - x_j| > R \\ J & \text{if } r < |x_i - x_j| < R \end{cases} \quad , \tag{4.2.17}$$

and infinite energy for $|x_i - x_j| < r$, giving therefore a hard core repulsion radius equal to $r/2$. As will be discussed further below, the hard core repulsive interaction

is necessary for obtaining a non-trivial phase diagram, and mimics the interaction found in the dynamical triangulation model, where the minimum distance between any two spins is restricted to be one lattice spacing. For $r \to 0, J_{ij} = J[1-\theta(|x_i-x_j|-R)]$.

The weights W_{ij} and W_i appearing in Eq. (4.2.16) could in principle contain geometric factors associated with the random lattice subtended by the points, and involve quantities such as the areas of the triangles associated with the vertices, as well as the lengths of the edges connecting the sites. In the following we will consider only the simplest case of unit weights, $W_{ij} = W_i = 1$. On the basis of universality of critical behavior one would expect that the results should not be too sensitive to such a specific choice, which only alters the short distance details of the model, and should not affect the exponents.

The full partition function for coordinates and spins is then written as

$$Z = \prod_{i=1}^{N} \sum_{S_i=\pm 1} (\prod_{a=1}^{d} \int_0^L dx_i^a) \exp(-I[x,S]) \quad . \tag{4.2.18}$$

In the following we will only consider the two-dimensional case, $d = 2$, for which specific predictions are available from the work of KPZ and the matrix model solution.

It should be clear that if the interaction range R is of order one, then, for sufficiently large hard core repulsion, $r \to \sqrt{5}/2 < R$, the spins will tend to lock in into an almost regular triangular lattice. As will be shown below, in practice this crossover happens already for quite small values of r. The critical behavior is then the one expected for the regular Ising model in two dimensions, namely a continuous second order phase transition with the Onsager exponents. Indeed for the Ising model on a triangular lattice it is known that $J_c = \frac{1}{2}\sqrt{3}\ln 3 = 0.9514\ldots$. On the other hand if the hard core repulsion is very small, then for sufficiently low temperatures the spins will tend to form tight ordered clusters, in which each spin interacts with a large number of neighbors. As will be shown below, this clustering transition is rather sudden and strongly first order. Furthermore, where the two

transition lines meet inside the phase diagram one would expect to find a tricritical point.

In order to investigate these issues further, we have chosen to study the above system by numerical simulation, with both the spins and the coordinates updated by a standard Monte Carlo method. We choose any spin on the lattice, flip its spin, and increment its (x, y) coordinates by a random amount (between 0 and 1.) The motion of the spin particles results in new neighbors within the interaction range. The probability for both of these occurring is computed, and compared to a random number. If the probability is larger than the random number, both spin flip and change in coordinates are accepted, otherwise both are ejected. This procedure is repeated for every spin in the lattice to give a new configuration. Before any thermodynamic quantities can be computed, many sweeps of the spin configuration must be done to bring the system to the thermal equilibrium state. The computation of thermodynamic averages is quite time consuming in this model, since any spin can in principle interact with any other spin as long as they get sufficiently close together. As a consequence, a sweep through the lattice requires a number of order N^2 operations, which makes it increasingly difficult to study larger and larger lattices. In order to extend our study to even larger lattices, we have applied a binning procedure in such a way that the time for the updating of a given configuration grows as zN, where z is the average coordination number of the lattice, instead of N^2. This binning procedure consists of dividing the system in cells of unit length, and keeping track of the spins in each cell. Since all the moves are local, and spins can only move from a given cell to the neighboring ones, we only need to consider the spins in a given cell and its neighbors at each updating step. This procedure is very effective when the average coordination number is relatively small ($J < J_c$ and r large), however, if $z \sim N$ the updating time grows again as N^2.

There are a number of local averages and fluctuations which can be determined and used to compute the critical exponents. The spontaneous magnetization per spin can be determined as

$$M = \frac{1}{N}\frac{\partial}{\partial h}\ln Z|_{h=0} = \frac{1}{N} < |\sum_i S_i| > \quad , \tag{4.2.19}$$

was measured (here the averages involve both the x and S variables, $< >\equiv< >_{x,S}$), and the zero field susceptibility

$$\chi = \frac{1}{N}\frac{\partial^2}{\partial h^2}\ln Z|_{h=0} = \frac{1}{N} < \sum_{ij} S_i S_j > - \frac{1}{N} < |\sum_i S_i| >^2 . \tag{4.2.20}$$

It is customary to use the absolute value on the r.h.s., since on a finite lattice the spontaneous magnetization, defined without the absolute value, vanishes identically even at low temperatures. In addition, the latent heat and the specific heat exponent can be determined from computing the average Ising energy per spin defined as

$$E \;=\; -\frac{1}{N}\frac{\partial}{\partial J}\ln Z|_{h=0} = -\frac{1}{JN} < \sum_{i<j} J_{ij}(x_i, x_j)\; W_{ij}\; S_i S_j > \quad , \tag{4.2.21}$$

and its fluctuation,

$$C \;=\; \frac{1}{N}\frac{\partial^2}{\partial J^2}\ln Z|_{h=0} \quad . \tag{4.2.22}$$

4.3 Results and Analysis

In the simulations we have investigated lattice sizes varying from $5^2 = 25$ sites to $30^2 = 900$ sites. The length of our runs varies in the critical region ($J \sim J_c$) between 2M sweeps on the smaller lattices and 200k sweeps on the largest lattices. A standard binning procedure then leads to the errors reported in the figures.

As it stands, the model contains three coupling parameters, the ferromagnetic coupling J, the interaction range R and the hard core repulsion parameter r. We have fixed $R = 1$; comparable choices should not change the universality class. As we alluded previously, for small r we find that the system undergoes a sharp first

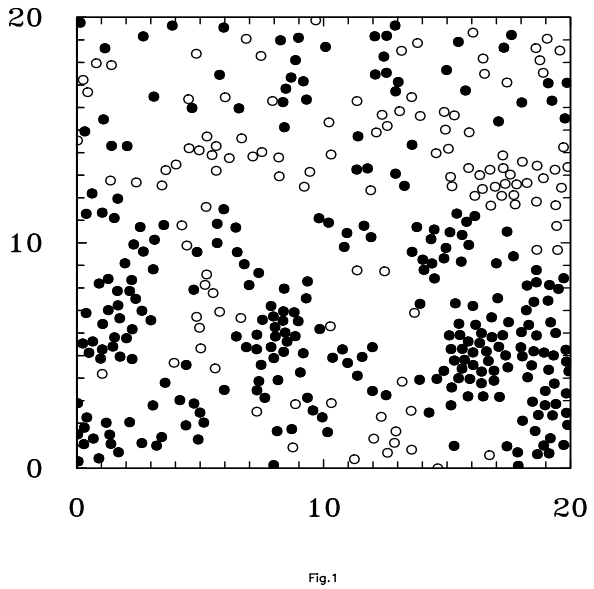

Figure 4.1: A system configuration with $N = 400$ spins and $r = 0.4$ for $J = 0.35$. Spins ± 1 are represented by empty and solid circles, respectively.

order transition, between the disordered phase and a phase in which all spins form a few very tight magnetized clusters, in which the number of neighbors is of the order N. These clusters persist even for larger values of the hard core repulsion, r, but the number of interacting neighbors does not become as large as N in this case.

In Figs. 4.1 and 4.2 we show the existence of these clusters when the hard core repulsion is as large as $r = 0.4$. In Fig. 4.1 we observe ferromagnetic order in small domains even though we are below J_c. On the other hand, in Fig. 4.2, where we are above J_c, the system has practically clustered into a single ferromagnetic domain. For sufficiently large r, the transition is Ising-like, between ordered and disordered, almost regular, Ising lattices (for our choice of range R, the transition appears to be very close to regular Ising-like for $r \approx 0.6$ and larger, see below).

In Fig. 4.3 we show a particular configuration for $r = 0.98$ where the regular, almost triangular, lattice is clearly visible. In this case the average coordination number z is very close to 3, as expected for a regular triangular lattice.

In Fig. 4.4 we show the average number of neighbors z for several values of r

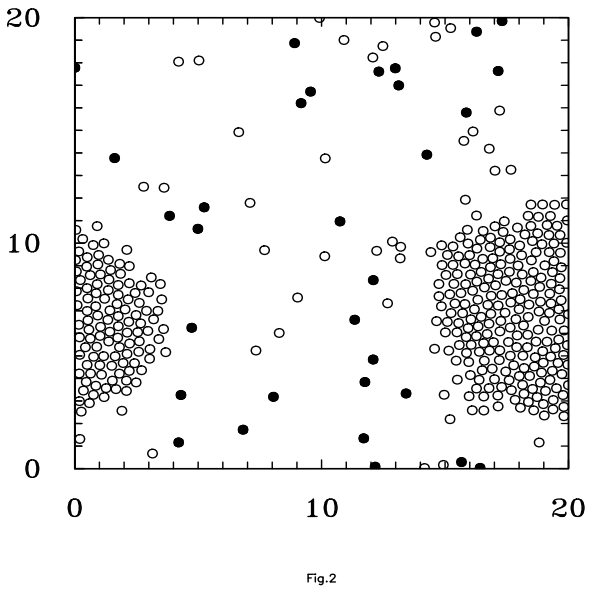

Figure 4.2: A system configuration with $N = 400$ spins and $r = 0.4$ for $J = 0.65$. Spins ± 1 are represented by empty and solid circles, respectively.

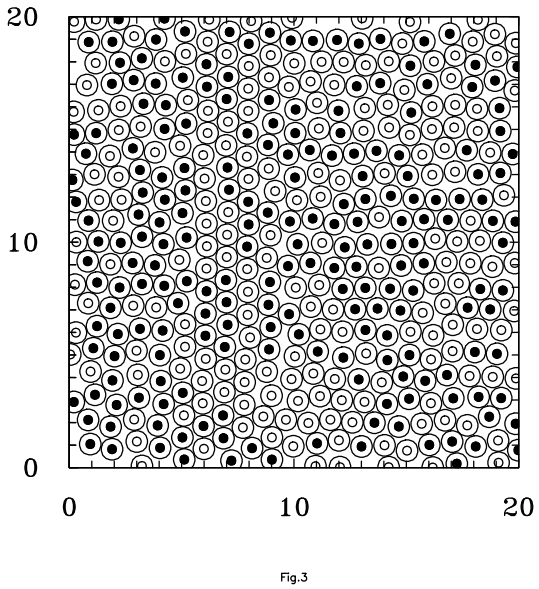

Figure 4.3: A system configuration with $N = 400$ spins and $r = 0.98$ for $J = 0.25$. The hard core repulsion radius is shown as a circle around the spin.

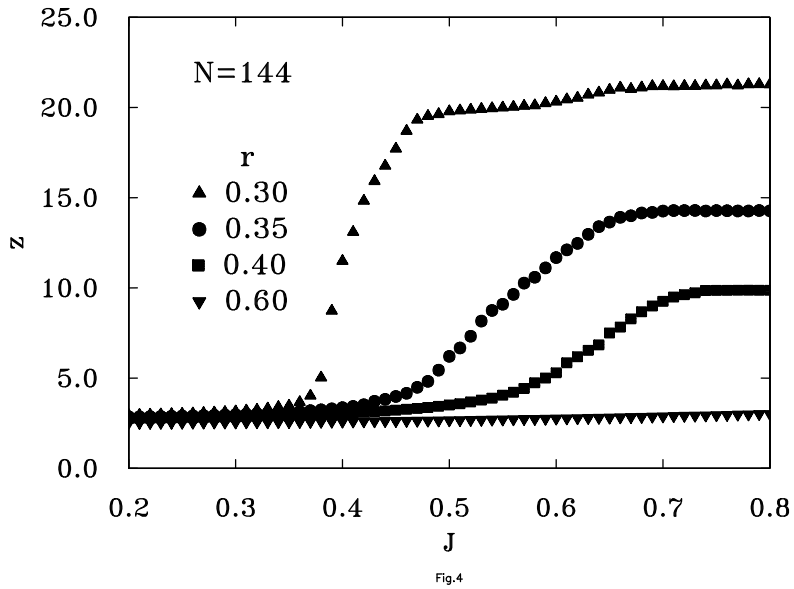

Figure 4.4: The average number of neighbors as a function of J on a lattice with $N = 144$ spins for several choices of the hard core repulsion r.

on a system with $N = 144$ spins. We find that for small values of r the coordination number increases very rapidly as we approach the critical point. On the other hand, for intermediate choices of r, z saturates to a smaller value. When $r = 0.6$, the coordination number saturates to a value of $z = 3.1$, which is already very close to the value on a regular triangular lattice ($z = 3$).

In Fig. 4.5 we plot the average energy per bond E_z as a function of J for several choices of the hard core repulsion r. The jump discontinuity, which is visible for small hard core repulsion r, indicates the existence of a first order transition. For larger values of r, the discontinuity is reduced and eventually vanishes. A determination of the discontinuity in the average energy of Fig. 4.5 at the critical coupling J_c shows that it gradually decreases as r is increased from zero.

Fig. 4.6 shows a plot of the latent heat per bond Δ_z versus r at the transition point J_c. In general we do not expect the latent heat to vanish linearly at the endpoint, but our results seem to indicate a behavior quite close to linear. From the data we estimate that the latent heat vanishes at $r = 0.344(7)$, thus signaling the presence of

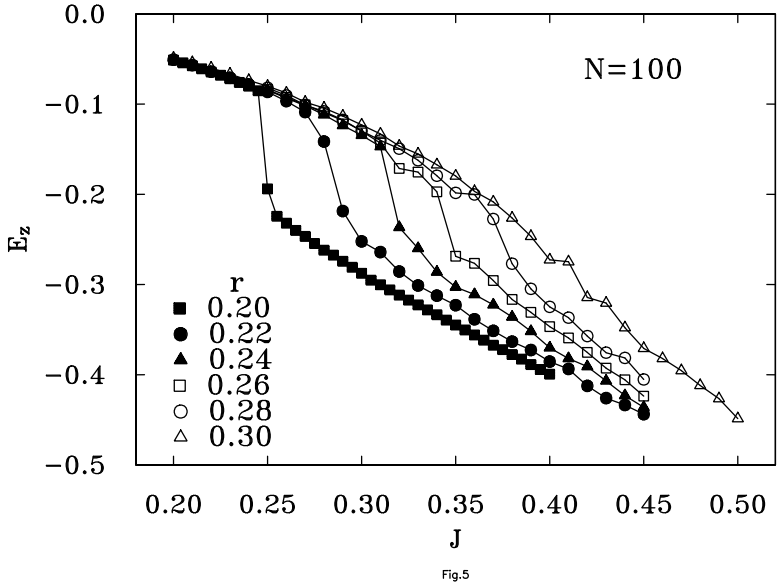

Figure 4.5: The average energy per bond E_z as a function of J for several choices of the hard core repulsion r for a system with $N = 100$ sites.

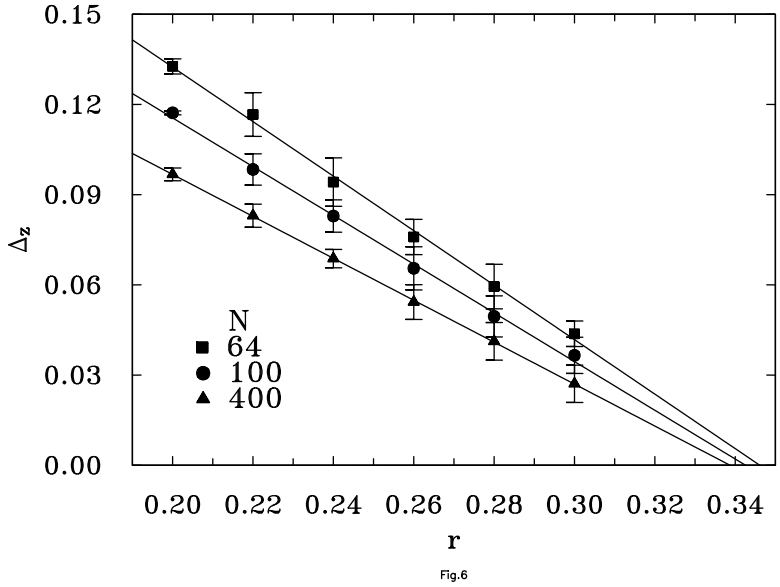

Figure 4.6: The latent heat per bond Δ_z along the first order transition line, plotted against the hard core repulsion parameter r. The tricritical point is located where the latent heat vanishes.

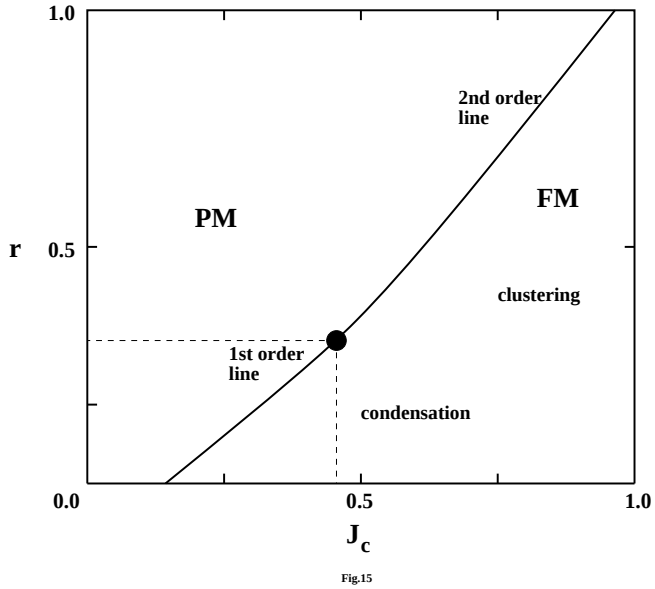

Figure 4.7: The phase diagram for the dynamical random Ising model on a two dimensional flat space. The critical point (denoted by the solid circle) separates the first order from the second order transition lines. The paramagnetic (PM) and ferromagnetic (FM) phases are also shown.

a tricritical point at the end of the first order transition line. Beyond this point, the transition stays second order, as will be discussed further below.

The phase transition line is shown in Fig. 4.7; for $r = 0$ we found on the largest lattices $J_c = 0.19(2)$, while for $r = 0.98$ we found $J_c = 0.93(3)$.

In Fig. 4.8 we plot the spin susceptibility as a function of J for several system sizes near the tricritical point, showing a growth of the peak with system size. To determine the critical exponents, we will resort to a finite-size scaling analysis. In the following we will be mostly concerned with the values for the critical exponents in the vicinity of the tricritical point. In the case of the spin susceptibility, from finite-size scaling, we expect a scaling form of the type

$$\chi(N, J) = N^{\gamma/2\nu}\, \bar{\chi}(N^{1/2\nu}|J - J_c|) \quad . \tag{4.3.23}$$

To recover the correct infinite volume result one needs $\bar{\chi}(x) \sim x^{-\gamma}$ for large arguments. Thus, in particular the peak in χ should scale like $N^{\gamma/2\nu}$ for sufficiently large N.

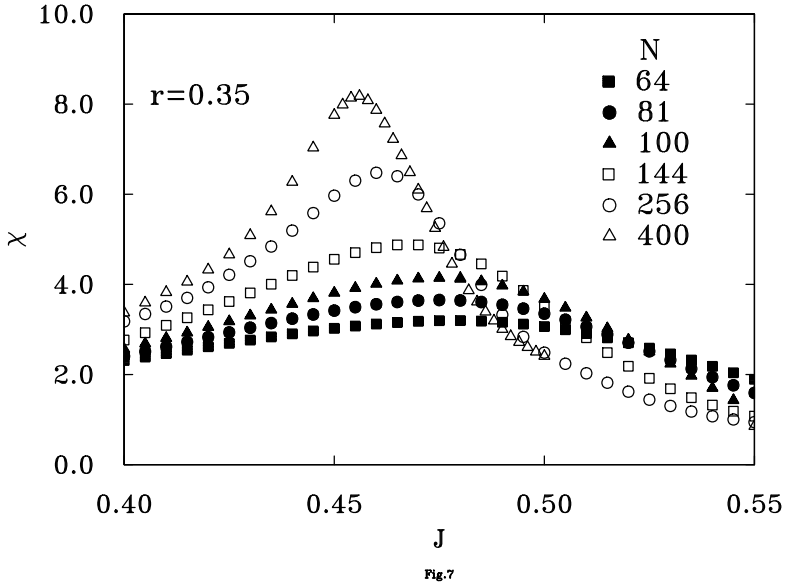

Figure 4.8: The magnetic susceptibility χ versus J for fixed hard core repulsion parameter $r = 0.35$ and different system sizes.

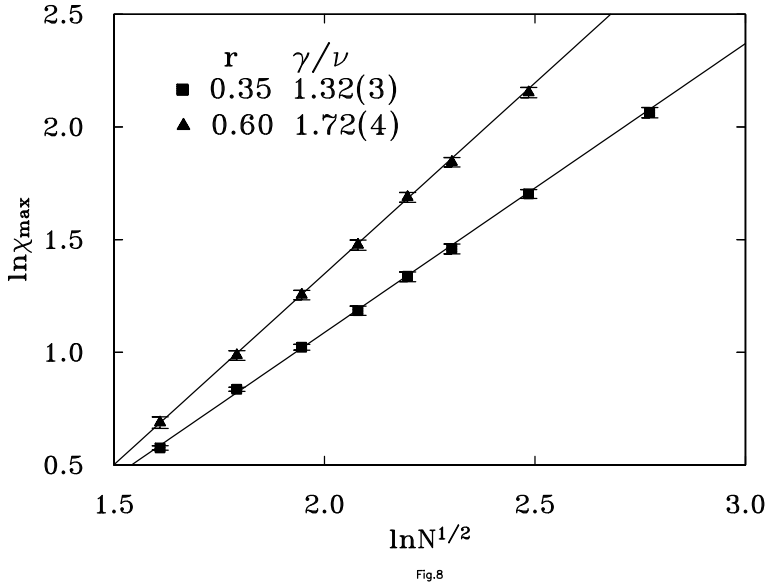

Figure 4.9: The peak in the magnetic susceptibility χ_{max} versus the number of Ising spins N for choices of the hard core repulsion parameter corresponding to $r = 0.35$ and $r = 0.6$.

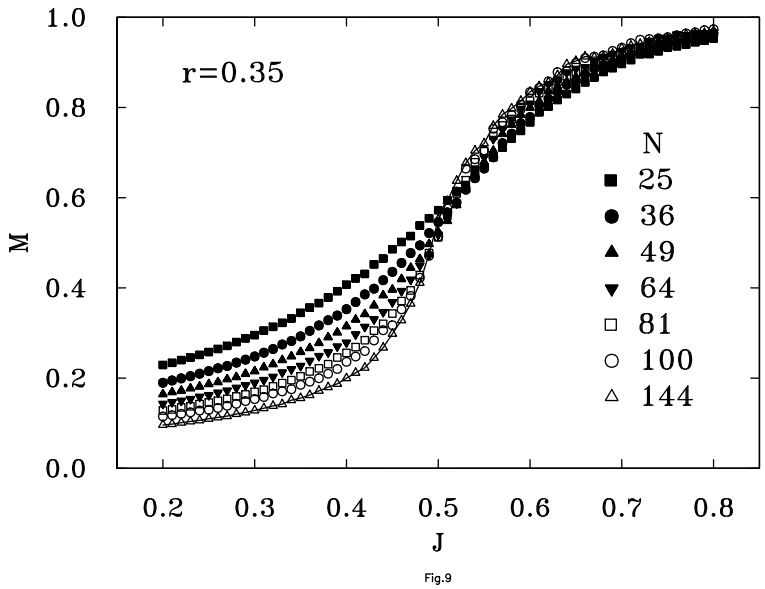

Figure 4.10: The magnetization M versus J, for fixed hard core repulsion parameter $r = 0.35$ and different system sizes. The solid line is a spline through the data for $n = 144$.

Despite the fact that the lattices are quite small, as can be seen from the graph, a linear fit to the data at the tricritical point is rather good, with relatively small deviations from linearity, $\chi^2/d.o.f. \sim 10^{-4}$. Using least-squares one can estimate γ/ν. For $r = 0.35$ we find $\gamma/\nu = 1.32(3)$, which is much smaller than the exact regular Ising result $\gamma/\nu = 1.75$. From scaling one then obtains the anomalous dimension exponent $\eta = 2 - \gamma/\nu = 0.68(3)$. To further gauge our errors, we have computed the same exponent for the regular Ising limit, for $r = 0.6$. In this case we indeed recover the Onsager value: we find on the same size lattices and using the same analysis method $\gamma/\nu = 1.72(4)$. We also note that the shift in the critical point on a finite lattice is expected to be determined by the correlation length exponent ν, namely $J_c(N) - J_c(\infty) \sim N^{-1/2\nu}$. This relationship can be used to estimate ν, but it is not very accurate. From a fit to the known values of $J_c(N)$ we obtain a first rough estimate $\nu = 1.3(2)$. A more precise determination of ν will be given later.

A similar finite-size scaling analysis can be performed for the magnetization, which is shown in Fig. 4.10 for several system sizes. Close to and above J_c we

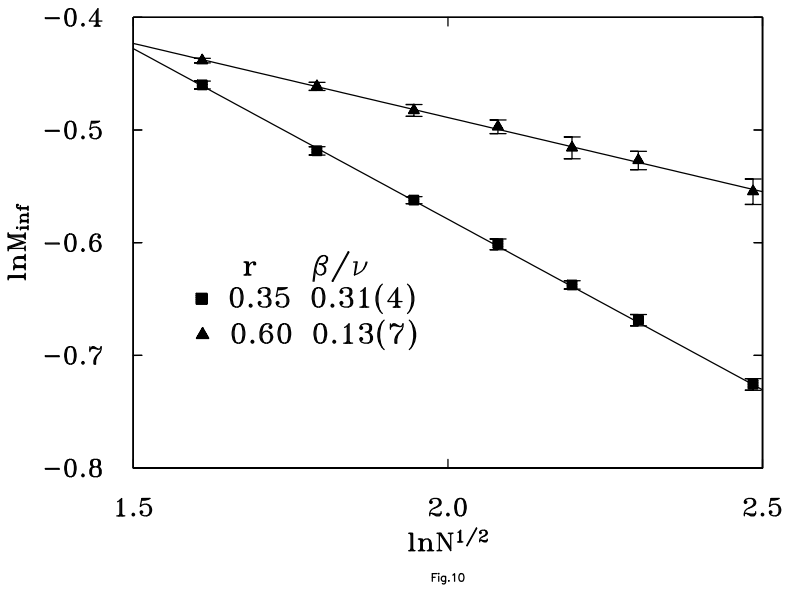

Figure 4.11: Finite size scaling of the magnetization at the inflection point M_{inf} versus the total number of Ising spins N for choices of the hard core repulsion parameter corresponding to $r = 0.35$ and $r = 0.6$.

expect $M \sim (J - J_c)^{\beta}$. At the critical point on a finite lattice, as determined from the peak in the susceptibility (which incidentally is very close to the inflection point in the magnetization versus J), M should scale to zero as $M_N(J_c) \sim N^{\beta/2\nu}$.

In Fig. 4.11 we show the magnetization M computed in this way for different size lattices At the tricritical point we find $\beta/\nu = 0.31(4)$, which again clearly excludes the pure Ising exponent, $\beta/\nu = 0.125$. For the pure Ising limit ($r = 0.6$) we obtain $\beta/\nu = 0.13(7)$, which is close to the expected Onsager value.

The results for the Ising specific heat C at the tricritical point as a function of lattice size N are shown in Fig. 4.12. One expects the peak to grow as $C \sim N^{\alpha/2\nu}$, but the absence of any growth for the larger values of N implies that $\alpha/\nu < 0$ (a weak cusp in the specific heat). In general close to a critical point, the free energy can be decomposed into a regular and a singular part. In our case the singular part does not seem to be singular enough to emerge above the regular background, leading to an intrinsic uncertainty in the determination of an $\alpha < 0$, and which can only be overcome by determining still higher derivatives of the free energy with respect

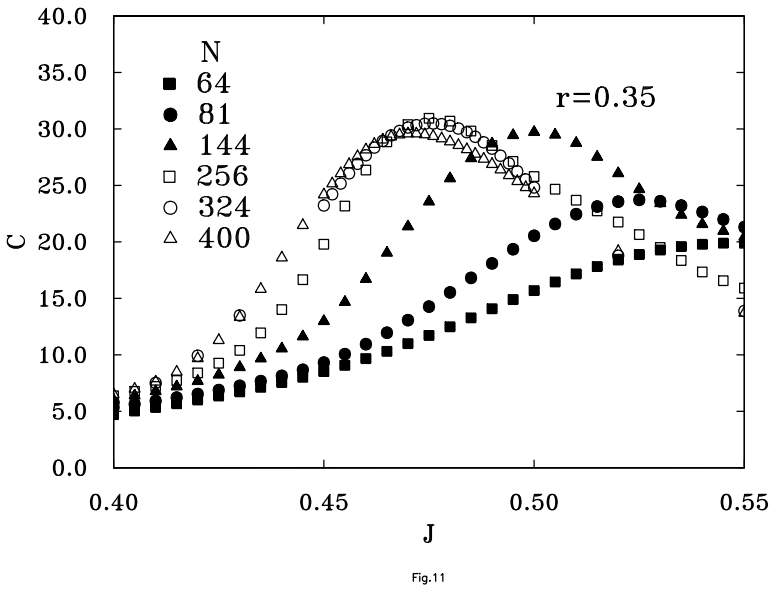

Figure 4.12: Plot of the specific heat C versus ferromagnetic coupling J at $r = 0.35$, showing the absence of a growth in the peak with increasing lattice size (for the larger systems), in contrast to the behavior of the magnetic susceptibility. The errors (not shown) are smaller than the size of the symbols.

to the coupling J. In order to isolate the singular part of the specific heat we have therefore calculated dC/dJ from the expression

$$\frac{dC}{dJ} = N^2 \left[3\langle E \rangle \langle E^2 \rangle - \langle E^3 \rangle - 2\langle E \rangle^3 \right] . \tag{4.3.24}$$

In the infinite system dC/dJ should diverge according to

$$\frac{dC}{dJ} \sim |J - J_c|^{-(\alpha+1)}. \tag{4.3.25}$$

In particular, if $\alpha = -1$, dC/dJ should diverge logarithmically. In Fig. 4.13 we show the scaling of dC/dJ on a lattice with $N = 256$ spins according to Eq. (4.3.25). From the slope of the curve we determine the critical exponent to be $\alpha \approx -0.98(4)$.

We have also tried to assume a logarithmic scaling behavior as shown in Fig. 4.14. It is clear that from the linear behavior of dC/dJ we can conclude that our results are completely consistent with an exponent of $\alpha = -1$. We attribute the small discrepancy between the results of Figs. 4.13 and 4.14 to the fact that we are not sufficiently close to J_c and that we are on a finite lattice with N sites. We have

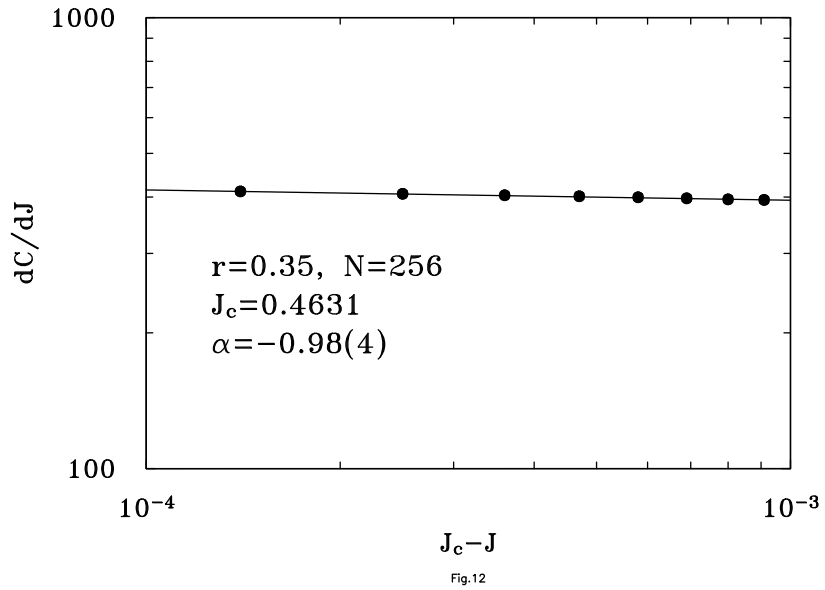

Figure 4.13: The derivative of the specific heat dC/dJ as a function of $J_c - J$ on logarithmic axes for $N = 256$.

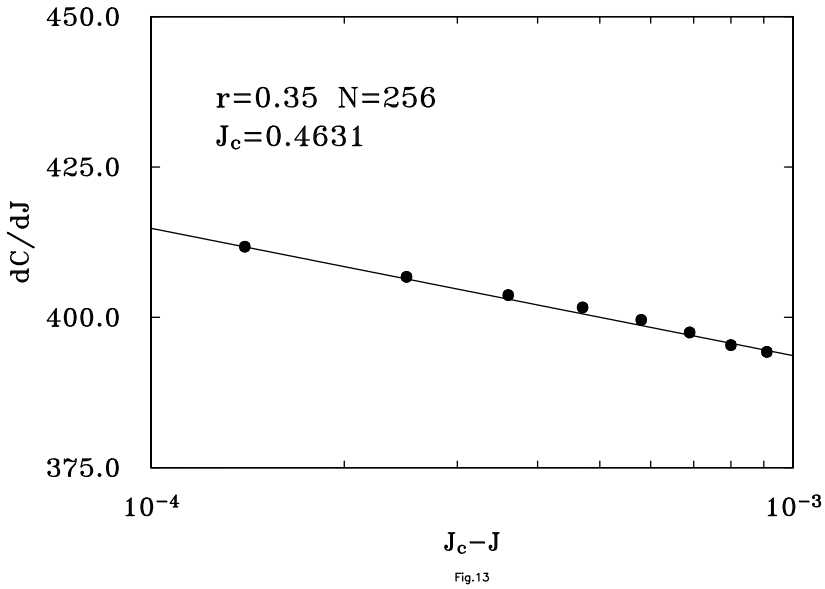

Figure 4.14: The derivative of the specific heat dC/dJ as a function of $J_c - J$ on semi-logarithmic axes for $N = 256$.

also performed a similar analysis for the fluctuation in the energy per bond (as opposed to the energy per site as defined previously). In this case we find close to the tricritical point $\alpha \approx -0.96(2)$.

In the *regular* Ising case one has in a finite volume a logarithmic divergence $C \sim \ln N$ (and $\alpha/2\nu = 0$), and we indeed see such a divergence clearly for $r = 0.6$, which corresponds to the almost regular triangular Ising case.

Another approach to obtaining α is to determine the correlation length exponent ν directly instead, and use scaling to relate it to $\alpha = 2 - 2\nu$. The exponent ν can be obtained in the following way. First one can improve on the estimate for J_c by considering the fourth-order cumulant [88]

$$U_N(J) = 1 - \frac{< m^4 >}{3 < m^2 >^2} \quad , \tag{4.3.26}$$

where $m = \sum_i S_i / N$. It has the scaling form expected of a dimensionless quantity

$$U_N(J) = \bar{U}(N^{1/2\nu}|J - J_c|). \tag{4.3.27}$$

The curves $U_N(J)$, for different and sufficiently large values of N, should then intersect at a common point J_c, where the theory exhibits scale invariance, and U takes on the fixed point value U^*. In Fig. 4.15 we show the fourth-order cumulant as a function of J for $r = 0.35$ and for several lattice sizes. We have found that indeed the curves meet very close to a common point, and from the intersection of the curves for $N = 25$ to 400 we estimate $J_c = 0.472(9)$, which is consistent with the estimate of the critical point derived from the location of the peak in the magnetic susceptibility. We also determine $U^* = 0.47(4)$, which should be compared to the pure Ising model estimate for the invariant charge $U^* \approx 0.613$ [89].

One can then estimate the correlation length exponent ν from the scaling of the slope of the cumulant at J_c. For two lattice sizes N, N' one computes the estimator

$$\nu_{eff}(N, N') = \frac{\ln[N'/N]}{2\ln[U'_{N'}(J_c)/U'_N(J_c)]} \quad , \tag{4.3.28}$$

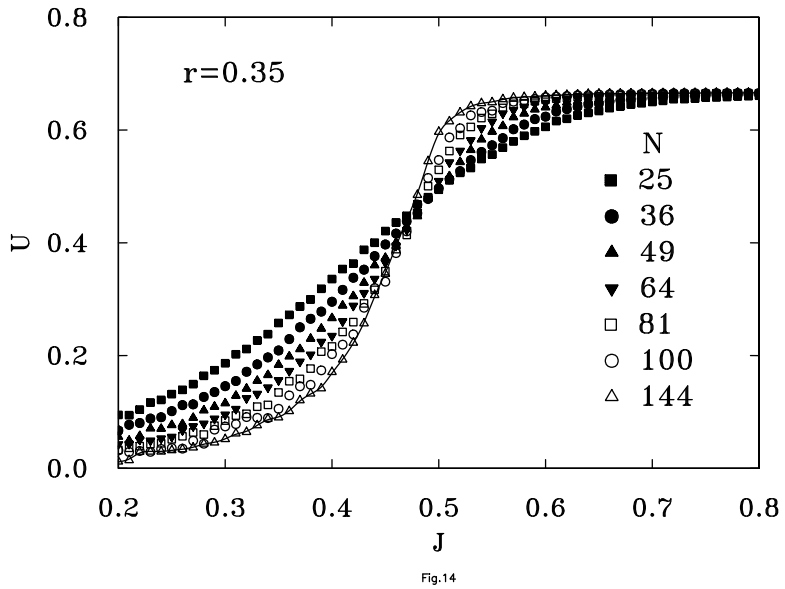

Figure 4.15: The Binder fourth-order cumulant U as a function of J for fixed hard core repulsion $r = 0.35$ and on several lattices with N spins. The solid line is a spline through the data for $N = 144$.

with $U'_N \equiv \partial U_N / \partial J$ defined by

$$U'_N = \frac{N}{3\langle m^2\rangle^2}\left[\langle m^4\rangle\langle E\rangle + \langle m^4 E\rangle - 2\frac{\langle m^4\rangle\langle m^2 E\rangle}{\langle m^2\rangle}\right]. \tag{4.3.29}$$

Using values of N from systems with 256, 400, and 900 spins we estimate ν from Eq. (4.3.29) to be $1.46(8)$. Using the scaling relationship $\alpha = 2 - 2\nu$, we obtain an estimate for α which is again quite consistent with our previous estimate derived from dC/dJ.

In Table 4.1 we summarize our results, together with the exponents obtained for the two-matrix model [74] (and which are the same as the KPZ values [82]), for the Onsager solution of the square lattice Ising model, and for the tricritical Ising model in two dimensions [86]. As can be seen, the exponents are quite close to the matrix model values (the pure Ising exponents seem to be excluded by several standard deviations).

Table 4.1: Estimates of the critical exponents for the random two-dimensional Ising model, as obtained from finite-size scaling at the tricritical point.

	γ/ν	β/ν	α/ν	α	ν
This work	1.32(3)	0.31(4)	-0.65(4)	-0.98(4)	1.46(8)
Matrix model	1.333...	0.333...	-0.666...	-1.0	1.5
Onsager	1.75	0.125	0.0	0.0	1.0
Tricritical Ising	1.85	0.075	1.60	0.888...	0.555...

4.4 Conclusions

In the previous sections we have presented some results for the exponents of a random Ising model in flat two-dimensional space. The model reproduces some of the features of a model for dynamically triangulated Ising spins, and in particular its random nature, but does not incorporate any effects due to curvature. Due to the non-local nature of the interactions of the spins, only relatively small systems have been considered so far, which is reflected in the still rather large uncertainties associated with the exponents. Still a rich phase diagram has emerged, with a tricritical point separating first from second order transition lines. The phase diagram we obtain is shown in Fig. 4.7. We have localized the tricritical point at $J_c = 0.471(5)$ and $r = 0.344(7)$. The thermal and magnetic exponents determined in the vicinity of the tricritical point (presented in Table 4.1) have been found to be consistent, within errors, with the matrix model solution of the random Ising model and the KPZ values. Our results would therefore suggest that matrix model solutions can also be used to describe a class of annealed random systems in flat space.

One might wonder at this point if the spin system discussed in this chapter can be found among the models in the FQS classification scheme [90] of two-

dimensional conformally invariant field theories [1]. Since the model is apparently not unitary (it contains short range repulsion and long range attraction terms), it should fall into the wider class of degenerate theories considered by BPZ [91]. The allowed scaling dimensions in these theories are given by the well-known Kac formula,

$$\Delta_{p,q} = \frac{1}{4}\left[(p\alpha_+ + q\alpha_-)^2 - (\alpha_+ + \alpha_-)^2\right] \tag{4.4.30}$$

with p, q positive integers, and $\alpha_\pm = \alpha_0 \pm (1+\alpha_0^2)^{1/2}$. α_0 is related to the conformal anomaly c of the theory by $c = 1 - 24\alpha_0^2$. Often the central charge is then written as $c = 1 - 6/\,m(m+1)$. One of the difficulties in this approach is the identification of a given realization of conformal symmetry with a particular universality class. The simplest possibility appears to be $m = 4/5$, corresponding to $m = r/(s-r)$ with $s = 9$ and $r = 4$. One then obtains for this choice the central charge $c = -19/6$, and $\alpha_0 = 5/12$, $\alpha_+ = 3/2$ and $\alpha_- = -2/3$. The matching scaling dimensions are then $\Delta_{1,4} = \Delta_{3,5} = 1/6$ (which gives $\eta = 2/3$), and $\Delta_{1,5} = \Delta_{3,4} = 2/3$ (which gives $\nu = 3/2$). Negative values of c are allowed in non-unitary theories. It would be of interest to compute the central charge directly in the random spin model and verify this assignment, using the methods described in Ref. [93].

We should mention that the above values for s and r appear to be rather close to the ones associated with the Yang-Lee edge singularity, which describes the behavior of the magnetization in the Ising model in the presence of an imaginary external field, and for which Cardy [92] has suggested the identification $s = 5$ and $r = 2$, which yields $m = 2/3$ and $c = -22/5$. It is known that the Yang-Lee edge singularity also describes the critical properties of large branched dilute polymers and of the Ising model in a quenched random external field in $d+2$ dimension [94].

[1] We thank Giorgio Parisi for suggesting to look into this aspect.

Chapter 5

Conclusion

In this thesis we have presented results for 1) the quantum corrections to the Newtonian potential in the long distance scale; 2) Feynman rules for simplicial gravity in two dimensions; 3) critical exponents for the dynamically triangulated random Ising model in flat two dimensional space. For the Newtonian potential correction to the order of G^2, we obtain

$$V(r) = -G\frac{m_1 m_2}{r}\left[1 - \frac{G(m_1+m_2)}{2c^2 r} - \frac{122G\hbar}{15\pi c^3 r^2}\right]. \tag{5.0.1}$$

The first correction term at the scale of $2Gm_i/c^2$ represents the classical relativistic correction, and the second term at the Planck scale $(G\hbar/c^3)^{1/2}$ represents the genuine quantum mechanical correction. The relativistic correction we obtained are in complete agreement with the result obtained by using classical relativistic method (Einstein-Hoffmann-Infeld.) The quantum correction to the potential to the one loop order is finite, despite the theory is non-renormalizable in perturbation theory. The sign of the quantum correction we obtained indicates an increase (slowly) of gravitational potential with distance. This result is in agreement with the intuitive expectation that gravity couples universally to all forms of energy, and cannot be easily screened by quantum fluctuations. Further investigation in this study will be to see if higher loop order corrections in G can still lead to finite corrections in the long distance limit. In case they are not finite, should one need to add higher derivative terms in the Hilbert-Einstein action to control the ultraviolet divergences.

In the chapter of “Feynman Rules for Simplicial Gravity", We derived the *lattice Feynman rules* for gravity coupled to a D-component massless scalar field. Even though the lattice Feynman rules derived are necessary more complicated than their corresponding continuum Feynman rules (involved *sine* of the momentum,) in the lowest order in momentum expansion, they completely reduce to the familiar continuum form. As an application, the conformal anomaly due to a massless scalar field was computed by diagrammatic methods. In the continuum theory, it has been shown (Polyakov) the conformal anomaly is canceled when $D = 26$. It is interesting to see if the anomaly can also be canceled in the lattice theory.

In the last chapter we presented the results for the exponents of a dynamically triangulated random Ising model in flat two-dimensional space using computer simulation method. The model describes Ising spins moving randomly on a two dimensional surface with no curvature (gravity.) The obtained phase diagram shows a tricritical point separating first from second order transition lines at $J_c = 0.471(5)$ and $r = 0.344(7)$. The thermal and magnetic exponents determined in the vicinity of the tricritical point (presented in Table 4.1) have been found to be consistent, within errors, with the matrix model solution of the random Ising model and the KPZ values. Our results would therefore suggest that matrix model solutions can also be used to describe a class of annealed random systems in flat space (without gravity.)

Bibliography

[1] C. J. Isham, R. Penrose, and D. W. Sciama, *Quantum Gravity: A Second Oxford Symposium.* Clarendon Press, 1981.

[2] A. H. Guth, *Phys. Rev.* **23D** (1981), 347.

[3] A. D. Linde, *Phys. Lett.*, **108B** (1982), 389.

[4] R. H. Brandenberger, *Rev. Mod. Phys.* **57**, 1.

[5] A. Vilenkin, *Phys. Rep.* **160**, (1988), 1.

[6] S. W. Hawking, Particle Creation by Black Hole. *Comm. Math. Phys.*, **43** (1975), 199.

[7] J. D. Berkenstein, The Quantum Mass Spectrum of a Kerr Black Hole, *Lett. Nuov. Cim.*, **11** (1974), 467.

[8] G. W. Gibbons, M. J. Perry, *Black Holes in Thermal Equilibrium*, *Phys. Rev. Lett.*, **36**, (1976), 985.

[9] G. 'tHooft, *On the Quantum Structure of a Black Hole*, *Nucl. Phys.*, **B256**, (1984), 727.

[10] L. Susskind, L. Thorlacius, J Uglum, *The Stretched Horizon And Black Hole Complementary*, *Phys. Rev.*, **D48**, (1993), 3743.

[11] J. B. Hartle, S. W. Hawking, *Wave Function of the Universe*, *Phys. Rev.*, **D28**, (1983), 46.

[12] S. W. Hawking, *The Quantum State of the Universe*, *Nucl. Phys.*, **B239**, (1984), 257.

[13] A. Ashtekar, New Variables for Classical and Quantum Gravity, *Phys. Rev. Lett.*, **57** (1986), 80.

[14] C. Rovelli and L. Smolin, Loop space representation of Quantum General Relativity, *Nucl. Phys.*, **331B** (1990), 80.

[15] L. Fedeev and V. Popov, Feynman Rules for Young-Mills theory, *Phys. Lett.* **25B** (1967), 27.

[16] R. P. Feynman, *Acta Phys. Polon.* **24** (1963) 697.

[17] R. P. Feynman, *"Lectures on Gravitation"*, Caltech Notes, edited by F. Morengo and W. Wagner (1963).

[18] B. DeWitt, *Phys. Rev.* **160** (1967) 1113; *Phys. Rev.* **162** (1967) 1195 and 1239.

[19] G. 't Hooft and M. Veltman, *Ann. Inst. H. Poincar*, **20** (1974) 69.

[20] S. Deser and P. van Nieuwenhuizen, *Phys. Rev.* **D10** (1974) 401 and 410;
S. Deser, H. S. Tsao and P. van Nieuwenhuizen, *Phys. Lett.* **50B** (1974) 491; *Phys. Rev.* **D10** (1974) 3337.

[21] J. F. Donoghue, *Phys. Rev. Lett.* **72** (1994) 2996; preprint UMHEP-408 (gr-qc/9405057).

[22] B. DeWitt and R. Utiyama, *J. Math. Phys.* **3** (1962) 608;
K. S. Stelle, *Phys. Rev.* **D16** (1977) 953.

[23] S. Weinberg, in *'General Relativity - An Einstein Centenary Survey'*, edited by S.W. Hawking and W. Israel, (Cambridge University Press, 1979).

[24] M. Ro£ek and R. M. Williams, *Phys. Lett.* **104B** (1981) 31, and *Z. Phys.* **C21** (1984) 371.

[25] I. J. Muzinich and S. Vokos, preprint UW/PT-94-12 (December 1994).

[26] T. T. Wu, CERN Th, unpublished.

[27] D. M. Capper, G. Leibrandt, and M. Ramon Medrano, *Phys. Rev.* **D8** (1973) 4320.

[28] L. D. Fadeev and V. N. Popov, *Phys. Lett.* **25B** (1967) 29.

[29] E. S. Fradkin and I. V. Tyutin, *Phys. Rev.* **D2** (1970) 2841.

[30] M. Veltman, in *'Methods in Field Theory'*, Les Houches Lecture notes, Session XXVIII (North Holland, 1975).

[31] D. G. Boulware and S. Deser, *Ann. Phys.* **89** (1975) 193.

[32] M. J. Duff, *Phys. Rev.* **D7** (1972) 2317; *Phys. Rev.* **D9** (1974) 1837.

[33] Y. Iwasaki, *Progr. Theor. Phys.* **46** (1971) 1587.

[34] F. Radkowski, *Ann. Phys.* **56** (1970) 314.

[35] S. Weinberg, *'Gravitation and Cosmology'*, Ch. 9 (Wiley, New York 1972).

[36] G. Modanese, *Phys. Lett.* **325B** (1994), 354; *Nucl. Phys.* **B434** (1995) 697; preprint MIT-CTP-2217 (June 1993).

[37] H. Hamber and R. Williams, *Nucl. Phys.* **B435** (1995) 361.

[38] M. Goroff and A. Sagnotti, *Phys. Lett.* **160B** (1985) 81; *Nucl. Phys.* **B266** (1986) 709.

[39] T. Regge, *Nuovo Cimento* **19** (1961) 558.

[40] H. W. Hamber, in the *1984 Les Houches Summer School*, Session XLIII, (North Holland, 1986).

[41] M. Ro£ek and R. M. Williams, *Phys. Lett.* **104B** (1981) 31, and *Z. Phys.* **C21** (1984) 371.

[42] J. B. Hartle, *J. Math. Phys.* **26** (1985) 804; **27** (1985) 287; and **30** (1989) 452.

[43] H. W. Hamber and R. M. Williams, *Nucl. Phys.* **B248** (1984) 392; **B260** (1985) 747; *Phys. Lett.* **157B** (1985) 368; and *Nucl. Phys.* **B269** (1986) 712.

[44] B. Berg, *Phys. Rev. Lett.* **55** (1985) 904; and *Phys. Lett.* **B176** (1986) 39.

[45] H. W. Hamber, *Nucl. Phys.* **B** (Proc. Supp.) **20** (1991) 728; *Phys. Rev.* **D45** (1992) 507; and *Nucl. Phys.* **B400** (1993) 347.

[46] W. Beirl, E. Gerstenmayer, H. Markum and J. Riedler, *Phys. Rev.* **D49** (1994) 5231.

[47] H. W. Hamber and R. M. Williams, *Nucl. Phys.* **B267** (1986) 482.

[48] Z. Tabor, preprint TPJU-10-95 (April 1995), 12pp.

[49] G. Modanese, *Phys. Lett.* **325B** (1994), 354; *Nucl. Phys.* **B434** (1995) 697.

[50] H. W. Hamber and R. M. Williams, *Nucl. Phys.* **B435** (1995) 361.

[51] H. W. Hamber and R. M. Williams, *Phys. Rev.* **D47** (1993) 510.

[52] A. M. Polyakov, *Phys. Lett.* **B103** (1981) 207.

[53] A. M. Polyakov, *Gauge Fields and Strings*, ch. 9 (Oxford Univ. Press, 1989).

[54] M. Gross and H. W. Hamber, *Nucl. Phys.* **B364** (1991) 703.

[55] C. Holm and W. Janke, *Phys. Lett.* **B335** (1994) 143; preprint FUB-HEP-17-95 (Nov. 1995).

[56] V. G. Knizhnik, A. M. Polyakov and A. B. Zamolodchikov, *Mod. Phys. Lett.* **A3** (1988) 819.

[57] F. David, *Mod. Phys. Lett.* **A3** (1988) 1651; J. Distler and H. Kawai, *Nucl. Phys.* **B321** (1989) 509.

[58] V. A. Kazakov, *Phys. Lett.* **A119** (1986) 140.

[59] M. Vekić, S. Liu, and H. W. Hamber, *Phys. Lett.* **B329** (1994) 444; *Phys. Rev.* **D51** (1995) 4287.

[60] W. Beirl and B. Berg, *Nucl. Phys.* **B452** (1995) 415.

[61] J. Nishimura and M. Oshikawa, *Phys. Lett.* **B338** (1994) 187.

[62] G. Parisi, *Nucl. Phys. B (Proc. Suppl.)* **29B,C** (1992) 247.

[63] D. Foerster, H. B. Nielsen and M. Ninomiya, *Phys. Lett.* **B94** (1980) 135;

[64] N. Christ, R. Friedberg and T. D. Lee, *Nucl. Phys.* **B202** (1982) 89; *Nucl. Phys.* **B210 [FS6]** (1982) 310,337.

[65] C. Itzykson, in *Progress in Gauge Field Theory* (CargŁse Lectures 1983, Plenum Press, New York, 1985).

[66] H. W. Hamber, in *Monte Carlo Methods in Theoretical Physics*, (ETS Editrice, 1992), pp. 119-144.

[67] M. Bander and C. Itzykson, *Nucl. Phys.* **B257 [FS14]** (1985) 531.

[68] A. Jevicki and M. Ninomiya, *Phys. Lett.* **B150** (1985) 115.

[69] M. Veltman, in *Methods in Field Theory*, Les Houches lectures, Session XXVIII (North Holland, 1975).

[70] H. W. Hamber and R. M. Williams, manuscript in preparation.

[71] H. W. Hamber and R. M. Williams, *Nucl. Phys.* **B451** (1995) 305.

[72] H. W. Hamber and S. Liu, to be published.

[73] P. Menotti and P. Peirano, *Phys. Lett.* **B353** (1995) 444.

[74] V.A. Kazakov, *Phys. Lett.* **A119** (1986) 140;
D.V. Boulatov and V.A. Kazakov, *Phys. Lett.* **B186** (1987) 379;
Z. Burda and J. Jurkiewicz, *Acta Physica Polonica* **20** (1989) 949.

[75] E. Brezin and S. Hikami, *Phys. Lett.* **B283** (1992) 203;
Phys. Lett. **B295** (1992) 209; S. Hikami, *Phys. Lett.* **B305** (1993) 327;
E. Brezin, M.R. Douglas, V. Kazakov and S.H. Shenker, *Phys. Lett.* **B237** (1990) 43.

[76] G.M. Cicuta, *Nucl. Phys.* **B** (Proc. Supp.) **5A** (1988) 54; and references therein.

[77] P. Ben-Av, J. Kinar and S. Solomon, *Int. Jour. Mod. Phys.* **C3** (1992) 279.

[78] C. Itzykson, JM. Drouffe, *Statistical Field Theory*, (Cambridge University Press, 1989).

[79] G. Parisi, *Statistical Field Theory*, (Addison-Wesley Pub. Co., 1988).

[80] J. B. Kogut, *An Introduction to Lattice Gauge Theory and Spin System*, *Reviews of Modern Physics*, V.51, No.4, 1979.

[81] J. Jurkiewicz, A. Krzywicki, B. Peterson and B. Sderberg, *Phys. Lett.* **B213** (1988) 511;
I.D. Aleinov, A.A. Migdal and V.V. Zmushko, *Mod. Phys. Lett.* **A5** (1990) 787;
C.F. Baille and D. A. Johnston, *Mod. Phys. Lett.* **A7** (1992) 1519;
S. Catterall, J. Kogut and R. Renken, *Phys. Rev.* **D45** (1992) 2957;
J. Ambjłrn, B. Durhuus, T. Jonsson and G. Thorleifsson, NBI-HE-92-35 (1992);
J.-P. Kownacki and A. Krzywicki, preprint LPTHE-Orsay 94/11 (Jan 1994).

[82] V.G. Knizhnik, A.M. Polyakov and A.B. Zamolodchikov, *Mod. Phys. Lett.* **A3** (1988) 819;
F. David, *Mod. Phys. Lett.* **A3** (1988) 1651;
J. Distler and H. Kawai, *Nucl. Phys.* **B321** (1989) 509.

[83] M. Gross and H.W. Hamber, *Nucl. Phys.* **B364** (1991) 703.

[84] D. Espriu, M. Gross, P. Rakow and J.F. Wheater, *Nucl. Phys.* **B265 [FS15]** (1986) 92;
W. Janke, M. Katoot and R. Villanova, *Phys. Lett.* **B315** (1993) 412.

[85] M. Vekić, S. Liu, and H.W. Hamber, *Phys. Lett.* **B329** (1994) 444.

[86] I.D. Lawrie and S. Sarbach, in *Phase Transitions and Critical Phenomena*, vol. 9, edited by C. Domb and J. Lebowitz (Academic Press, 1984); and references therein.

[87] U. Wolff, *Phys. Rev. Lett.* **62** (1989) 361.

[88] K. Binder, *Phys. Rev. Lett.* **47** (1981) 693; *Z. Phys.* **B43** (1981) 119.

[89] K. Binder and D. Landau, *Surf. Sci.* **151** (1985) 409;
D. Heerman and A. Burkitt, *Physica* **A 162** (1990) 210.

[90] D. Friedan, Z. Qiu and S. Shenker, *Phys. Rev. Lett.* **52** (1984) 1575.

[91] A.A. Belavin, A.M. Polyakov and A.B. Zamolodchikov, *J. Stat. Phys.* **34** (1984) 763.

[92] J. Cardy, *Phys. Rev. Lett.* **54** (1985) 1354;
J. Cardy, in *Phase Transitions and Critical Phenomena*, vol. 11 (edited by C. Domb and J.L. Lebowitz, Academic Press, 1987).

[93] H. Blte, J. Cardy and M.P. Nightingale, *Phys. Rev. Lett.* **56** (1986) 742;
I. Affleck, *Phys. Rev. Lett.* **56** (1986) 746;
C. Itzykson, H. Saleur and J.-B. Zuber, *Europhys. Lett.* **2** (1986) 91.

[94] G. Parisi and N. Sourlas, *Phys. Rev. Lett.* **46** (1981) 871.